UNCLASSIFIED

AD NUMBER
ADB017280
LIMITATION CHANGES

TO:

Approved for public release; distribution is unlimited.

FROM:

Distribution authorized to U.S. Gov't. agencies only; Test and Evaluation; JAN 1975. Other requests shall be referred to Air Force Materials Lab., Wright-Patterson AFB, OH 45433.

AUTHORITY
WL/DOA ltr 25 Feb 1994

THIS PAGE IS UNCLASSIFIED

AFML-TR-74-65, PART IV

DESIGN OF PARACHUTE COMPONENT MATERIALS
FROM KEVLAR 29 AND 49

Fabric Research Laboratories
1000 Providence Highway
Dedham, Massachusetts 02026

JULY 1976

AD-B017280

TECHNICAL REPORT AFML-TR-74-65, PART IV
REPORT FOR PERIOD JANUARY 1975 - APRIL 1976

Distribution limited to U. S. Government agencies only; test and evaluation;
January 1975. Other requests for this document must be referred to the Air
Force Materials Laboratory, Nonmetallic Materials Division, Composite and
Fibrous Materials Branch, AFML/MBC, Wright-Patterson Air Force Base
Ohio 45433.

AIR FORCE MATERIALS LABORATORY
AIR FORCE WRIGHT AERONAUTICAL LABORATORIES
AIR FORCE SYSTEMS COMMAND
WRIGHT-PATTERSON AIR FORCE BASE, OHIO

This technical report has been reviewed and is approved for publication.

S. Schulman, Project Monitor

For the Director

T. J. REINHART, CHIEF
Composites and Fibrous Materials Branch
Nonmetallic Materials Division

AIR FORCE - 23 MARCH 77 - 350

REPORT DOCUMENTATION PAGE		READ INSTRUCTIONS BEFORE COMPLETING FORM
1. REPORT NUMBER AFML-TR-74-65, Part IV	2. GOVT ACCESSION NO.	3. RECIPIENT'S CATALOG NUMBER
4. TITLE *(and Subtitle)* DESIGN OF PARACHUTE COMPONENT MATERIALS FROM KEVLAR 29 and 49		5. TYPE OF REPORT & PERIOD COVERED Technical Report January 1975 - April 1976
		6. PERFORMING ORG. REPORT NUMBER
7. AUTHOR(s) Norman J. Abbott, Robert J. Coskren, James G. Donovan		8. CONTRACT OR GRANT NUMBER(s) F33615-73-C-5034
9. PERFORMING ORGANIZATION NAME AND ADDRESS Fabric Research Laboratories 1000 Providence Highway Dedham, Mass. 02026		10. PROGRAM ELEMENT, PROJECT, TASK AREA & WORK UNIT NUMBERS Project 7320, Task 732002
11. CONTROLLING OFFICE NAME AND ADDRESS		12. REPORT DATE July 1976
		13. NUMBER OF PAGES 121
14. MONITORING AGENCY NAME & ADDRESS*(If different from Controlling Office)*		15. SECURITY CLASS. *(of this report)* Unclassified
		15a. DECLASSIFICATION/DOWNGRADING SCHEDULE

16. DISTRIBUTION STATEMENT *(of this Report)*

Distribution limited to U. S. Government agencies only; test and evaluation; January 1975. Other requests for this document must be referred to the Air Force Materials Laboratory, Nonmetallic Materials Division, Composite and Fibrous Materials Branch, AFML/MBC, Wright-Patterson Air Force Base, Ohio 45433.

17. DISTRIBUTION STATEMENT *(of the abstract entered in Block 20, if different from Report)*

Same

18. SUPPLEMENTARY NOTES

None

19. KEY WORDS *(Continue on reverse side if necessary and identify by block number)*

parachute materials, Kevlar, Kevlar processing, narrow fabrics, canopy fabrics, webbings, ribbons, tapes, cords, sewing threads, impact properties, high speed cutting.

20. ABSTRACT *(Continue on reverse side if necessary and identify by block number)*

Designs for Kevlar parachute component materials have been developed, including ribbons, tapes, webbings, tubular webbings, canopy and pack fabrics, braided cords, and sewing threads. Kevlar materials weigh approximately 1/3 as much as corresponding nylon materials of the same strength. This permits a saving of about 50% as the weight and bulk of parachutes made from Kevlar instead of nylon.

DD $_{1\ JAN\ 73}^{FORM}$ 1473   EDITION OF 1 NOV 65 IS OBSOLETE

TABLE OF CONTENTS

LIST OF ILLUSTRATIONS

LIST OF ILLUSTRATIONS (Cont)

LIST OF ILLUSTRATIONS (Cont)

LIST OF TABLES

LIST OF TABLES (Cont)

I.   INTRODUCTION

One of the main reasons for wanting to use Kevlar in parachutes is the potential it offers in reducing weight and bulk for a given strength, in relation to the commonly-used high tenacity nylon. This is because the tenacity of Kevlar fiber is 3 to 4 times that of high tenacity nylon fiber. However, it is apparent that maximum benefit can only be derived from this high tenacity if the fiber strength is translated efficiently into the strength of the structure.

The fabric designer, as well as the processor, cannot assume that a new fiber can be handled or used exactly like another fiber with which he is familiar. Particularly if the fiber has a totally new, hitherto unavailable set of properties, as Kevlar has, one can expect to have to learn how to handle it through yarn and fabric processing, and how to design structures which retain and reflect the desirable characteristics of the fiber, in this case its high tenacity.

This report describes the problems encountered in developing efficient designs for Kevlar parachute component materials, and the solutions arrived at in the design of some 60 structures in the form of tapes, ribbons, webbings, tubular webbings, braided cords, sewing threads and broad woven fabrics.

II.   PROCESSING PROCEDURES

Because of Kevlar's peculiar tensile characteristics, particularly its low rupture elongation and high modulus, and its sensitivity to abrasive damage, it is much more susceptible to damage during all phases of processing than a fiber like nylon. A study was made of the effect of several critical processing steps on yarn or fabric strength, with a view to optimizing conditions in each of those steps for maximum strength retention.

Yarn Twist

1.   Singles Yarn Twist Optimization

Prior to conducting any fabric weaving studies the relation between yarn twist and strength was determined for each of four commercially available deniers of Kevlar 29 yarn, as well as one denier available to this program in experimental quantities.

The data from the singles yarn twist studies are presented graphically in Figures 1, 2 and 3. Figure 1 shows the breaking tenacity in grams per denier for each of the five yarn sizes as a function of Twist Multiplier.* Optimum values range from 1.0 for the 200 denier yarn to 1.75 to 2.0 for the 100 and 1000 deniers. The strength of the 400 and 1500 yarns is maximized at a twist multiplier of 1.25 to 1.50.

---

*Twist Multiplier (TM) = $\dfrac{\text{tpi }\sqrt{\text{denier}}}{73}$, a parameter normalized with respect to yarn diameter. Thus yarns having the same twist multiplier contain fibers lying at approximately the same helix angle.
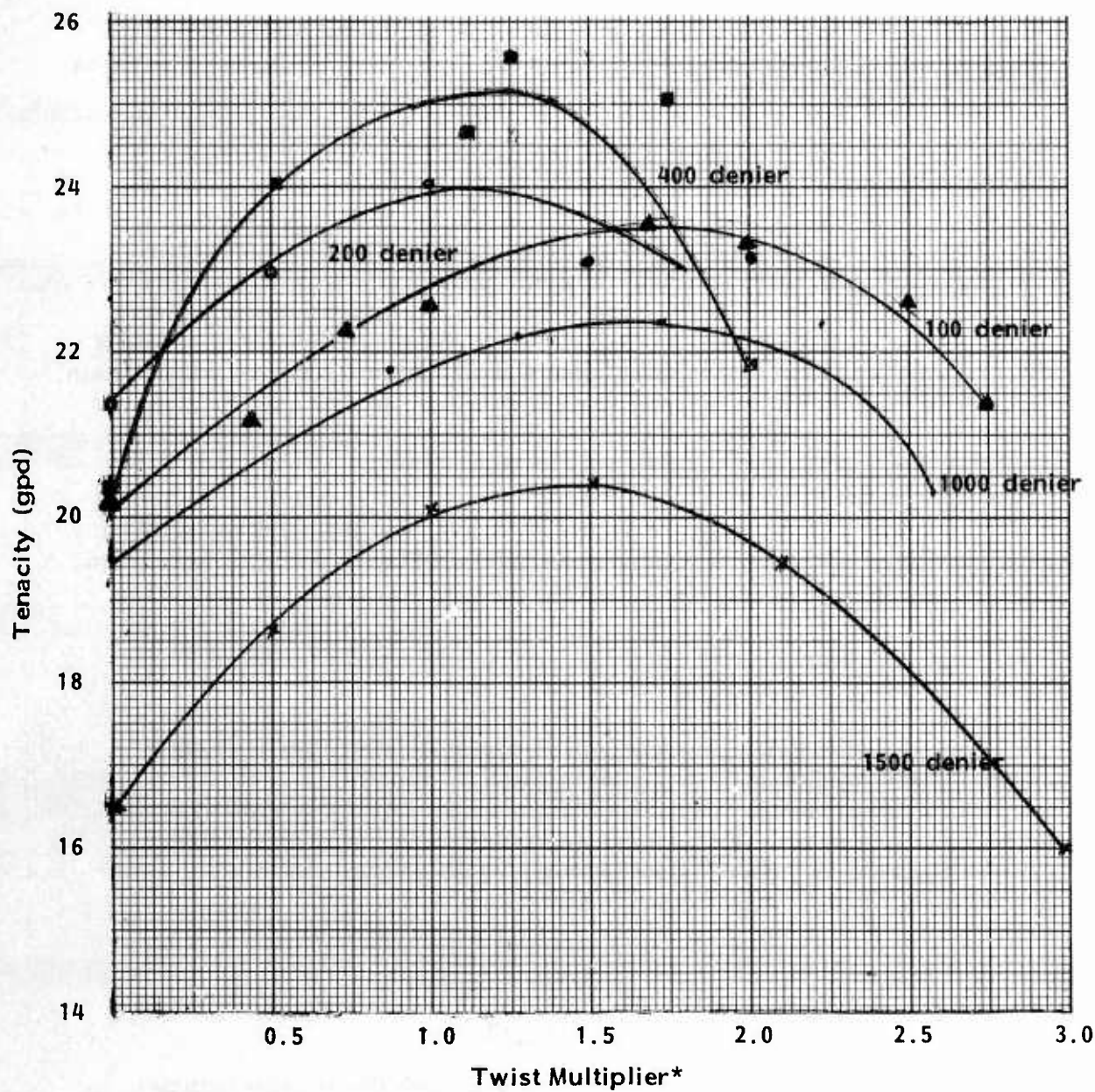
$$\text{Twist Multiplier} = \frac{\text{tpi}\sqrt{\text{denier}}}{73}.$$

Figure 1.   Effect of Twist on Tensile Strength of Kevlar 29 Yarns
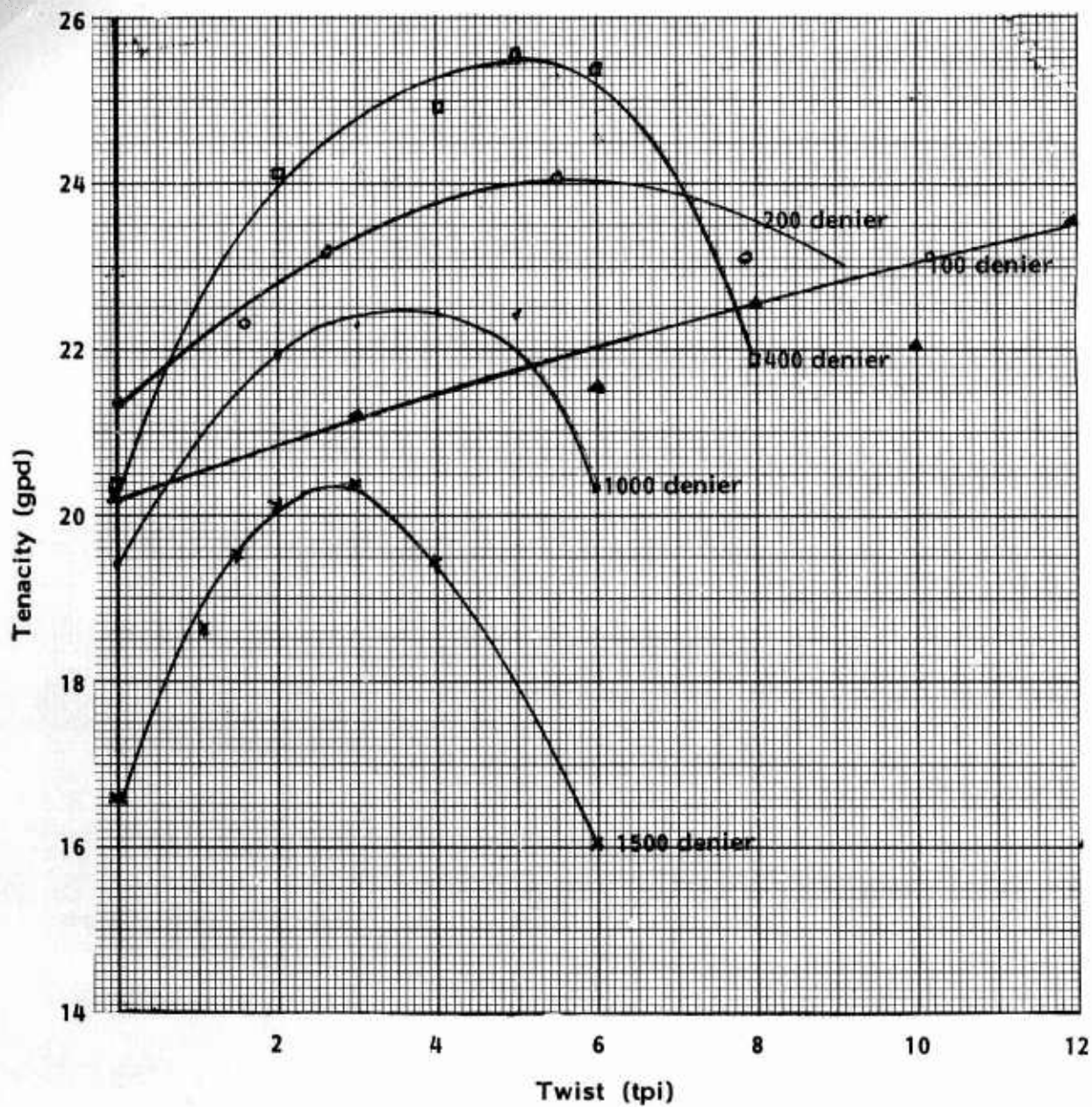
Figure 2. Effect of Twist on Tensile Strength of Kevlar 29 Yarn

3
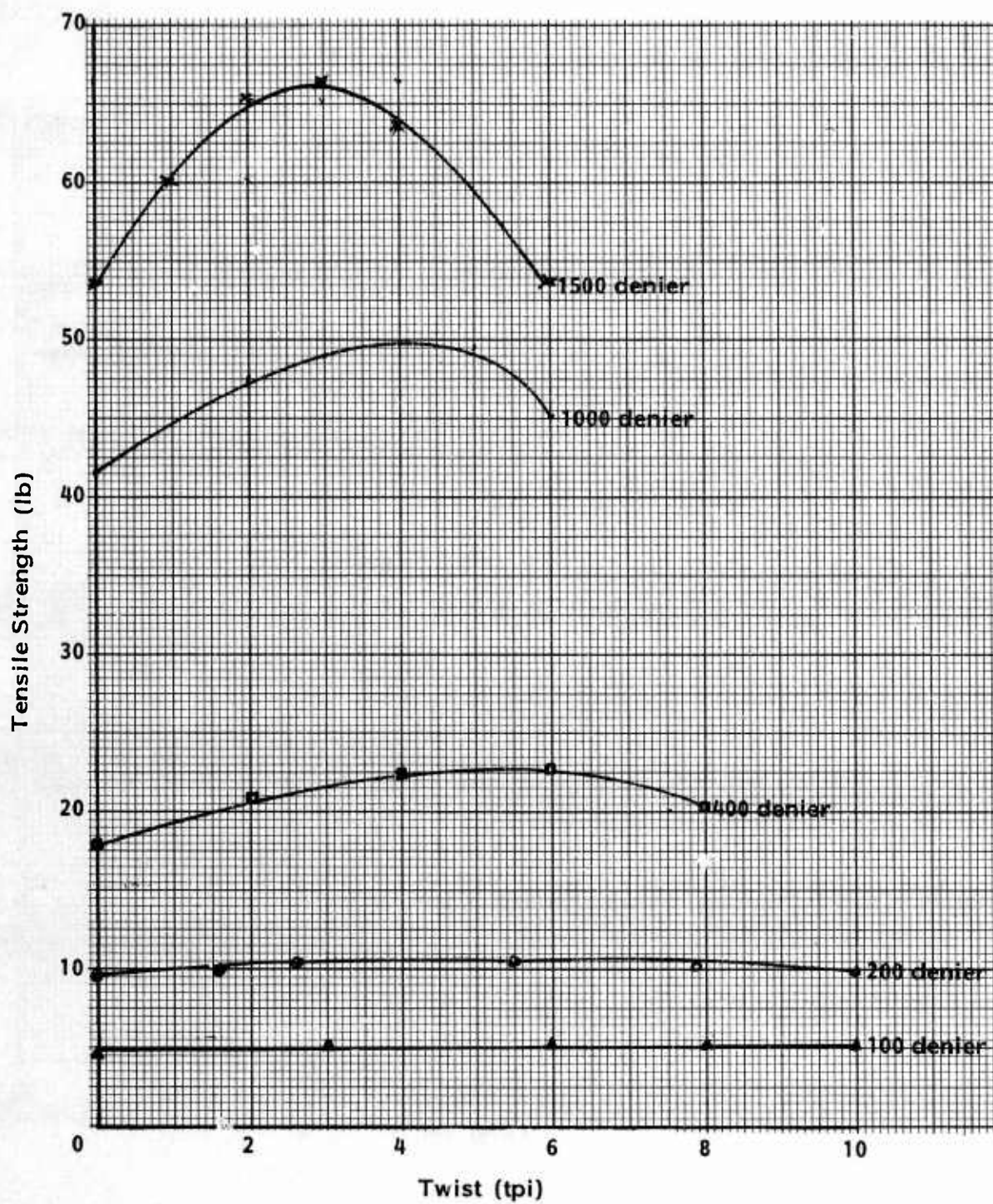
Figure 3. Effect of Twist on Tensile Strength of Kevlar 29 Yarns

4

Figure 2 is a plot of yarn tenacity versus actual turns of twist inserted into each of the five yarns. Optimum values are found to be 10 to 12 turns per inch in the 100 denier, 4 to 6 turns per inch for the 200 and 400 deniers, 3 to 5 for the 1000 denier and 2.5 to 3.5 for the 1500 denier.

Figure 3 shows how the absolute breaking strength of each yarn size varies with twist. Optimizing the twist raises the breaking strength of the 100 and 200 denier yarns approximately ten percent while the 400, 1000 and 1500 denier yarn strengths are raised by approximately twenty percent.

2.   Optimization of Ply Twist

Many of the planned Kevlar structures required the use of plied yarn in order to attain the desired ultimate tensile strength. A study was made, therefore, to determine the relation between twist and strength in plied yarns. The results are given in Tables 1, 2 and 3.

TABLE 1

OPTIMIZATION OF PLY TWIST
FOR 400 DENIER KEVLAR 29 YARN

Ply/Twist	Tenacity (gpd), Made with Zero Twist in Singles
2/1.79S	24.4
2/2.08S	24.7
2/2.5S	24.5
2/3.03S	24.0
3/1.79S	23.9
3/2.08S	24.0
3/2.5S	24.4
3/3.03S	24.3
4/1.79S	23.4
4/2.08S	23.7
4/2.5S	24.1
4/3.03S	23.2
5/1.79S	23.4
5/2.08S	23.9
5/2.5S	24.5
5/3.03S	23.5

TABLE 2

OPTIMIZATION OF PLY TWIST
FOR 1000 DENIER KEVLAR 29 YARN

| | Tenacity (gpd), | |
Ply/Twist	Made with Zero Twist in Singles	Made with 5Z tpi in Singles
2/1.0S	20.4	20.1
2/1.79S	20.7	20.7
2/2.08S	21.9	22.1
2/2.5S	21.7	22.0
2/3.03S	21.1	21.9
3/1.0S	20.4	21.1
3/1.79S	21.6	21.2
3/2.08S	21.6	21.2
3/2.5S	20.8	20.9
3/3.03S	20.0	21.1
4/1.0Z	22.6	----
4/1.79Z	22.6	----
4/2.08Z	22.6	----
6/1.0S	22.5	----
6/1.79S	21.7	----
6/2.08S	20.9	----
6/2.5S	19.5	----
6/3.03S	17.7	----
6/4.9S	13.2	----

TABLE 3

OPTIMIZATION OF PLY TWIST
FOR 1500 DENIER KEVLAR 29 YARN

| | Tenacity (gpd), | |
Ply/Twist	Made with Zero Twist in Singles	Made with 5Z tpi in Singles
2/1.0S	20.3	----
2/1.79S	20.9	----
2/2.08S	18.5	----
3/1.0S	17.7	17.2
3/1.79S	18.4	17.0
3/2.08S	18.4	16.8
4/1.0S	20.7	----
4/1.79S	18.8	----
4/2.08S	18.8	----
6/1.0S	20.7	----
6/1.79S	19.1	----
6/2.08S	18.6	----
3 x 2/1.79Z x 1.0S	19.9	----
3 x 2/1.79Z x 1.79S	19.5	----
8/1.0S	20.1	----
8/1.79S	16.9	----
8/2.08S	15.3	----

Two methods are possible for ply twisting. The first involves twisting the singles to its optimum value and then combining two or more of the yarns by inserting ply twist in the opposite direction. A second method is merely to combine two or more untwisted singles yarns by twisting them together at a relatively low level. Both methods have been evaluated selectively for both 1000 and 1500 denier Kevlar 29 yarns and there appears to be no significant difference between the two. The second method is preferable, therefore, since it involves only one twisting operation. More importantly, there does not appear to be any significant loss in strength between the singles and plied yarns. In general, the plied yarns made with the 400 denier singles have a breaking tenacity of 24 grams per denier, while the plied yarns made from the 1000 and 1500 denier yarn are ten to twenty percent weaker than this. This result indicates that wherever maximum emphasis is placed on strength to weight, 400 denier parent yarn should be used. If cost is more important than strength-to-weight ratio, however, allowance must be made for the fact that 400 denier yarn costs 50 to 100% more per pound than 1000 or 1500 denier yarn.

3. Yarn Twist Recommendations

Because twist has been found to have an unusually high influence on yarn strength, significant benefits will be derived from using the optimum twist for all load-bearing yarns. Accordingly, all of the narrow fabrics which were designed in this program used optimum twist yarns in the warp direction. The draft tentative Military Specifications which resulted from our work all contained the following table giving optimum levels of warp yarn twist (see Table 4).

TABLE 4

WARP YARN TWIST

Singles Yarn Denier	Ply	Ply Twist (turns/inch)
200	1	6.0
	3	4.0
400	1	5.0
	2	2.5
	3	2.5
	4	2.5
1000	1	4.0
	2	2.1
	3	1.8
	4	1.6
	5	1.4
	6	1.0
1500	1	3.0
	2	1.8
	3	1.6
	4	1.2
	5	1.0
	6	1.0
	8	0.8

Note: In all cases the singles yarn contains producer's twist.

These draft specifications also give some guidance to handling the yarn through twisting and winding operations to minimize damage, as follows:

(a)   Twisting precautions

(i)   Feed roll speed should be as follows for various Kevlar yarns and twist levels:

Yarn Denier	Twist (tpi)	Feed roll speed (yards per min)
200	5.0	70
400	4.0	90
1000	4.0	60
1500 & greater	1.8	20

(ii)   Slightly heavier travelers than those used for nylon yarn should be used.

(iii)   High humidity should be maintained to minimize electrostatic charge between filaments.

(b)   Winding Precautions - "Anti-wear" wide tension gates (Leesona Corporation), or their equivalent, should be used.

Warp Preparation

Kevlar yarns containing the recommended amount of twist can be woven into narrow fabrics without the addition of size. Thus, yarns may be drawn from the creel and wound directly on a warp beam. Because of Kevlar's low elongation, more than the usual degree of care is required to keep the tension uniform across the warp. Good dead-weight disc type tensioners can be used on the creel, provided the band of yarn is not allowed to relax until it is wound on the beam. All surfaces which the yarn contacts must be rounded or flat, and as smooth as possible to minimize snagging. The beam on which the warp yarns are wound must not be more than one half inch wider than the finished width of the woven fabric, or uneven edge yarn tensions will result.

Weaving

In the loom, the warp yarns contact many surfaces from the warp beam to take-up roll. Some of these are stationary, and some, such as the heddles and the reeds, move. All stationary surfaces must be smooth and contain no sharp edges. Take-up rolls should be covered with the smoothest surface which can be tolerated. An experiment was conducted to determine the effect of some variables in the heddle and reed surfaces on yarn strength.

As a means of determining the extent of damage incurred by the Kevlar yarn during the weaving process, an experiment was conducted whereby sec-

9

tions of warp yarns were withdrawn at various stages. The action of three types of reeds and heedles was studied:

1. Stainless steel reed and heddles.

2. Stainless steel reed and Teflon coated heddles.

3. Teflon coated reed and heddles.

Approximately thirty out of forty warp yarns in a given section were tested, 10 from the area near each edge and 10 from the middle of the warp. The tensile data obtained are shown in Table 5.

TABLE 5

EFFECT OF VARIOUS WEAVING OPERATIONS ON
STRENGTH OF 1000 DENIER KEVLAR 29 YARNS

| | | Tensile Strength Loss (%) | | |
		Left Edge	Middle	Right Edge
a.	After warping	0	0	0
b.	After Teflon heddles	0	− 2	+ 1
c.	After (b) and regular reed	− 6	− 5	− 6
d.	After (c) + shuttle moving	− 9	− 7	− 7
e.	After regular heddles	− 4	− 4	− 7
f.	After (e) + regular reed	−12	−13	−16
g.	After (f) + shuttle moving	−25	−15	−18
h.	After Teflon heddles, Teflon reed + shuttle moving	−21	−16	−12

It is apparent that the use of Teflon coated heddles reduces yarn damage significantly, but the Teflon coated reed damaged the yarn. The reason for damage in the reed was found to be due to the abrasion of the yarn against the reed wires which roughened the Teflon surface to the point where yarn damage occurred. We concluded from this study that all of our weaving would be done with Teflon coated heddles and a regular, rust-free reed. This recommendation is also included in the draft specifications.

Included in the draft specifications are also guidelines for adjusting the loom, based on our experience in weaving Kevlar. These are:

1. Harness times should be 2" before front center for 1/2" wide ribbon when using 400 denier yarn and 3/4" before front center for 1" and wider ribbons.

10

2. Warp line should be level.

3. Loom(s) selected for weaving Kevlar 29 yarns must be in good running condition with minimum wear or "play" in various mechanical components. Loom should be operated at reduced speed (90 to 100 picks per minute) when weaving 200 or 400 denier yarn into narrow ribbon.

4. Due to the low extensibility of Kevlar 29 yarn it is important that uniform yarn length be maintained at all times across the entire set of warp yarns.

5. High humidity should be maintained during weaving.

III. STRENGTH TRANSLATION EFFICIENCY

The success with which fiber strength is translated into the strength of the structure is usually indicated by a quantity known as the strength translation efficiency. This is the ratio of structure strength to the accumulated strengths of the components making up the structure, and is commonly expressed as a percentage. The value of this percentage will depend, of course, upon the base from which it is calculated, that is, the component whose strength is taken to represent the ultimate achievable.

This is illustrated in the example given in Table 6, in which three different reference bases have been used.

(a) the strength of the individual fibers,

(b) the strength of the yarn as received from the manufacturer, containing producer's twist (nominally zero),

(c) the strength of the twisted yarn used in the load-bearing direction of the structure in question.

The effect of these bases on the value of the strength translation efficiency is apparent in the last column of the table.

11

TABLE 6

STRENGTH TRANSLATION EFFICIENCY

Kevlar webbing, 1-3/4", 2500 lb nominal
2620 lb actual

Warp:	1000 denier, 4 tpi, 71 total ends
Filling:	1000 denier, 0 tpi, 22 picks per inch
Fiber:	1-1/2 denier

A 1000 denier yarn contains 666 fibers in its cross section.

Basis of Reference	Tenacity (gpd)	Unit Strength (lb)	Estimated Webbing Strength (lb)	Strength Translation Efficiency (%)
Kevlar 29 fiber	26.9	0.089	4210	62
0 tpi yarn	17.8	39.2	2780	94
4 tpi yarn	22.5	49.6	3520	74

The choice of the base to be used in calculating strength translation efficiency is an arbitrary one, but it is clear that if comparisons between structures are to be meaningful, the same base must always be used. In all of our work we have chosen the strength of the twisted load-bearing yarns as the reference in calculating strength translation efficiency. We believe that this represents best the influence of the weaving operation and the weave design on the strength of the structure. Efficiencies as low as 40 to 50% were encountered in our early attempts to design and weave efficient Kevlar structures, but during the course of the work we learned to obtain efficiencies in the range of 70 to 90%, relative to the strength of the twisted yarn used in the warp, with reasonable consistency. It has never been completely clear, however, how efficient structures can be designed with confidence. Minimum damage to the yarns during warp preparation in the loom is, of course, necessary and, as already described, we learned how to handle the yarns through these operations so as to virtually eliminate such damage. The construction of the fabric, however, has proven to be critical, particularly with respect to the number of picks per inch used. Often the addition of only one pick per inch will cause the strength to drop 10% or more.

The availability of some 50 samples of woven Kevlar webbings, tapes and ribbons afforded us an opportunity to learn more about the influences of changes in structural geometry on strength translation efficiency. Some preliminary cross sections indicated that there were significant differences in warp crimp level between fabrics, and suggested that this might be an important parameter. It seemed likely, however, that differences in warp crimp should be considered in relation to the denier of warp and filling yarns. The same absolute level of crimp in a 400 denier warp yarn, for example, might not have the same influence on strength translation efficiency as it would have in 1500 denier warp yarn.

12

Out of the samples currently available, eight comparisons were selected in each of which warp and filling yarn deniers were kept constant. Warp yarn crimp was determined for each of these materials by marking a 10" length on the fabric, and then removing 5 warp yarns, straightening them by application of a low tension, and measuring the distance between the gauge marks on the straightened yarn. The crimp is then expressed as

$$\text{crimp} = \frac{\ell_s - \ell_f}{\ell_f} \times 100\%$$

where

ℓ_s is the straightened distance between the gauge marks,

ℓ_f is the distance between gauge marks in the fabric = 10".

In Table 7, the entries are grouped by paired or three-way comparisons, and pertinent data given for each of the materials studied. In each case, the variability between the five individual measurements was relatively small, the maximum standard error being only 0.3%.

A plot of all the data is given in Figure 4 which makes it clear that a general trend exists in which decreases in warp crimp lead to increases in strength translation efficiency. There is, however, a significant scatter outside the area delineated by the remainder of the data. An examination of the selected comparisons in Table 7 shows clear evidence of the consistent trend existing between changes in warp crimp and changes in strength translation efficiency for the paired comparisons, except for two instances. Samples 5034-19 and -75, for example, apparently show an inverse trend. However, neither the translation efficiencies or warp crimps are significantly different from one another. The other case, which is the comparison between 5034-34 and -63, shows a significant difference in efficiency, but no difference in crimp. It is possible that additional measurements would clarify this apparent inconsistency.

Additional analysis of this relationship would be interesting, particularly to attempt to determine why apparently small changes in warp crimp can have a significant effect on strength translation efficiency. This was not done in the present program, however, for even the relatively small amount of data already obtained makes it clear that, in Kevlar woven narrow fabric structures, warp crimp should be kept at the lowest acceptable level to ensure that optimum strength translation efficiencies are achieved.

Structural Influences

The procedure used in the laboratory to develop efficient Kevlar structures was to set up a short (10-yard) warp containing the number of yarns of a suitable denier which would be needed to provide the desired strength, using 70% strength translation efficiency as the estimate of what should be achieved.

13
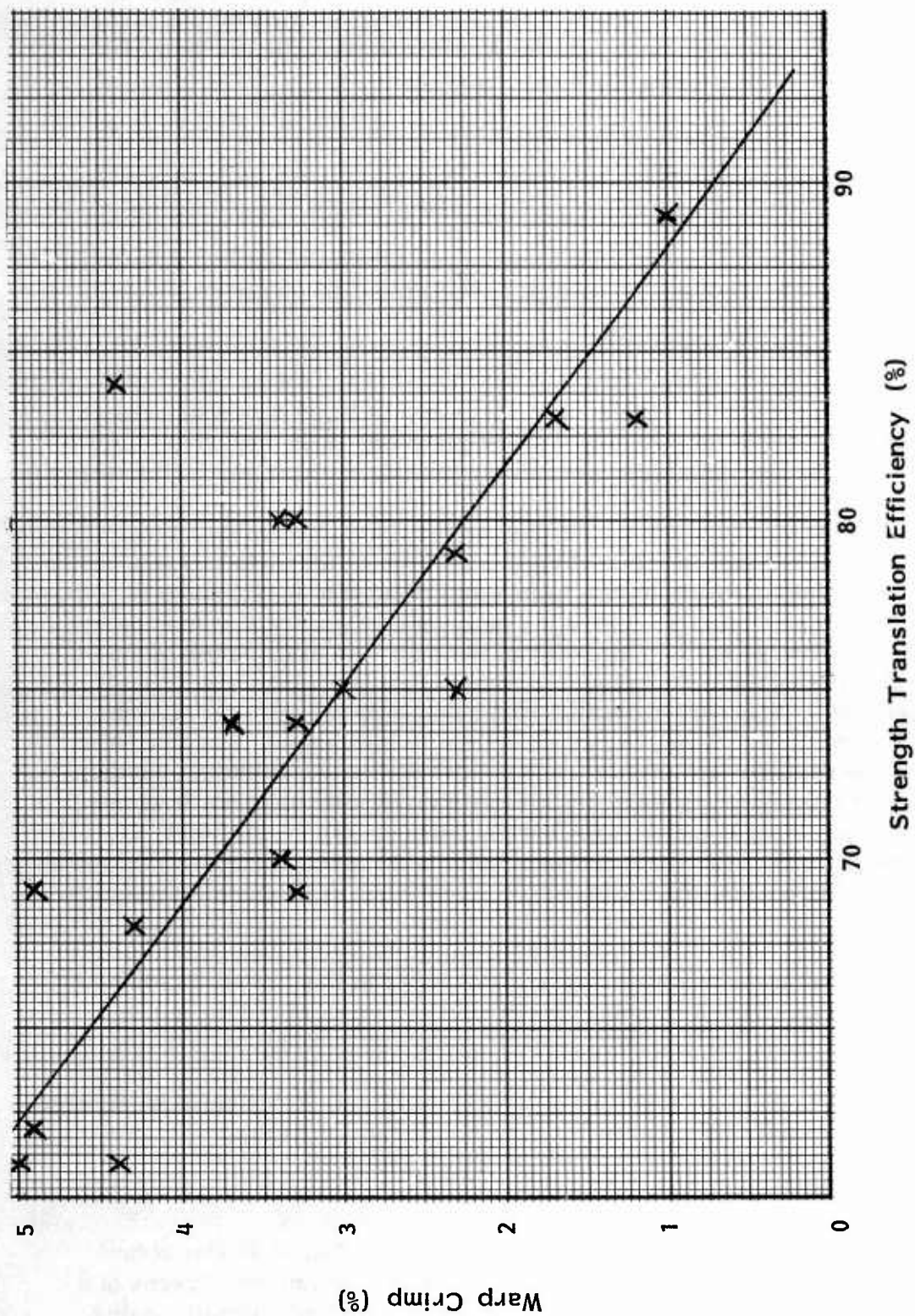
Figure 4. Influence of Warp Crimp on Strength Translation Efficiency

14

TABLE 7

WARP CRIMP MEASUREMENTS

FRL Sample No. 5034-	Yarn Denier Warp	Fill	Width (inch)	Ends Total No.	per Inch	Picks per Inch	Strength (lb)	Effi-ciency (%)	Warp Crimp (%)
42	400	400	1/2	39	78	23	590	69	3.3
55	400	400	1-3/4	104	59	24	1390	62	4.9
56	400	1000	2	148	74	22	2030	61	4.4
76	1000	1000	2	76	38	19	2300	61	5.0
90	1000	1000	1/2	39	78	20	1550	80	3.4
38	1000	1000	9/16T*	45	80	17	1820	83	1.7
64	1000	1000	9/16T*	43	76	17	1600	75	2.3
19	1000	1000	1-3/4	71	41	22	2620	74	3.7
75	1000	1000	1-3/4	84	48	16	2620	70	3.4
36	1500	1000	5/8T*	39	31	14	2180	83	1.2
37	1500	1500	3/4T*	59	39	14	3020	79	2.3
35	1500	1500	1T*	81	40	14	3950	75	3.0
34	1500/2	1000	1	47	47	11	4900	74	3.3
63	1500/2	1000	1	39	39	12	4780	80	3.3
65	1500/2	1500	3/4	31	41	12	3200	84	4.4
74	1500/2	1500	1-3/4	50	67	17	4850	69	4.9
61	1500/3	1500	1-3/4	137	78	9	22700	89	1.0
62	1500/3	1500	1-3/4	121	69	12	20400	68	4.3

*Tubular weave.

Various filling yarns, at various levels of picks per inch were then woven into this warp and it was found that the strength of the woven material is very critically dependent upon the picks per inch. Maximum strength is achieved with a structure woven so loosely as to be unusable. As the picks per inch are increased, a critical degree of packing is reached where the strength falls rapidly with each additional pick per inch. Unfortunately, the critical packing giving maximum strength is usually still too loose to be usable, so in most cases a compromise must be reached between tightness of weave and strength, neither one being at the optimum level.

Some results indicating this behavior are given in Table 8, which indicates that a change of as little as one or two picks per inch can alter the strength by as much as 25%.

TABLE 8

EFFECT OF PICKS PER INCH ON BREAKING STRENGTH
IN PLAIN WOVEN STRUCTURES

Width (inch)	Warp Yarn Denier	Total Ends	Filling Yarn Denier	Picks per Inch	Strength (lb)
2	200	72	200	58	430
				56	525
1	400	96	400	34	910
				32	1050
				30	1110
1-3/4	1500	140	1500	16	4800
				14	6075
				12	6715
1-3/4	1500/2	52	1500	17	4900
				15	5400
				13	5650
1	1500/3	76	1500	9	8600
				8	10800

During this experimentation the effect of weave was also studied, for twill or satin weaves which have relatively few warp/filling intersections per unit of area might be expected to show better strength translation efficiency than a plain weave, which has the maximum number of intersections per unit area.

It was found that, because of the need to reduce picks per inch as much as possible to maintain a reasonable strength translation efficiency, a more stable structure could be made using a plain weave rather than the more usual herringbone twill. Experiments with various weaves indicated that the best compromise between strength translation efficiency and firmness of structure could be obtained with the plain weave. This was adopted, therefore, for all narrow fabric designs except for those in which the strength/width relationship imposed very dense warp yarn packing, when a herringbone twill or a double-layer weave was used.

IV. DESIGN CONSIDERATIONS

The critical characteristics which dictate the design of webbings, ribbons and tapes used in parachute applications are width and strength. The strength of a narrow fabric is determined by the sum of the strengths of the lengthwise yarns used in its manufacture, modified by the strength translation efficiency of the structure, as discussed previously. These lengthwise yarns must be constrained by the weaving operation to lie within the desired width. Depending upon their size and number in relation to this width, the resultant packing may be loose, tight or even stacked into two, three or four levels.

16

Kevlar yarns are available only in 200, 400, 1000 and 1500 denier.*
Within these constraints, and assuming a 70% strength translation efficiency,
it is clear that any desired strength, for example 5000 lb, can be obtained in
the way shown in Table 9.

TABLE 9

YARN CHOICES FOR A STRUCTURAL STRENGTH OF 2500 POUNDS

Yarn Denier	Twisted Yarn Strength (lb)	Effective Yarn Strength (Strength x 0.7 lb)	Number Required for 5000 lb (n)	Twisted Yarn Diameter (inch)	Width of a Contiguous Array of n Yarns (inch)
200	10.7	7.5	333	0.0063	2.1
400	22.4	15	167	0.0119	2.0
1000	49.6	35	71	0.0169	1.2
1500	66.5	46	54	0.0264	1.4

The numbers in the right hand column of the table show clearly the degree
of lateral packing which must occur in relation to the yarn denier chosen, when
a width requirement is added to the strength requirement. For example, a 2",
2500 lb ribbon made from 1000 or 1500 denier yarns would be too open to be
usable. On the other hand, a 1", 2500 lb webbing might be made from 200 or
400 denier warp yarns, though this would involve tight lateral packing so that
either the cross section of the yarns would have to be distorted or a degree of
stacking into a second longitudinal layer of warp yarns would have to take place.
These changes from a simple structure would result in a tighter, firmer struc-
ture, but their effect on strength translation efficiency could only be determined
by a weaving trial. In fact, many of the structures selected for the draft speci-
fications involved this kind of tight warp packing without unacceptably low
strength translation efficiencies.

In addition to the structural factors discussed above, another consideration
entered into our choice of yarn denier for any given structure. The current price
of Kevlar yarns varies with the denier in the following manner**: 200 denier, $21.50/
lb; 400 denier, $14.50/lb; 1000 denier, $9.50/lb; 1500 denier, $7.50/lb. In all
of our work, we adopted the attitude that when a choice was to be made between
two yarn deniers for a structure, preference was given to the higher denier
because it was cheaper. Clearly, this does not necessarily result in structures
of optimum firmness of packing, and in a few cases, particularly in the ribbons,
it is probable that additional use requirements not considered in the work de-
scribed herein should be introduced, which could alter the recommended con-
struction to one which might be heavier and more expensive but, at the same
time, perform better in service.

---

*For this program a small amount of experimental 100 denier yarn was
available.

**Prices as of June, 1976.

A plot of the actual structures made in the work being described herein is shown in Figure 5. The two curved lines represent the envelopes of acceptable fabric strengths achievable for the various yarn deniers. It is clear from the shape of these curves that at the higher strengths, less choice of warp yarn denier is available than at the lower strengths, where acceptable structures can be made from two or even three different warp yarn deniers. These structures will differ, of course, in other characteristics such as thickness, tightness of weave, deformability and air permeability. The choice between available warp yarn deniers will have to be made, therefore, on the basis of the importance of these other characteristics.

V.   WOVEN NARROW FABRIC DESIGNS

The designs which were considered to be the best compromise between strength translation efficiency and structural firmness are given in Tables 10 through 13 for ribbons, tapes, webbings and tubular webbings. Stress-strain curves for each of these structures are given in Figures 6 through 34.

Ratios of the weights of these materials to their nylon counterparts which have the same strength and width average 0.36, with a low of 0.26 and a high of 0.46. In general, the ribbons and tubular webbings are somewhat heavier in relation to their nylon counterparts (weight ratio 0.40) than are the tapes and webbings (0.34). Limited experience with the ribbons in parachute drop tests indicate that the structures designed as indicated in Table 10 are in some cases too openly woven to provide adequate joint strength, and in some cases to retain their structural integrity during deployment. These structures may have to be woven tighter, with a corresponding slight weight increase, in order to perform well in service. Experience with the tapes and webbings has indicated that they appear to perform well.

VI.   BROAD WOVEN FABRIC DESIGNS

The most important characteristics of broad woven fabrics for most parachute applications are strength and air permeability. These are the characteristics which determined the design of the fabrics which were made from Kevlar.

An unexpected problem arose in the early experimental work. Because of the fact that the cross section of Kevlar yarns is shaped like a flat ribbon, permeabilities were very low at normal weaving densities. Thus, it became easy to design a low porosity pack fabric, but much more difficult to obtain the degree of openness needed in a canopy fabric without excessive sleaziness. Indeed, the pack fabrics which were designed tended to be somewhat sleazier than their nylon counterparts because they did not need to be woven as tightly. Thus, a new set of compromises is needed in designing Kevlar broad woven fabrics, which were not worked out in a completely satisfactory way within the scope of the contract under which this work was carried out. As a result, no draft tentative military specifications for pack or canopy fabrics were written. The following outlines some of the approaches which were taken in a study of the influence of some design variables.

18
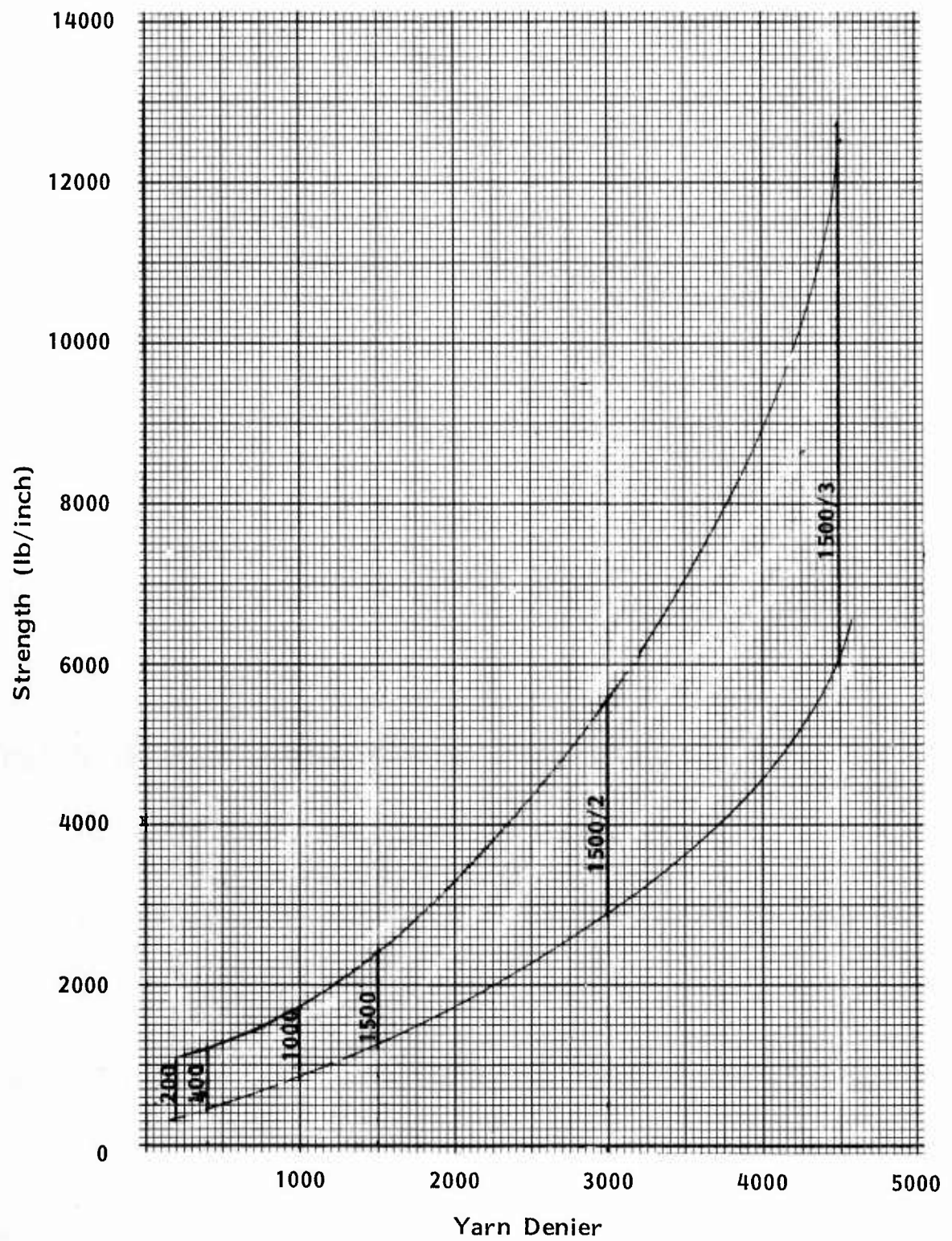
Figure 5. Yarn Deniers Needed for Various Fabric Strengths

TABLE 10

CONSTRUCTION AND CHARACTERISTICS OF KEVLAR RIBBONS

Draft Spec Type No.	FRL Sample No. 5034-	Width (inch)	Strength Mean (lb)	Strength Range Low	Strength Range High	Translation Efficiency (%)	Elong (%)	Weight oz/yd	Weight yd/lb	Thickness (inch)	Weave	Warp den/ply/twist[1]	Warp total ends	Filling den/ply/twist[1]	Filling picks /inch
IX	--	2	485	450	520	57	--[3]	--[3]	--[3]	--[3]	plain	200/1/6.0	80	200/1/0	46
X	82	2	1455	1430	1520	70	--[3]	--[3]	--[3]	--[3]	plain	1000/1/4.0	42	1000/1/0	35
XII	76	2	2300	2060	2440	61	4.4	0.43	37.3	0.017	plain	1000/1/4.0	76	1000/1/0	19
XIII	20	2	3650	3300	3780	77	4.1	0.49	33.0	0.020	plain	1000/1/4.0	96	1000/1/0	16
XIV	73	2	4530	4030	4825	99	5.2	0.68	23.5	0.026	plain	1500/1/1.8	92	1500/1/0	15
XV	95	2	6220	5950	6620	74	4.2	0.83	19.2	0.032	plain	1500/2/1.8	60	1500/1/0	12
XVI	94	2	9290	9050	9450	78	3.9	1.29	12.4	0.045	2x2 HBT[2]	1500/3/1.8	64	1500/1/0	17

1. When a plied yarn is used, this is the value of the ply twist. Singles twist is always zero, or producer's twist.

2. 2 x 2 herringbone twill, center reversal.

3. Not determined.

20

TABLE 11

CONSTRUCTION AND CHARACTERISTICS OF KEVLAR TAPES

Draft Spec Type No.	FRL Sample No. 5034-	Width (inch)	Strength Mean (lb)	Strength Range Low	Strength Range High	Translation Efficiency (%)	Elong (%)	Weight oz/yd	Weight yd/lb	Thickness (inch)	Weave	Warp den/ply/twist[1]	Warp total ends	Filling den/ply/twist[1]	Filling picks /inch
I	89	1/2	310	287	318	69	2.2	0.049	328	0.009	plain	200/1/6.0	42	200/1/0	40
II	115	3/4	560	510	620	58	--2	0.094	171	0.009	plain	200/1/6.0	90	200/1/0	38
III	110	1	565	--2	--2	59	--2	0.11	147	0.008	plain	200/1/6.0	90	200/1/0	50
IV	113	9/16	760	755	765	58	4.2	0.12	136	0.015	plain	400/1/5.0	58	400/1/0	32
V	107	1	1120	1040	1190	49	4.2	0.20	78	0.015	plain	400/1/5.0	102	400/1/0	31
VI	112	1-1/8	1580	--2	--2	73	--2	0.21	76	0.015	plain	400/1/5.0	96	400/1/0	34
VII	106	1-1/2	1700	1690	1710	70	3.3	0.24	66	0.012	plain	200/1/6.0	228	400/1/0	29

1.. When a plied yarn is used, this is the value of the ply twist. Singles twist is always zero, or producer's twist.

2. Not determined.

21

TABLE 12

CONSTRUCTION AND CHARACTERISTICS OF KEVLAR WEBBINGS

Draft Spec Type No.	FRL Sample No. 5034-	Width (inch)	Strength Mean (lb)	Strength Range Low	Strength Range High	Translation Efficiency (%)	Elong (%)	Weight oz/yd	Weight yd/lb	Thickness (inch)	Weave	Warp den/ply/twist[1]	Warp total ends	Filling den/ply/twist[1]	Filling picks /inch
I	42	1/2	.590	562	622	68	2.8	0.075	210.0	0.012	plain	400/1/5.0	39	400/1/0	22
II	65	3/4	3210	3140	3275	84	3.8	0.40	40.0	0.040	plain	1500/2/1.8	31	1500/1/0	12
III	66	3/4	4930	4800	5000	85	--[3]	0.52	31.0	0.044	plain	1500/2/1.8	41	1500/1/0	11
IV	81	1	2610	2475	2750	77	3.5	0.34	46.5	0.024	plain	1500/2/1.8	24	1500/1/0	14
V	63	1	4380	4300	4550	80	4.3	0.48	33.6	0.037	plain	1500/2/1.8	39	1000/1/0	12
VI	32	1	6780	6390	7000	75	4.1	0.90	17.7	0.065	plain	1500/3/1.8	49	1500/1/0	12
VII	93	1	10260	10100	10500	73	4.3	1.37	11.7	0.094	2x2 HBT[2]	1500/3/1.8	76	1500/1/0	8
VIII	119	1	13600	13200	14200	84	--[3]	1.48	10.8	0.105	plain	1500/3/1.8	89	1500/1/0	9
IX	117	1-1/4	870	746	890	65	4.8	0.21	75.0	0.013	plain	400/1/5.0	60	1000/1/0	26
X	55	1-3/4	1400	1310	1595	61	4.2	0.31	52.0	0.014	plain	400/1/5.0	103	1000/1/0	23
XI	75	1-3/4	2910	2660	3030	70	4.8	0.42	37.7	0.019	plain	1000/1/4.0	84	1000/1/0	16
XII	16	1-3/4	4370	4200	4480	80	3.8	0.50	31.9	0.021	plain	1000/2/2.1	55	1000/1/0	15
XIII	74	1-3/4	4850	4730	5120	69	5.1	0.74	21.7	0.030	plain	1500/2/1.8	50	1500/1/0	17
XIV	15	1-3/4	7100	6900	7200	76	5.6	0.90	17.7	0.034	plain	1500/1/3.0	140	1500/1/0	11
XV	31	1-3/4	9000	8920	9180	73	5.9	1.09	14.7	0.043	plain	1500/2/1.8	88	1000/1/0	10
XVI	108	1-3/4	11800	--[3]	--[3]	66	--[3]	1.60	10.0	0.064	2x2 HBT[2]	1500/2/1.8	127	1500/1/0	12
XVII	62	1-3/4	18000	16500	19500	85	--[3]	2.16	7.4	0.079	double plain	1500/3/1.8	121	1500/1/0	12
XVIII	61	1-3/4	22600	21950	23360	89	3.3	2.36	6.8	0.092	double plain	1500/3/1.8	137	1500/1/0	9
XIX	116	3	--[3]	--[3]	--[3]	--[3]	--[3]	0.59	26.9	0.016	plain	400/1/5.0	200	1000/1/0	24

1. When a plied yarn is used, this is the value of the ply twist. Singles twist is always zero, or producer's twist.

2. 2 x 2 herringbone twill, center reversal.

3. Not determined.

TABLE 13

CONSTRUCTION AND CHARACTERISTICS OF KEVLAR TUBULAR WEBBINGS

Draft Spec Type No.	FRL Sample No. 5034-	Width (inch)	Strength Mean (lb)	Strength Range Low	Strength Range High	Translation Efficiency (%)	Elong (%)	Weight oz/yd	Weight yd/lb	Thickness (inch)	Weave	Warp den/ply/twist[1]	Warp total ends	Filling den/ply/twist[1]	Filling picks /inch
I	90	1/2	1505	1475	1520	78	3.6	0.25	71.0	0.034	plain	1000/1/4.0	39	1000/1/0	40
II	64	9/16	1600	1530	1650	72	3.6	0.23	70.4	0.032	plain	1000/1/4.0	45	1000/1/0	34
III	36	9/16	2180	2050	2320	80	2.9	0.29	55.8	0.038	plain	1500/1/1.8	41	1000/1/0	27
IV	37	3/4	3020	2850	3100	77	3.3	0.44	36.4	0.045	plain	1500/1/1.8	59	1500/1/0	27
V	35	1	3950	3800	4030	73	4.0	0.62	26.0	0.046	plain	1500/1/1.8	81	1500/1/0	27

1. When a plied yarn is used, this is the value of the ply twist. Singles twist is always zero, or producer's twist.

23

Figure 6. Average Load-Elongation Diagram for 2-Inch Wide Kevlar 29 Ribbon, Type XII (FRL Sample No. 5034-76)
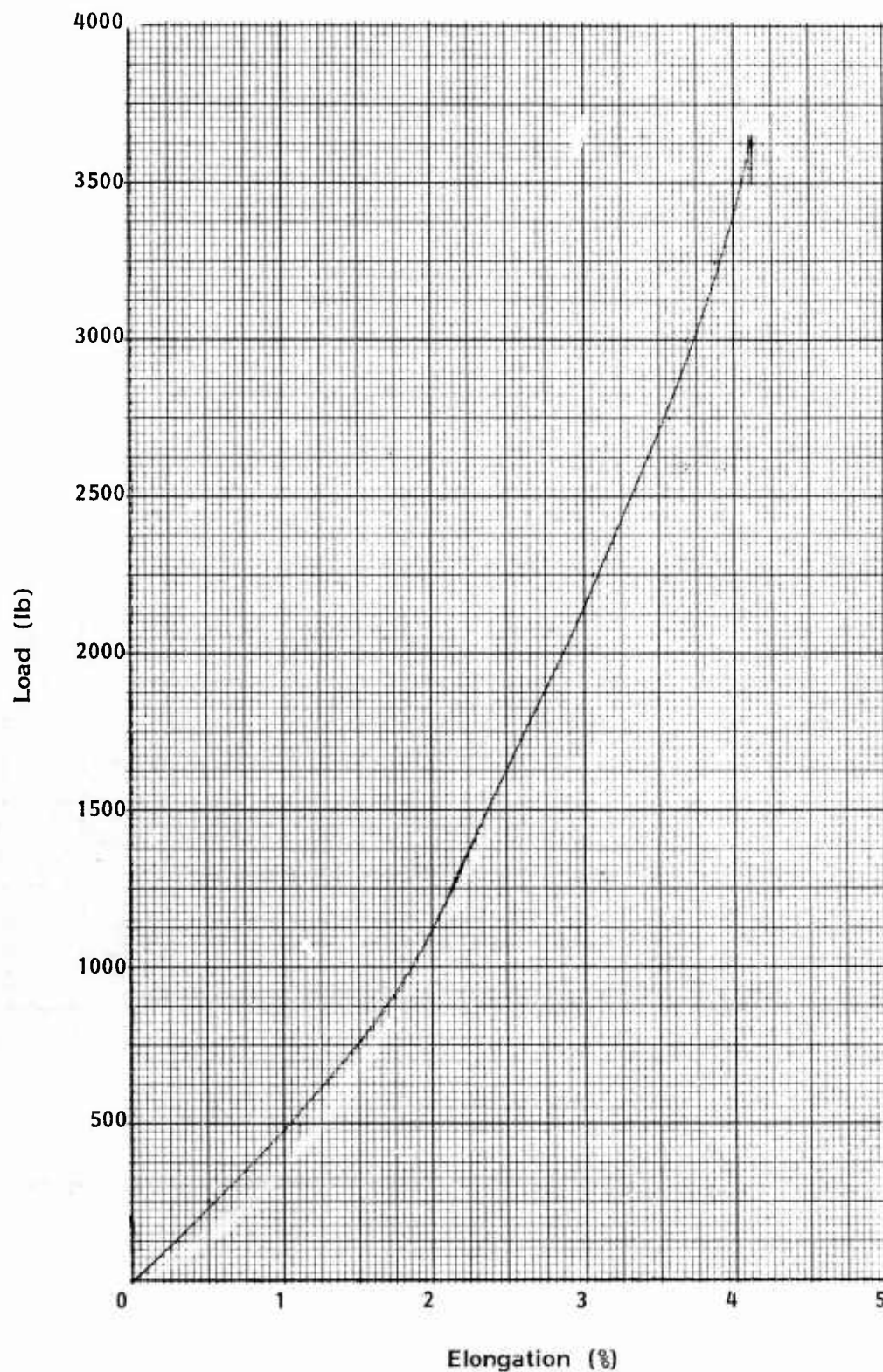
Figure 7. Average Load-Elongation Curve for 2-Inch Wide Kevlar 29 Ribbon, Type XIII (FRL Sample No. 5034-20)

Figure 8. Average Load-Elongation Diagram for 2-Inch Wide Kevlar 29
Ribbon, Type XIV (FRL Sample No. 5034-73)

26
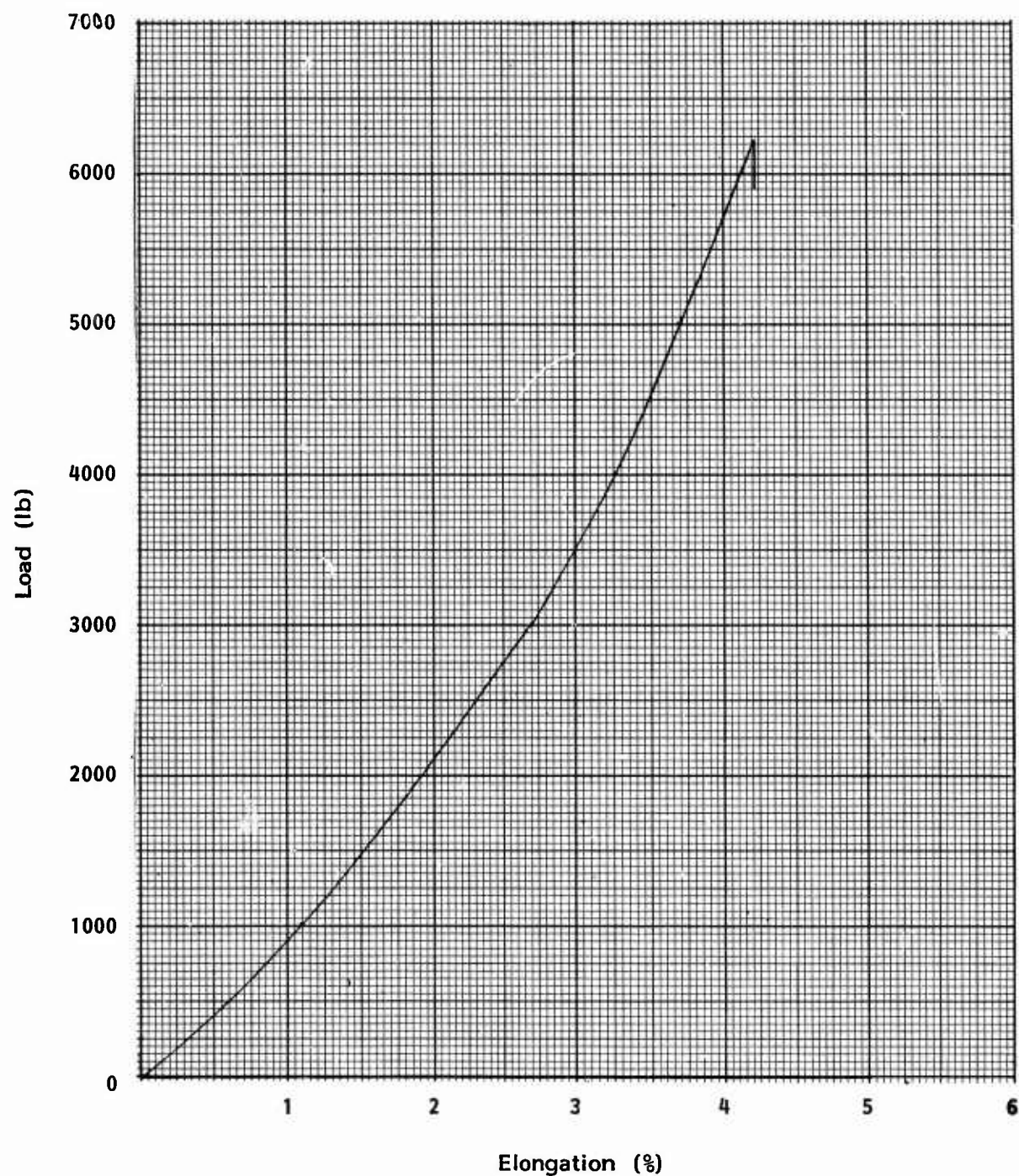
Figure 9. Average Load-Elongation Curve for 2-Inch Wide Kevlar 29 Ribbon, Type XV (FRL Sample No. 5034-95)
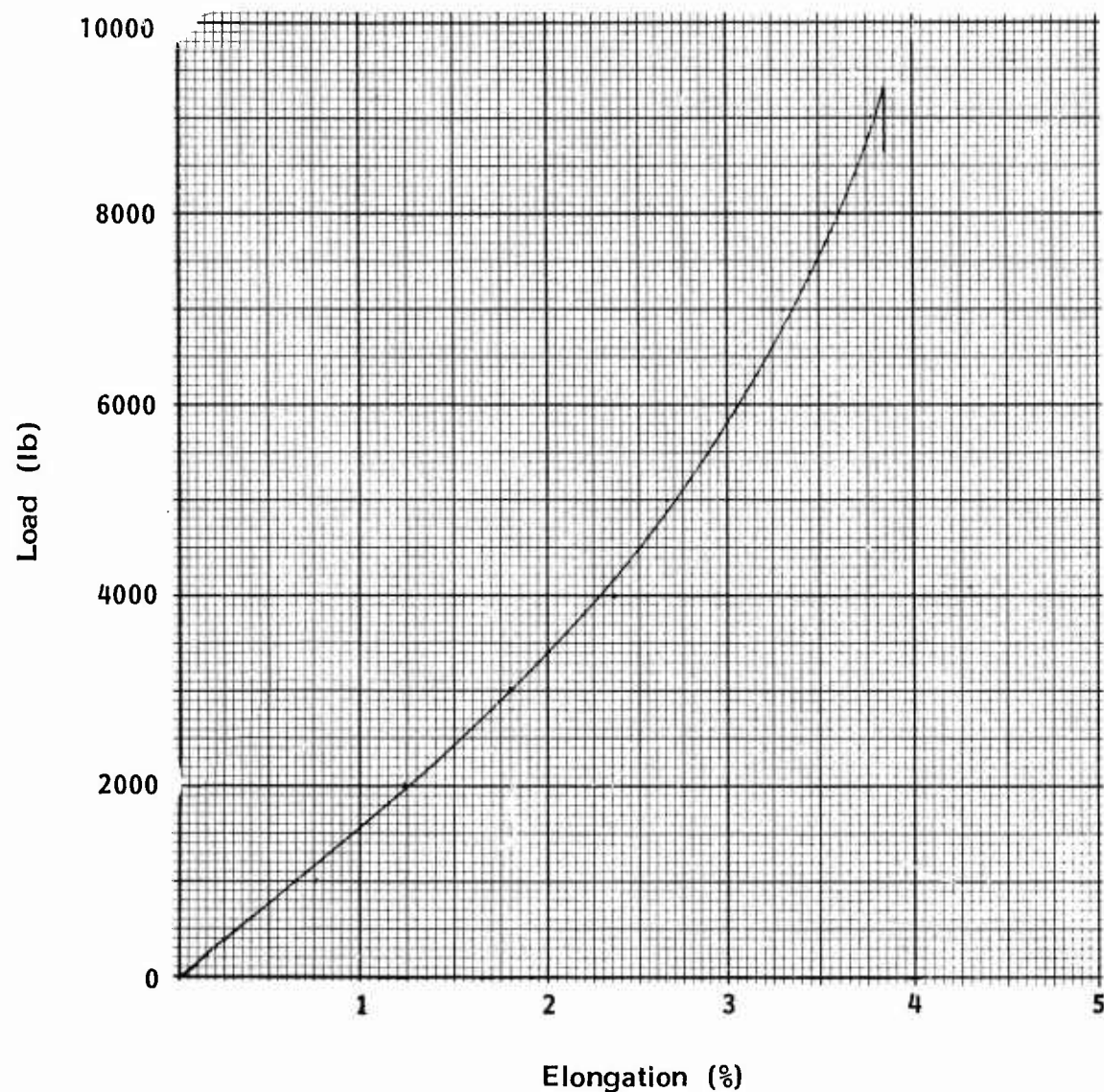
Figure 10. Average Load-Elongation Curve for 2-Inch Wide Kevlar 29 Ribbon, Type XVI (FRL Sample No. 5034-94)
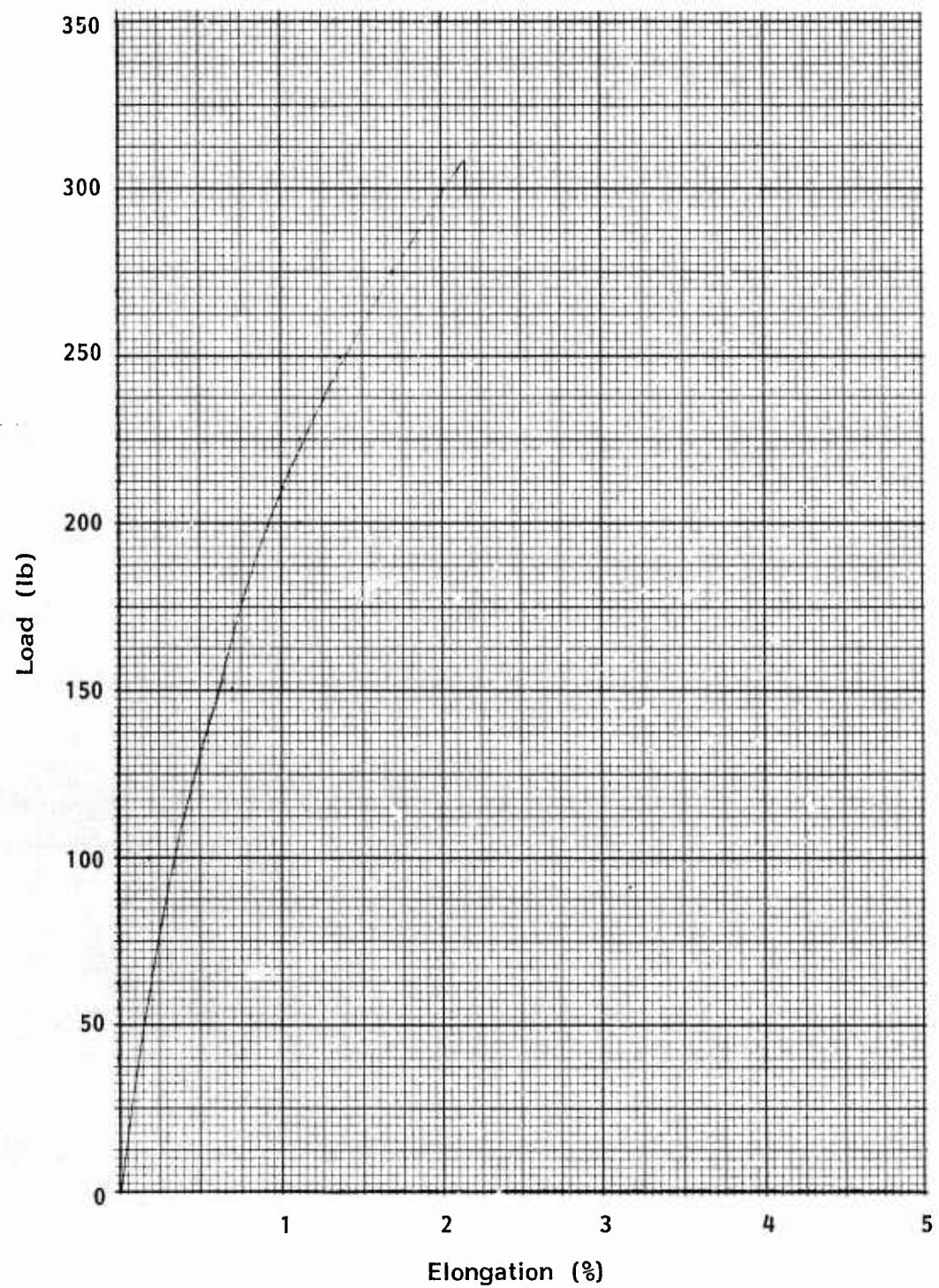
Figure 11. Average Load-Elongation Curve for 1/2-Inch Wide Kevlar 29 Tape, Type I (FRL Sample No. 5034-89)

29
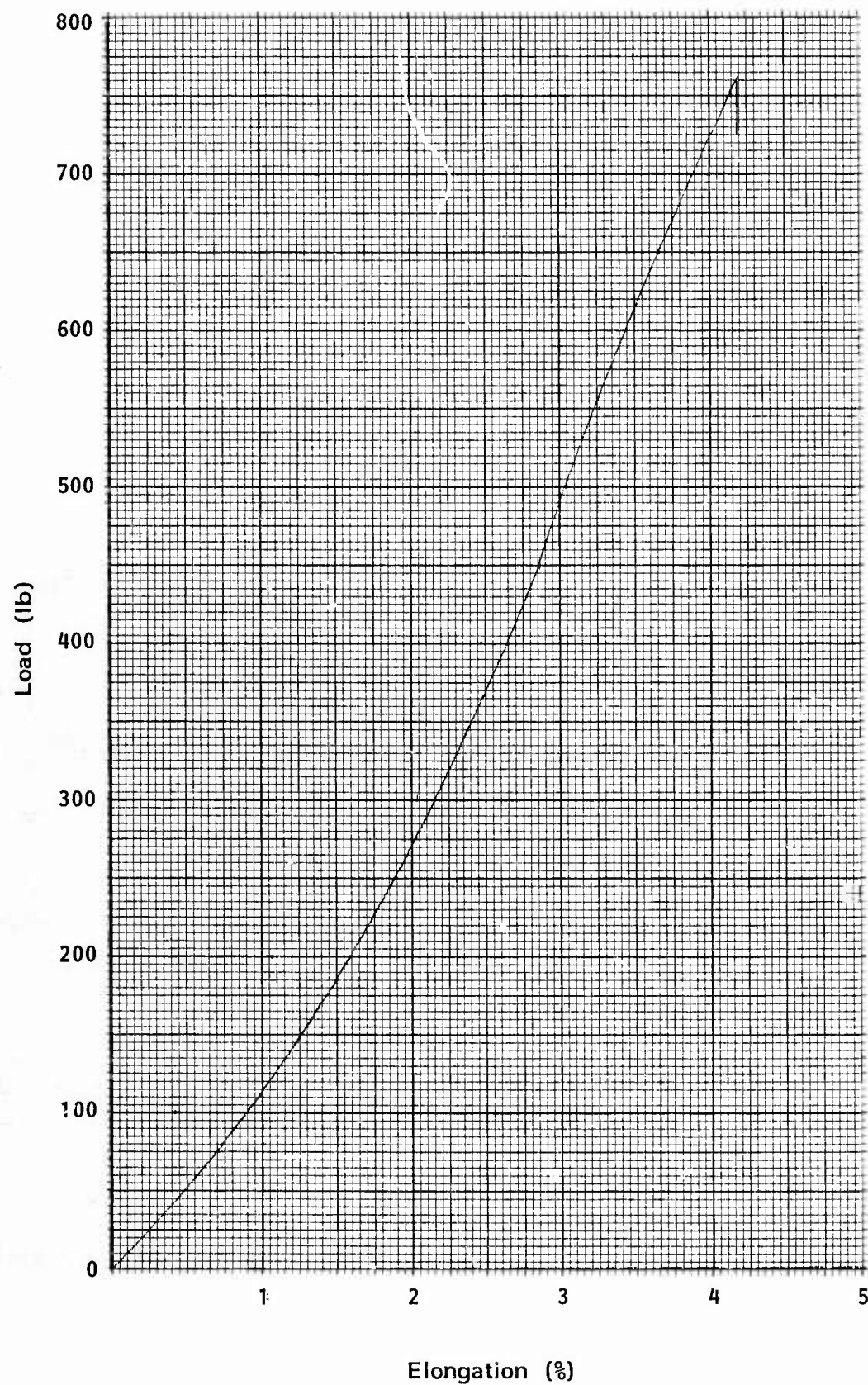
Figure 12. Average Load-Elongation Curve for 9/16-Inch Wide
Kevlar 29 Tape, Type IV (FRL Sample No. 5034-113)

30
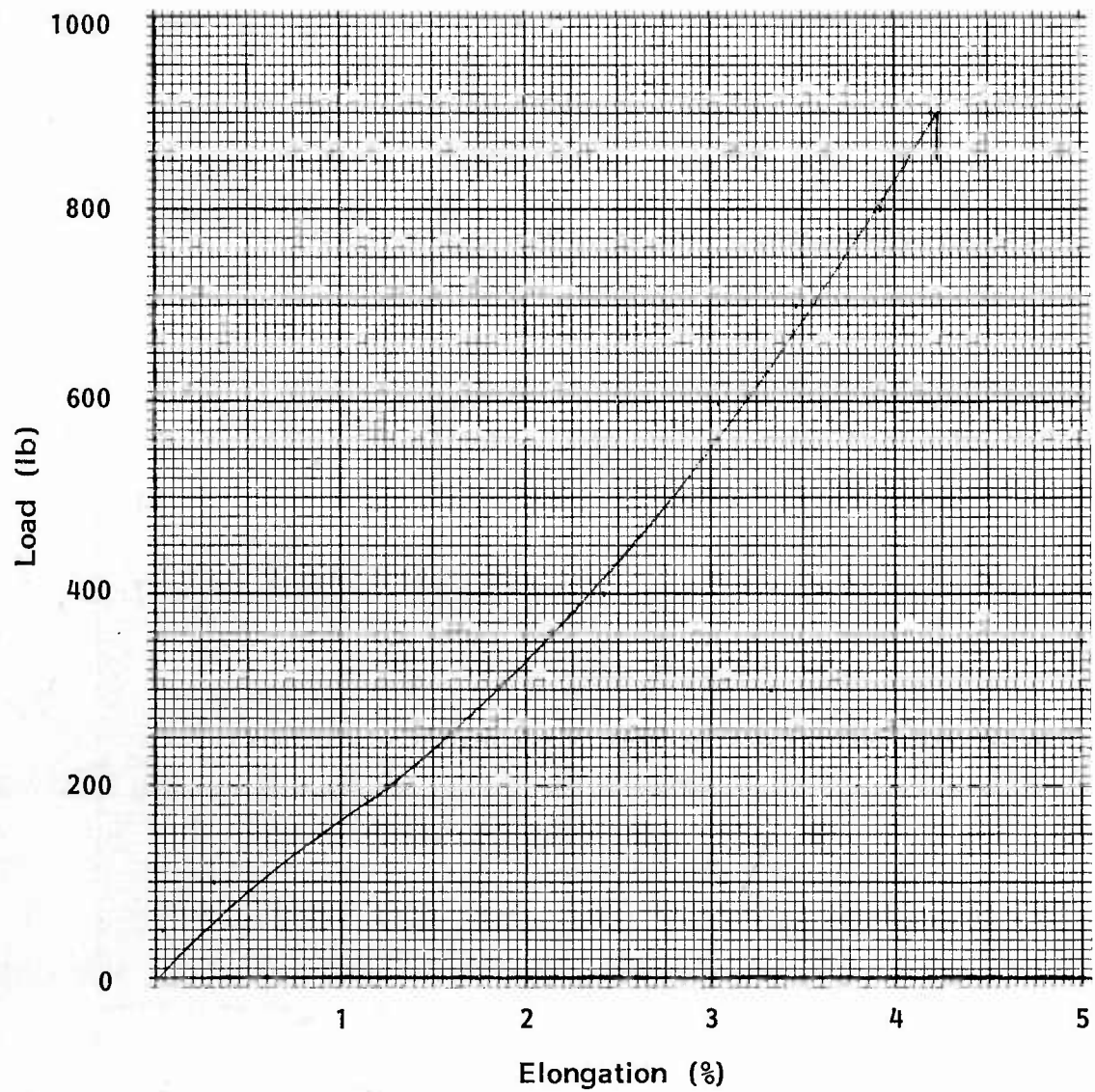
Figure 13. Average Load-Elongation Curve for 1-Inch Wide Kevlar 29 Tape, Type V (FRL Sample No. 5034-107)
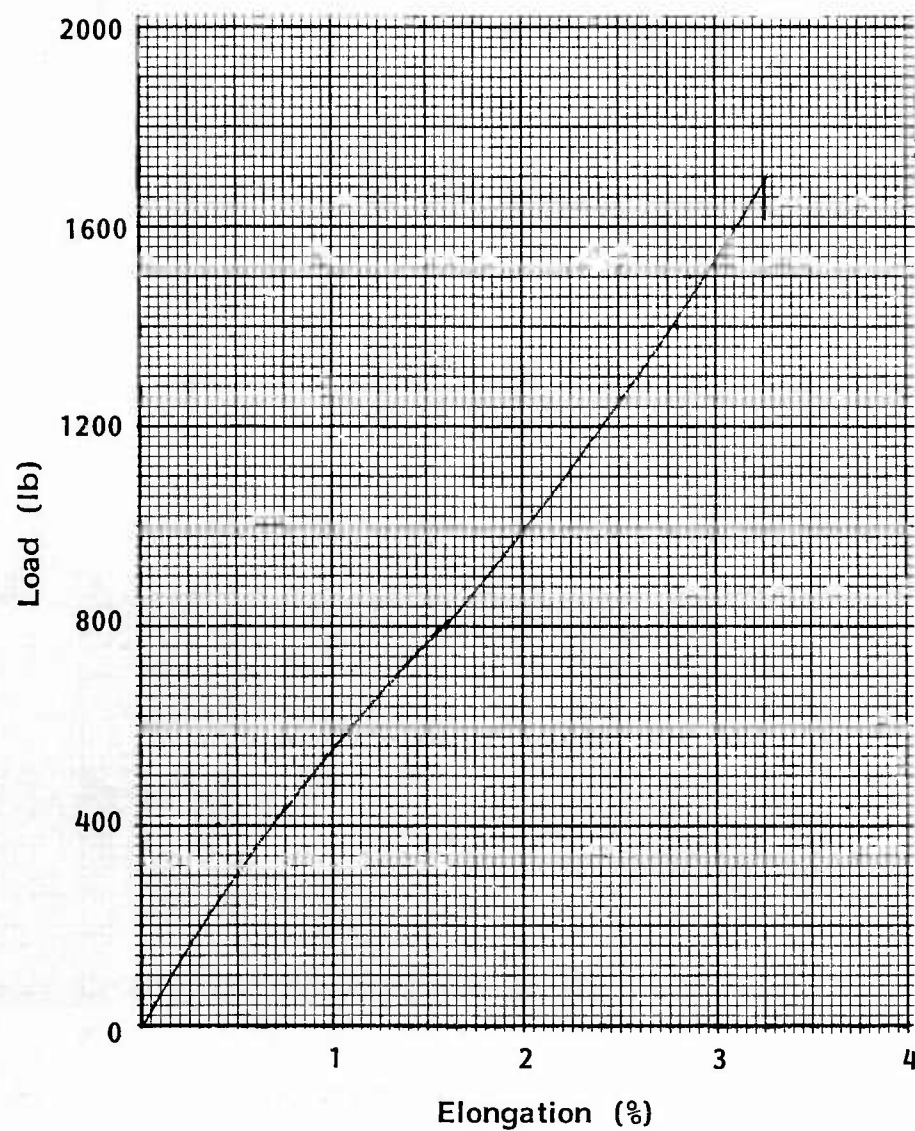
Figure 14. Average Load-Elongation Curve for 1-1/2-Inch
Wide Kevlar 29 Tape, Type VII (FRL Sample No.
5034-106)

32
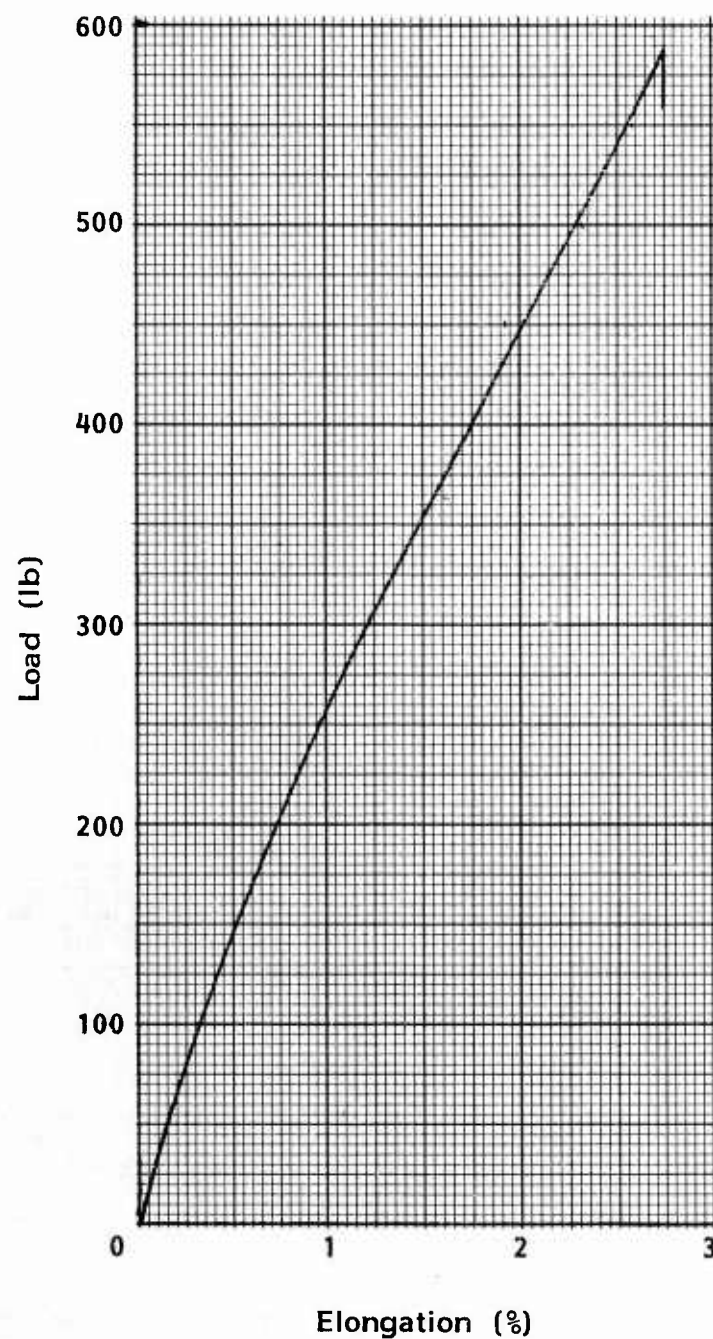
Figure 15. Average Load-Elongation Curve for
1-Inch Wide Kevlar Webbing, Type I
(FRL Sample No. 5034-42)

Figure 16. Average Load-Elongation Curve for 3/4-Inch Wide Kevlar 29
Webbing, Type II (FRL Sample No. 5034-65)

34
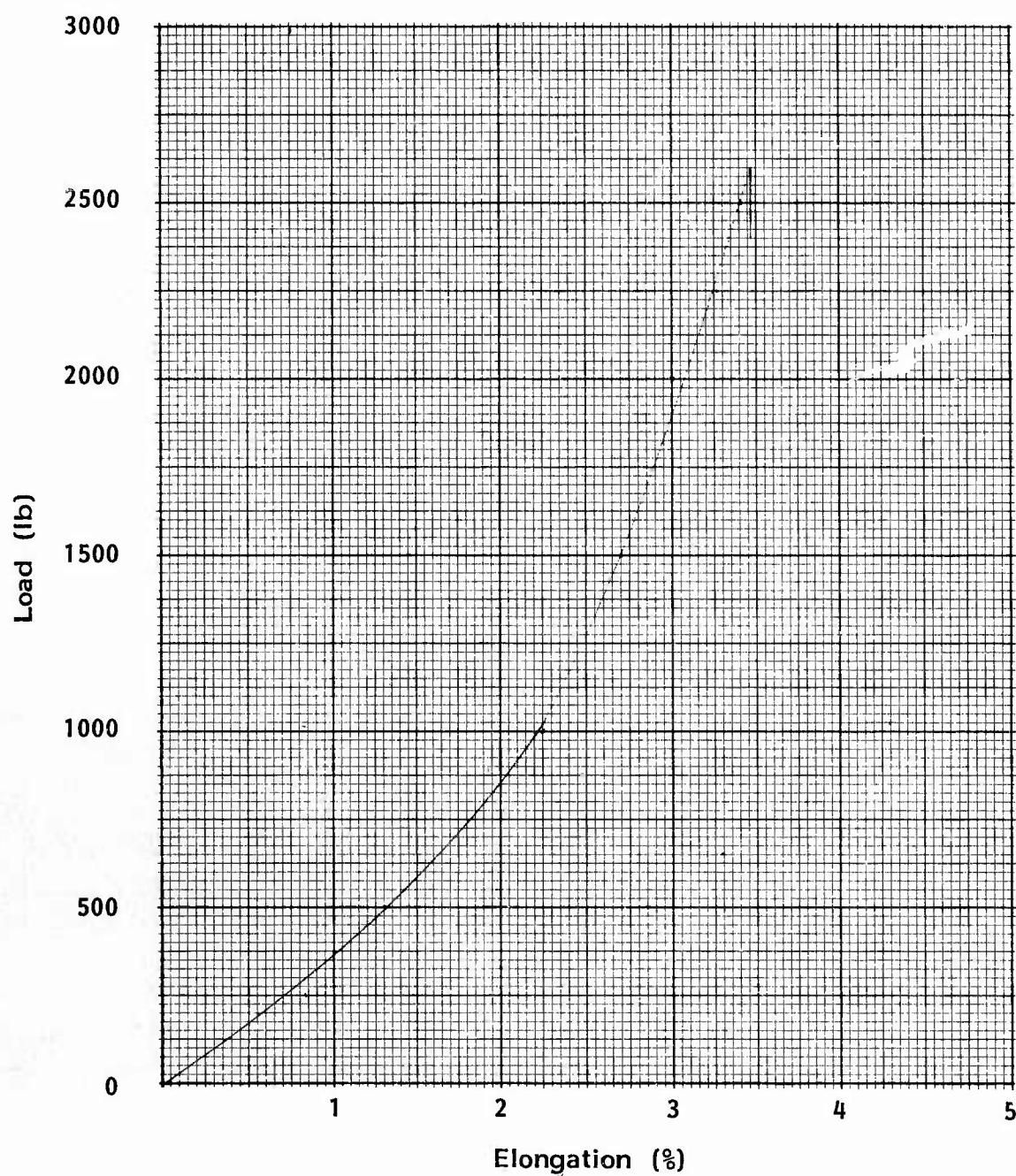
Figure 17. Average Load-Elongation Curve for 1-Inch Wide Kevlar 29 Webbing, Type IV (FRL Sample No. 5034-81)
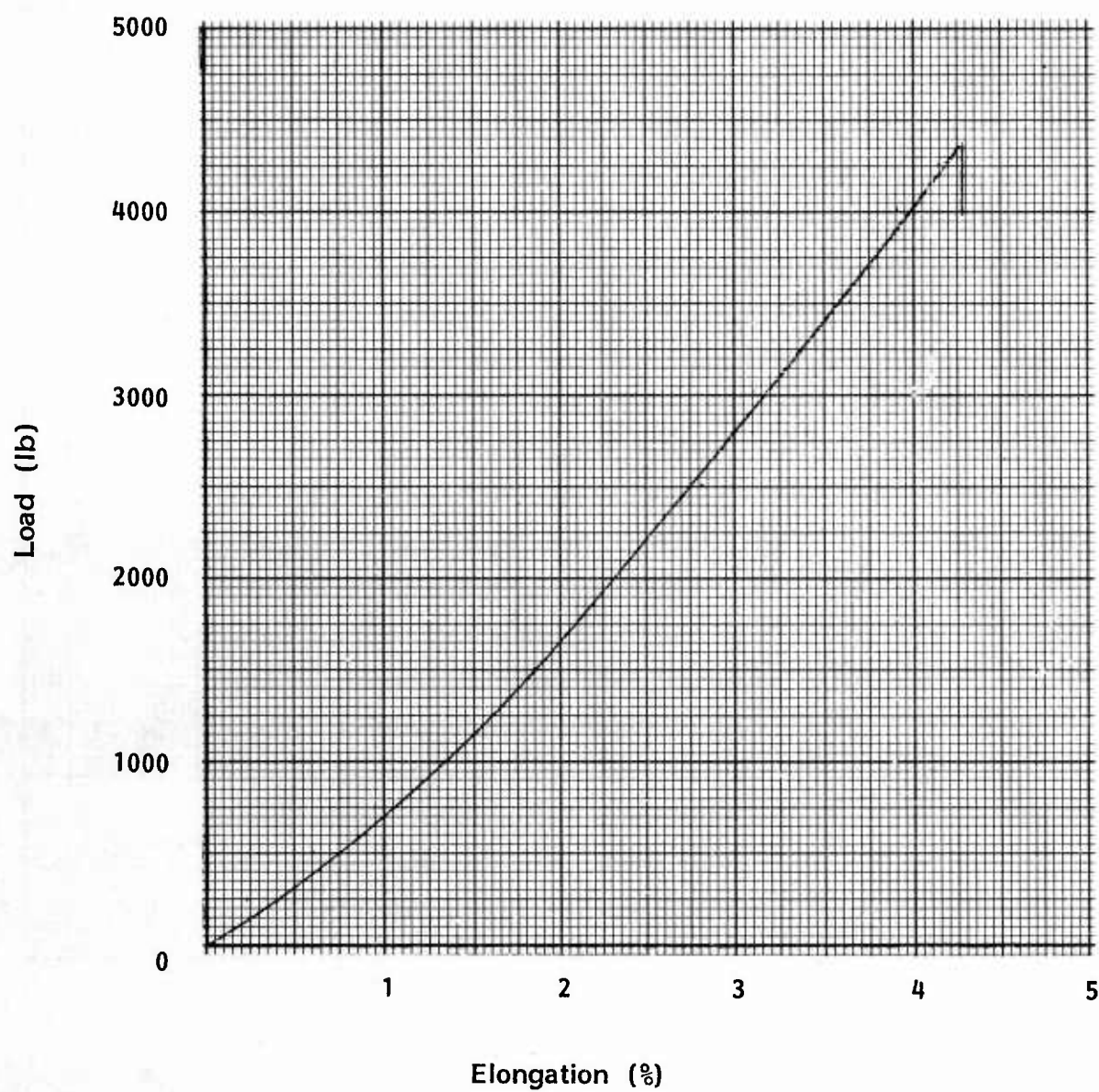
Figure 18. Average Load-Elongation Diagram for 1-Inch Wide Kevlar 29 Webbing, Type V (FRL Sample No. 5034-63)
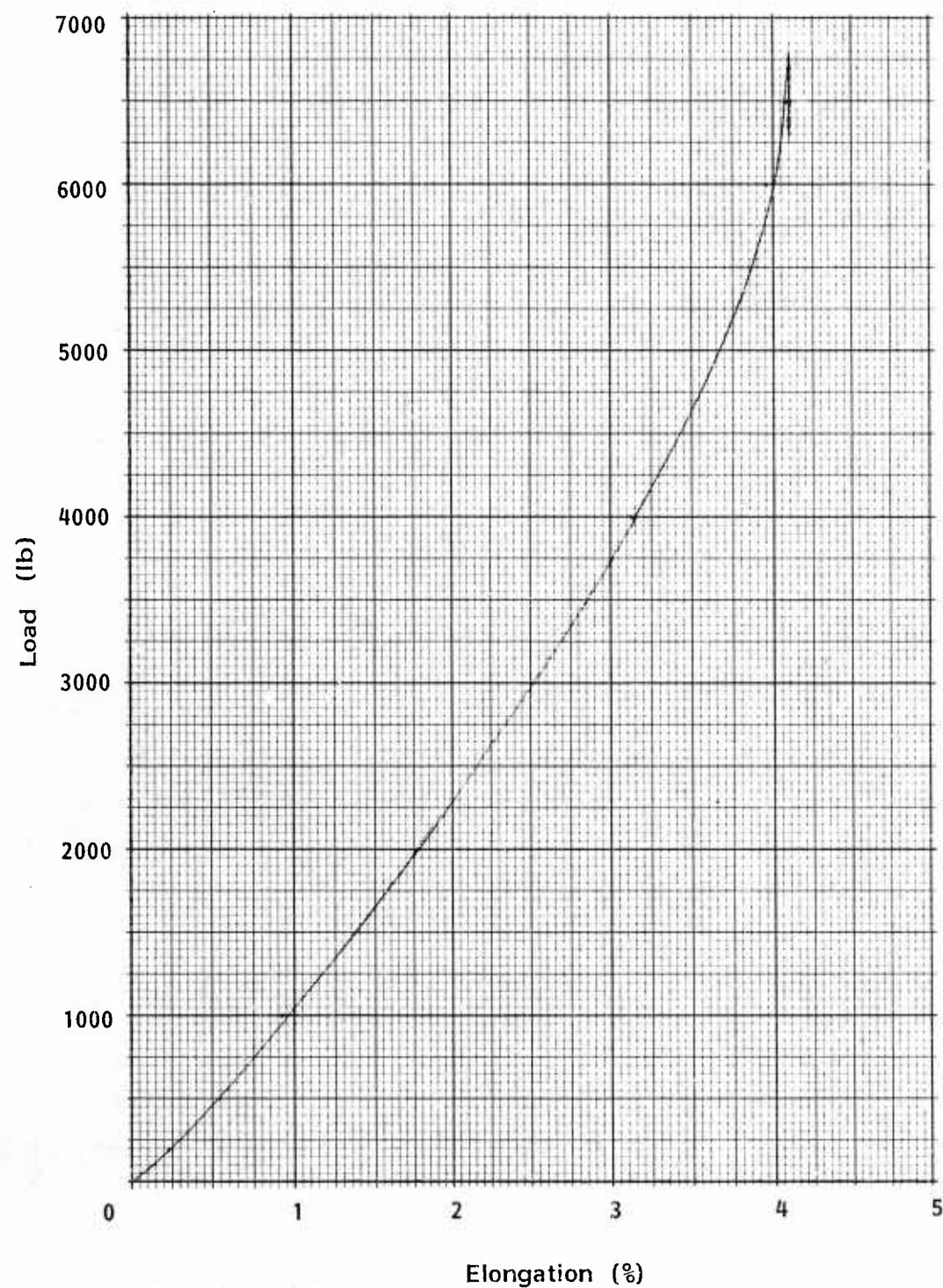
Figure 19. Average Load-Elongation Curve for 1-Inch Wide Kevlar
Webbing, Type VI (FRL Sample No. 5034-32)
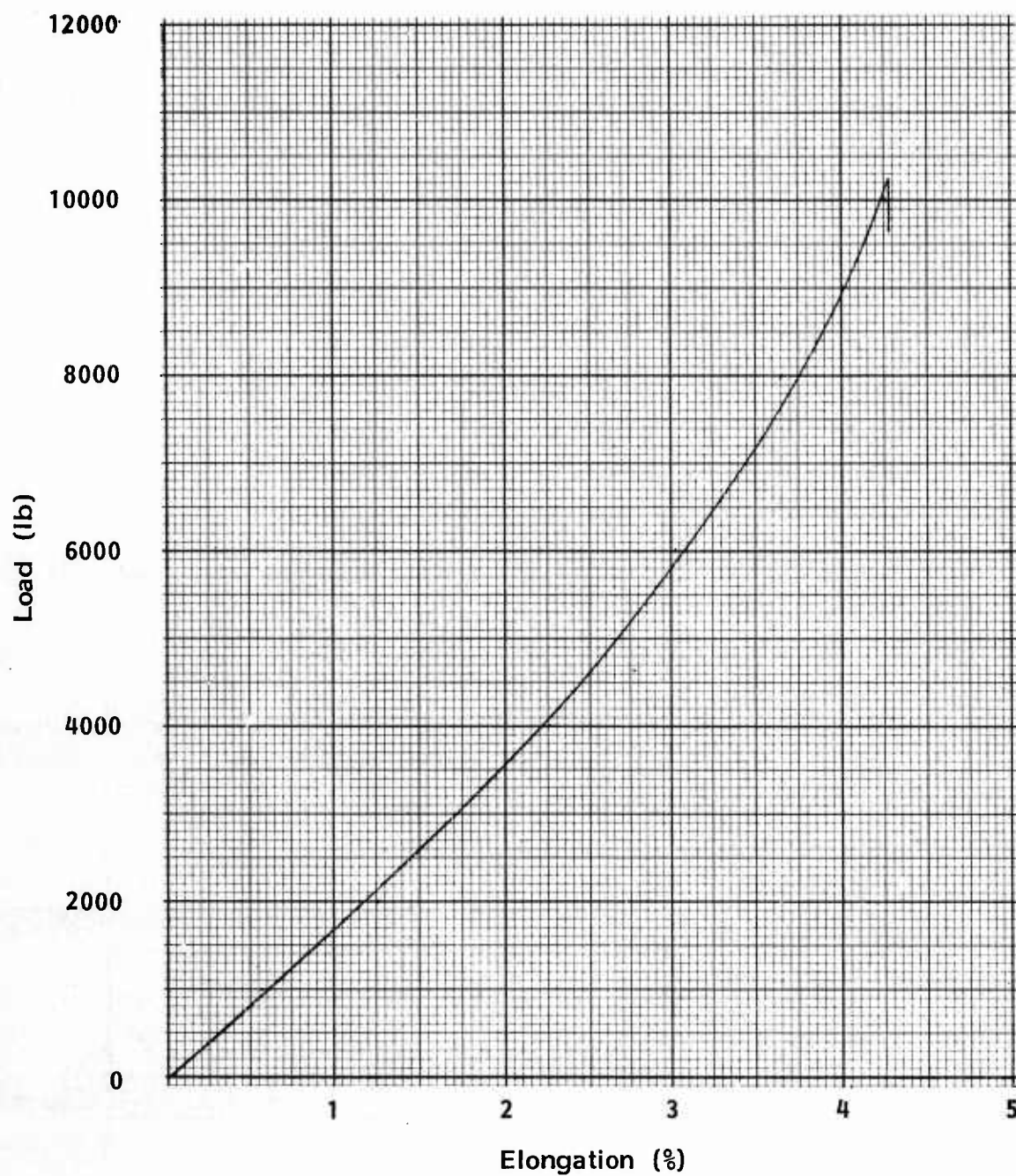
Figure 20. Average Load-Elongation Curve for 1-Inch Wide Kevlar 29
Webbing, Type VII (FRL Sample No. 5034-93)
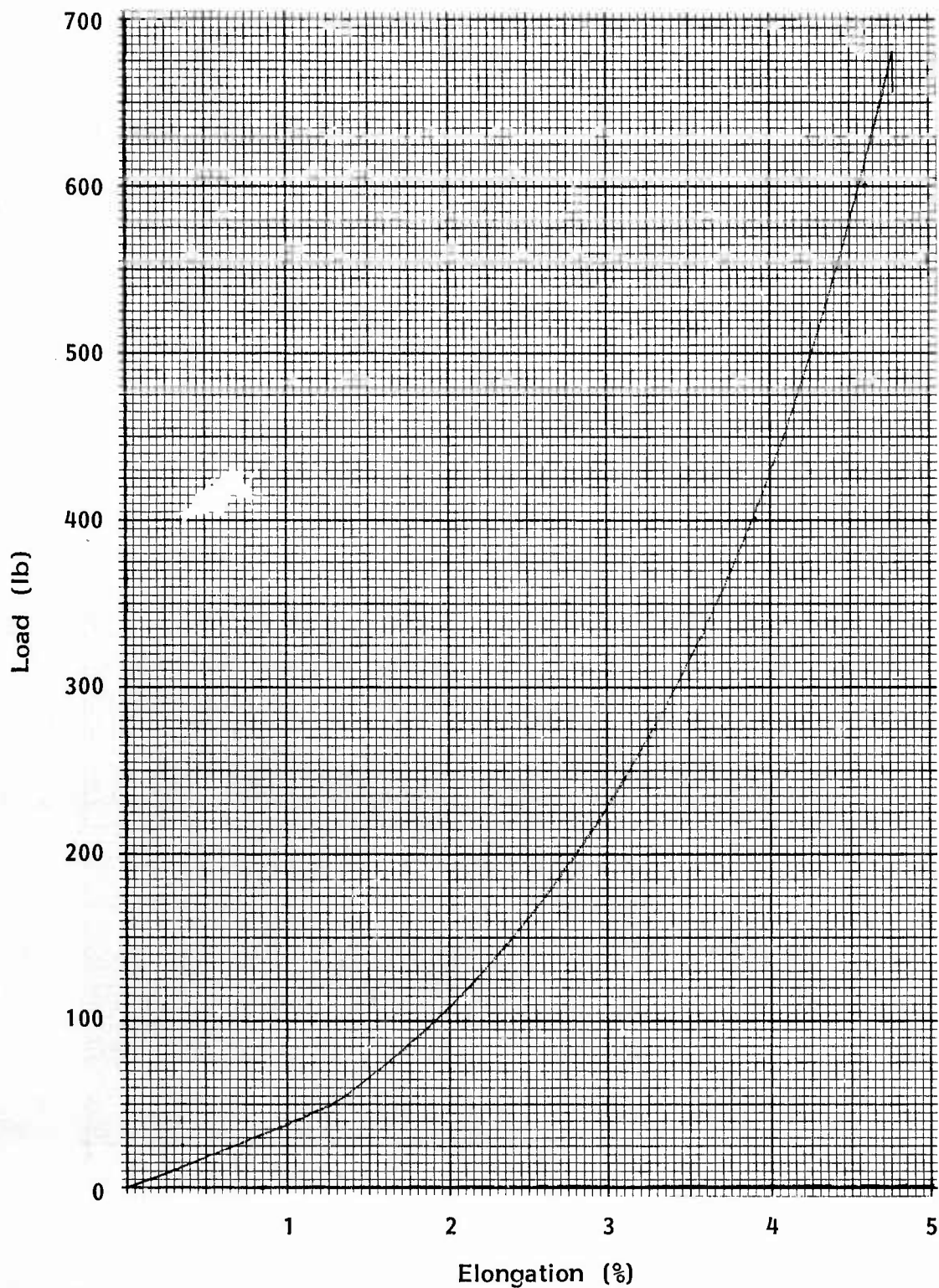
Figure 21. Average Load-Elongation Curve for 1-Inch Wide Kevlar 29 Webbing, Type VIII (FRL Sample No. 5034-117)
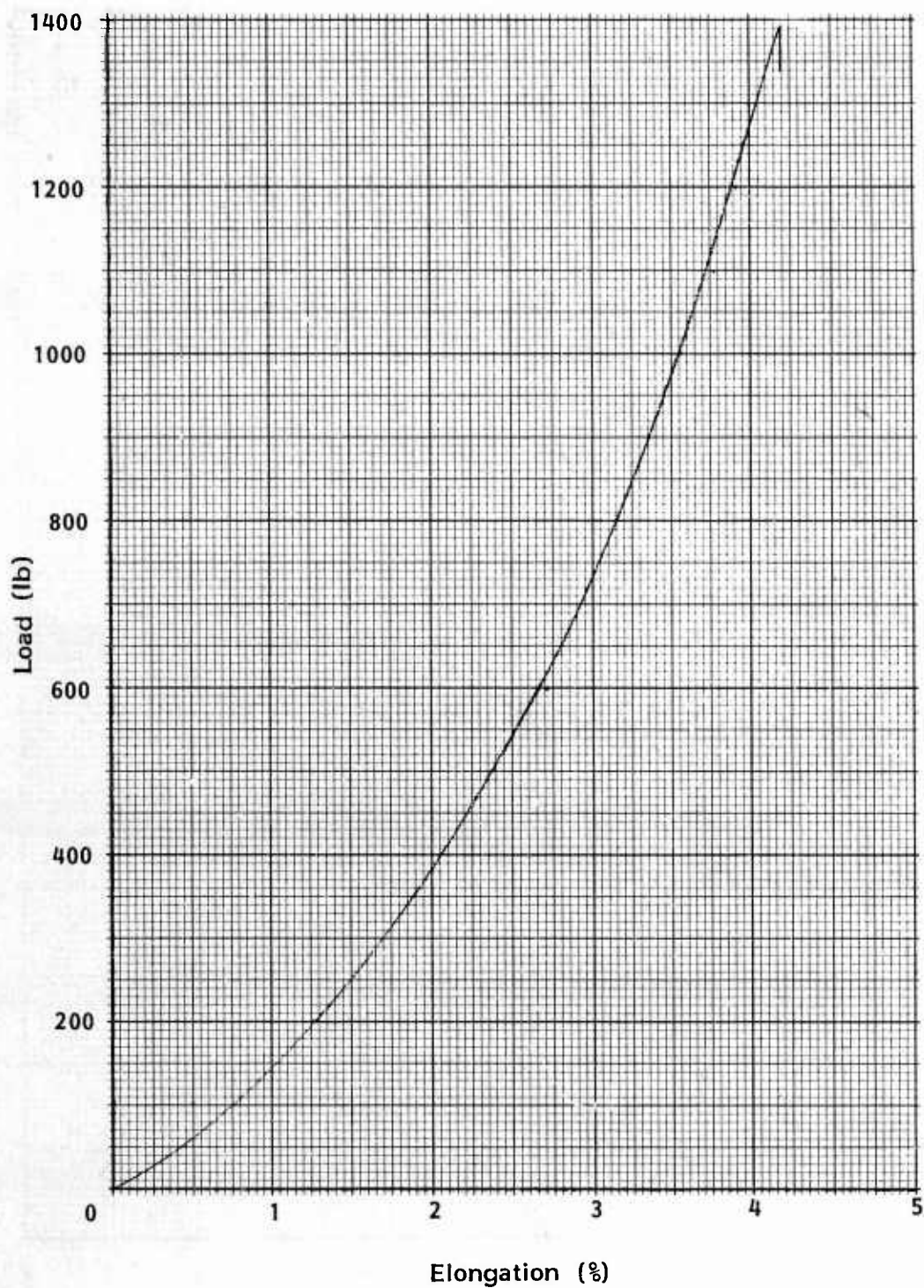
Figure 22.   Average Load-Elongation Curve for 1-3/4-Inch Wide Kevlar
Webbing, Type X (FRL Sample No. 5034-55)
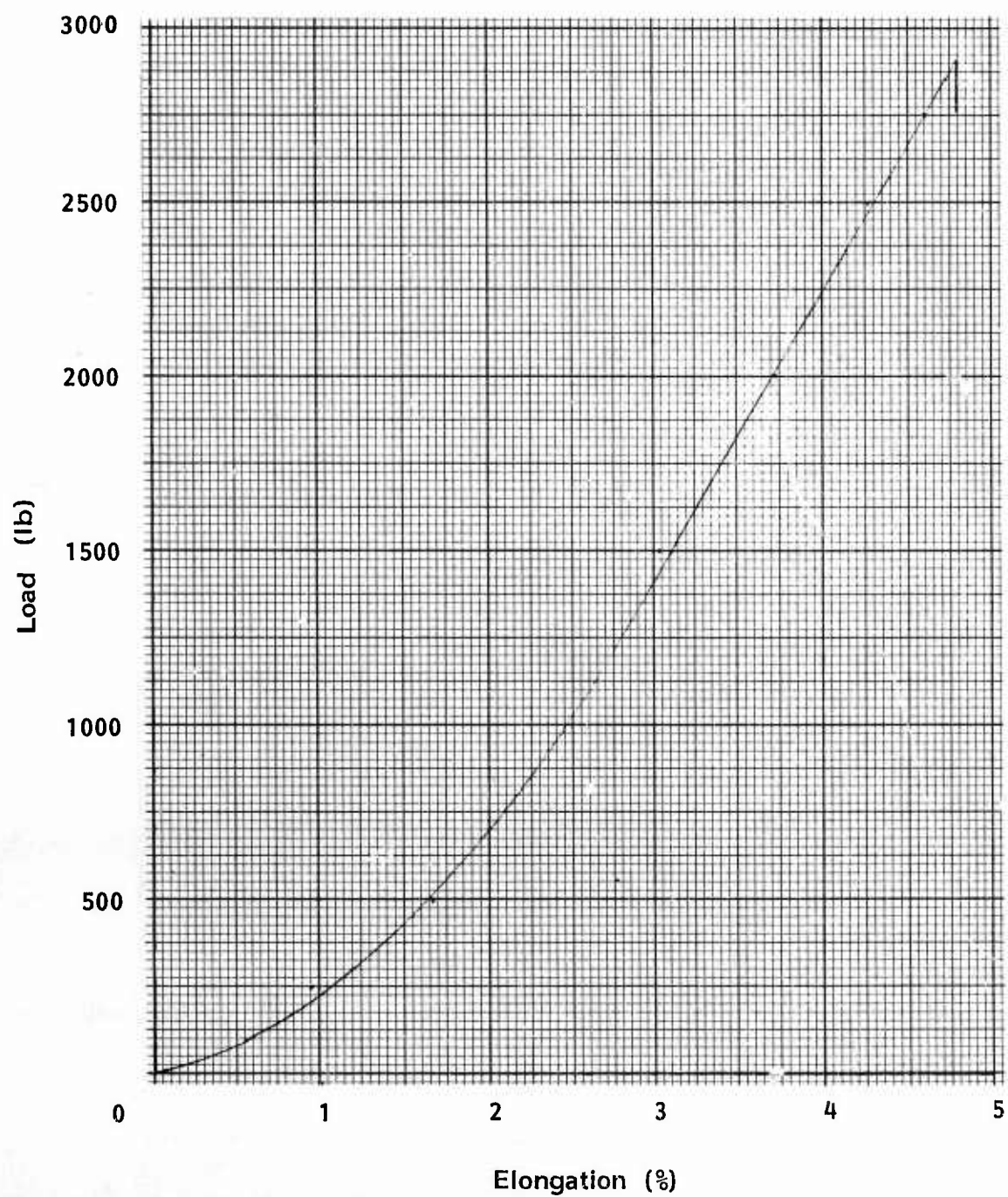
Figure 23. Average Load-Elongation Diagram for 1-3/4-Inch Wide Kevlar 29 Webbing, Type XI (FRL Sample No. 5034-75)

41
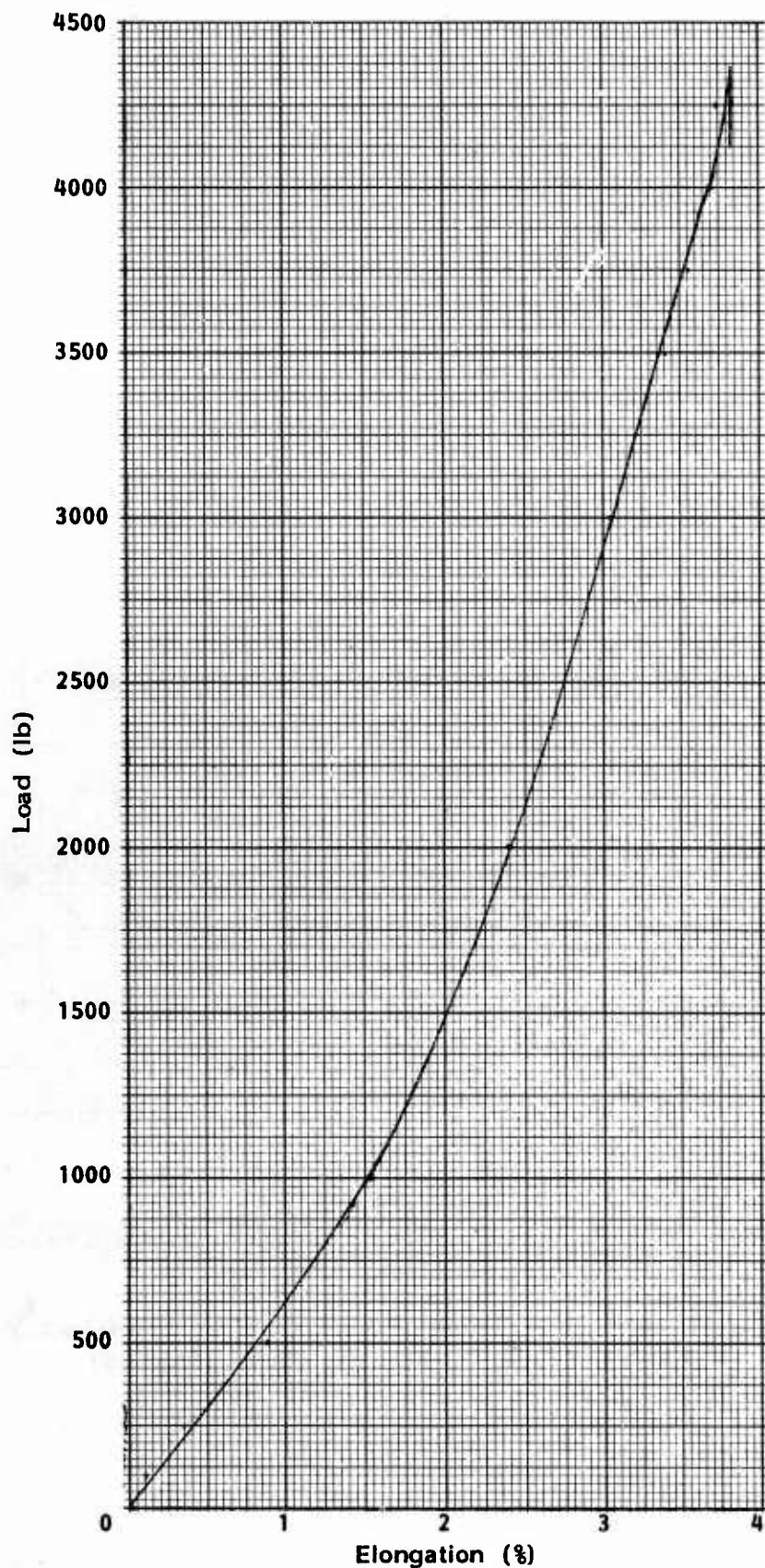
Figure 24.   Average Load-Elongation Curve for 1-3/4-Inch Wide
Kevlar Webbing, Type XII (FRL Sample No. 5034-16)
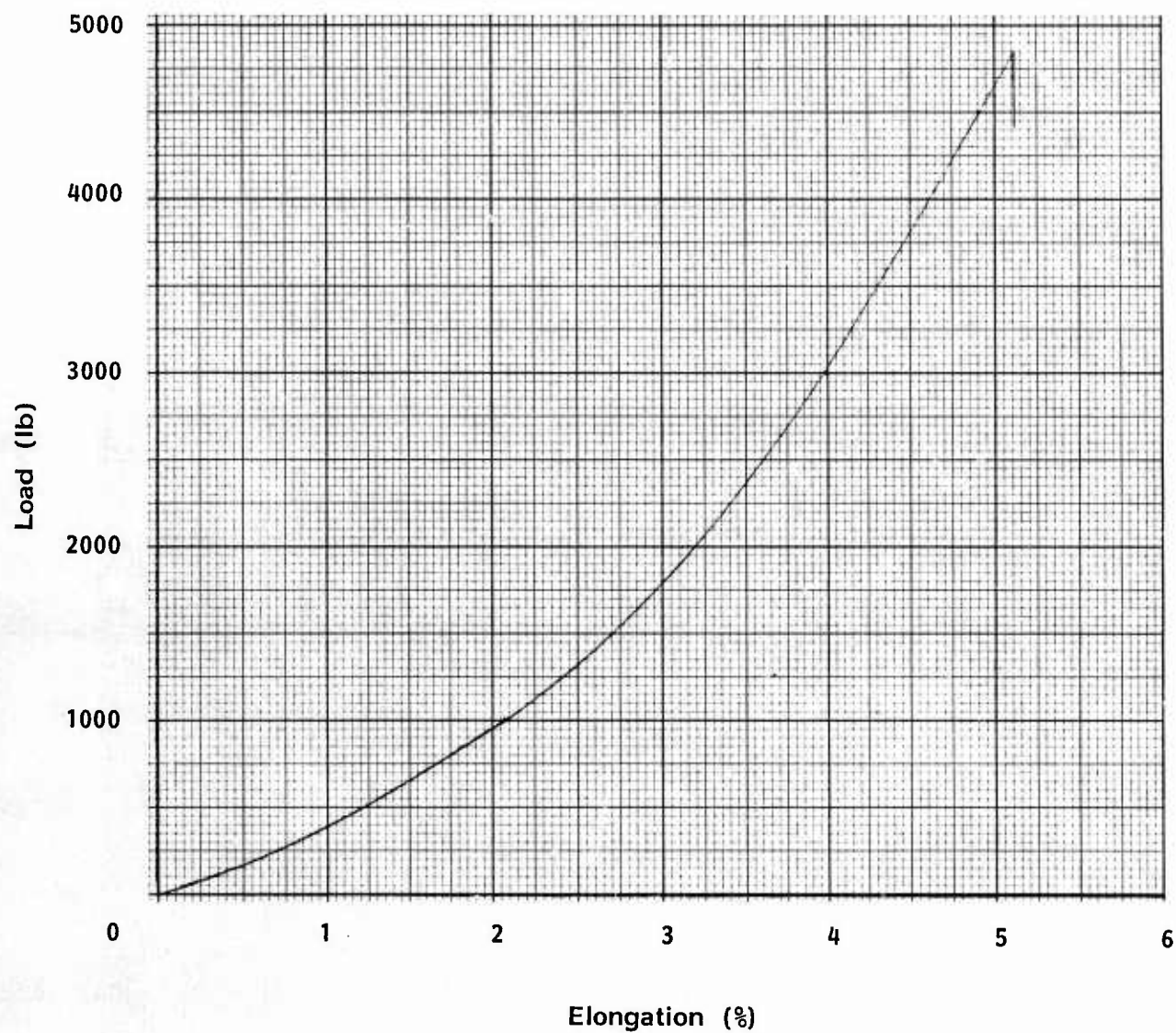
Figure 25. Average Load-Elongation Diagram for 1-3/4-Inch Wide Kevlar 29 Webbing, Type XIII (FRL Sample No. 5034-74)

43
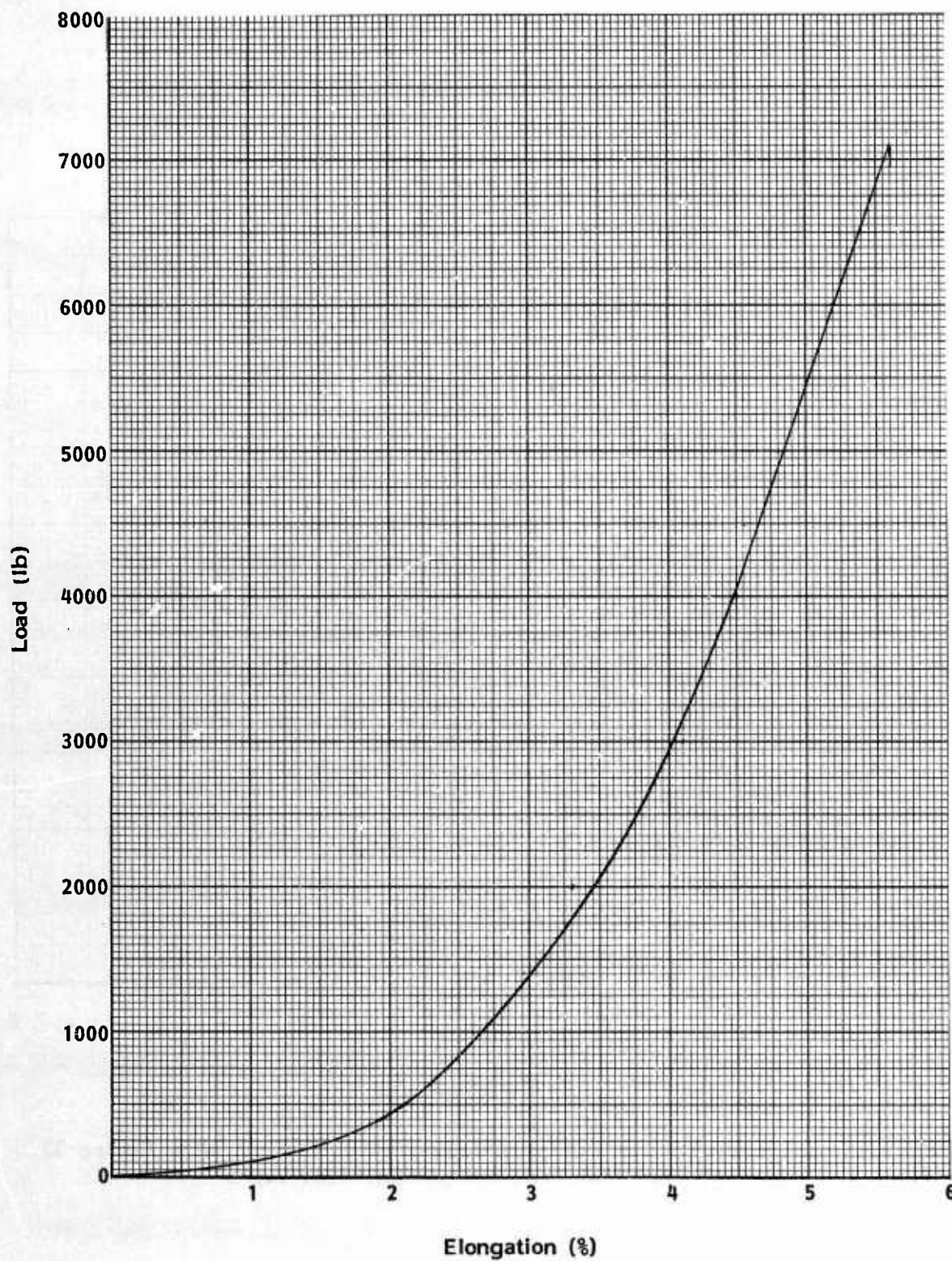
Figure 26. Average Load-Elongation Diagram for 1-3/4-Inch Wide Kevlar 29 Webbing, Type XIV (FRL Sample No. 5034-15)

44
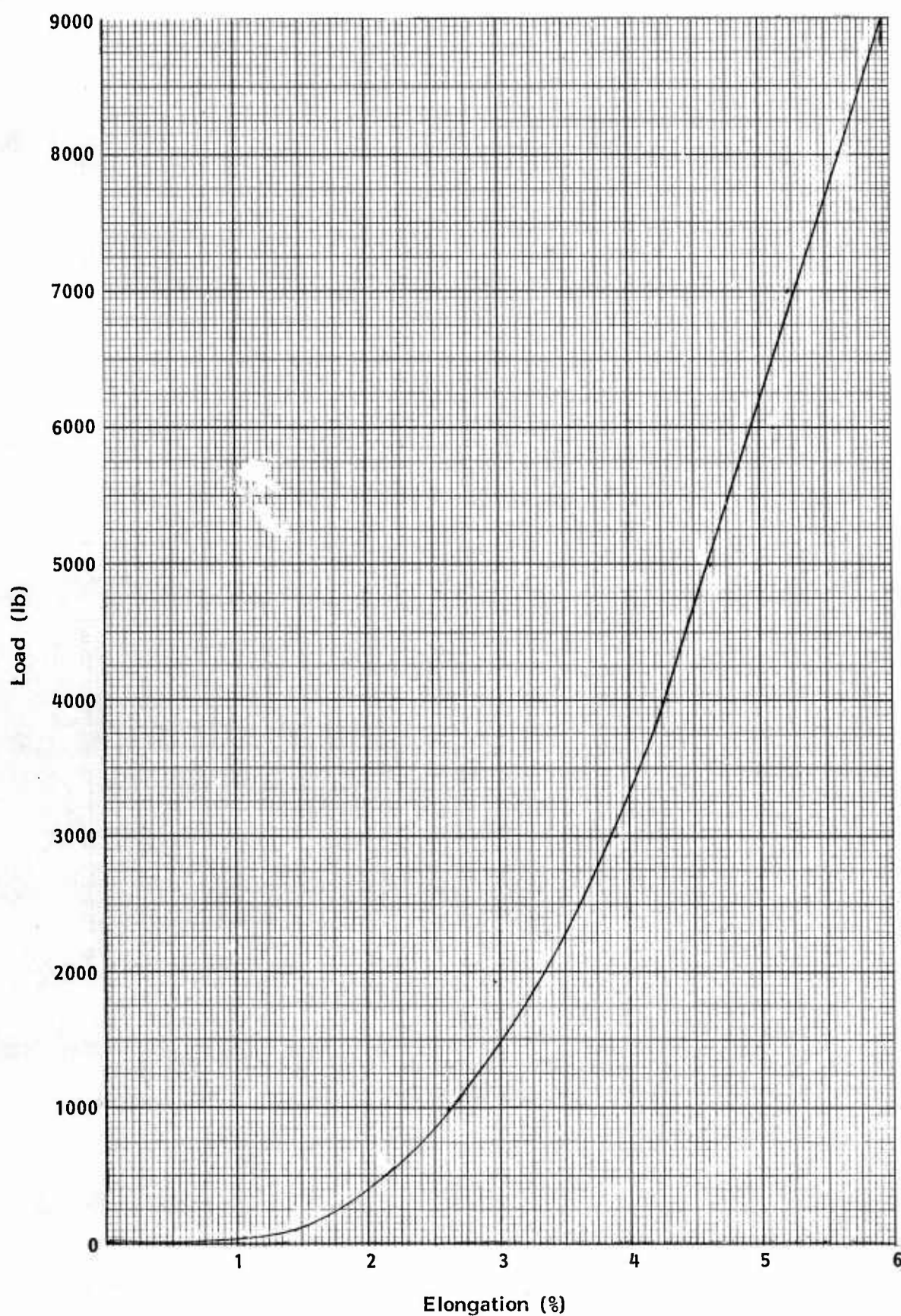
Figure 27. Average Load-Elongation Diagram for 1-3/4 Inch Wide Kevler 29 Webbing, Type XV (FRL Sample No. 5034-31)

45
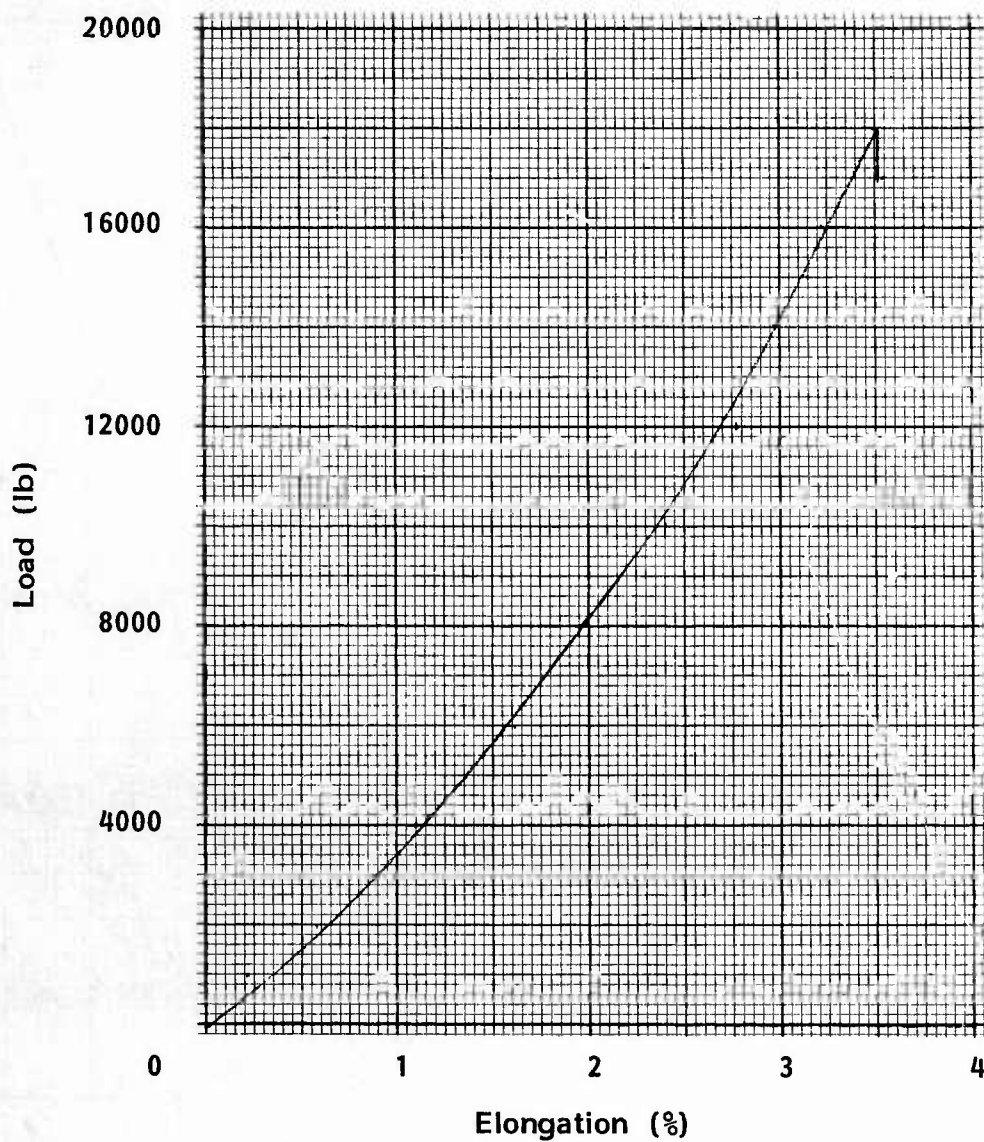
Figure 28. Average Load-Elongation Diagram for 1-3/4 Inch Wide Kevlar 29 Webbing, Type XVII (FRL Sample No. 5034-62)
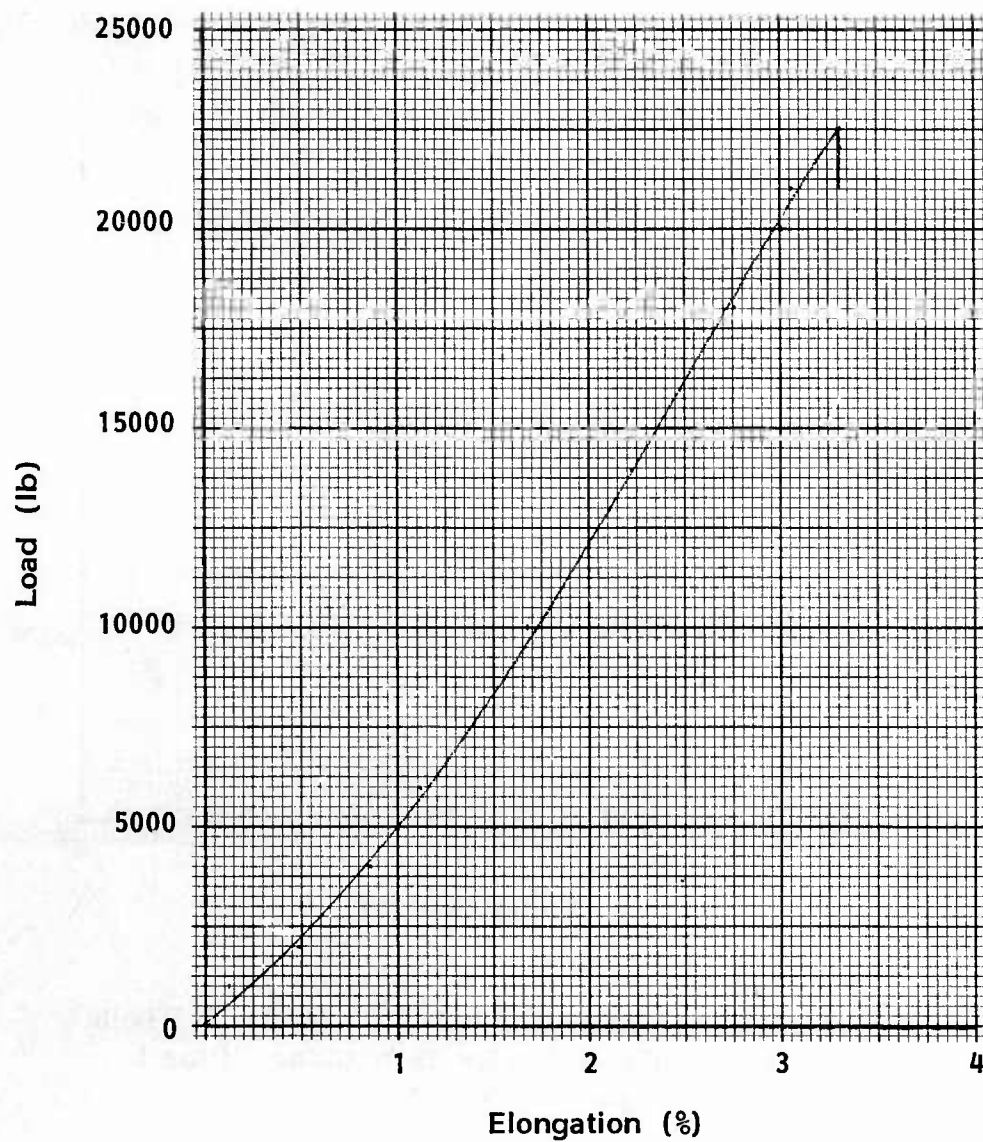
Figure 29. Average Load-Elongation Diagram for 1-3/4 Inch Wide Kevlar 29 Webbing, Type XVIII (FRL Sample No. 5034-61)
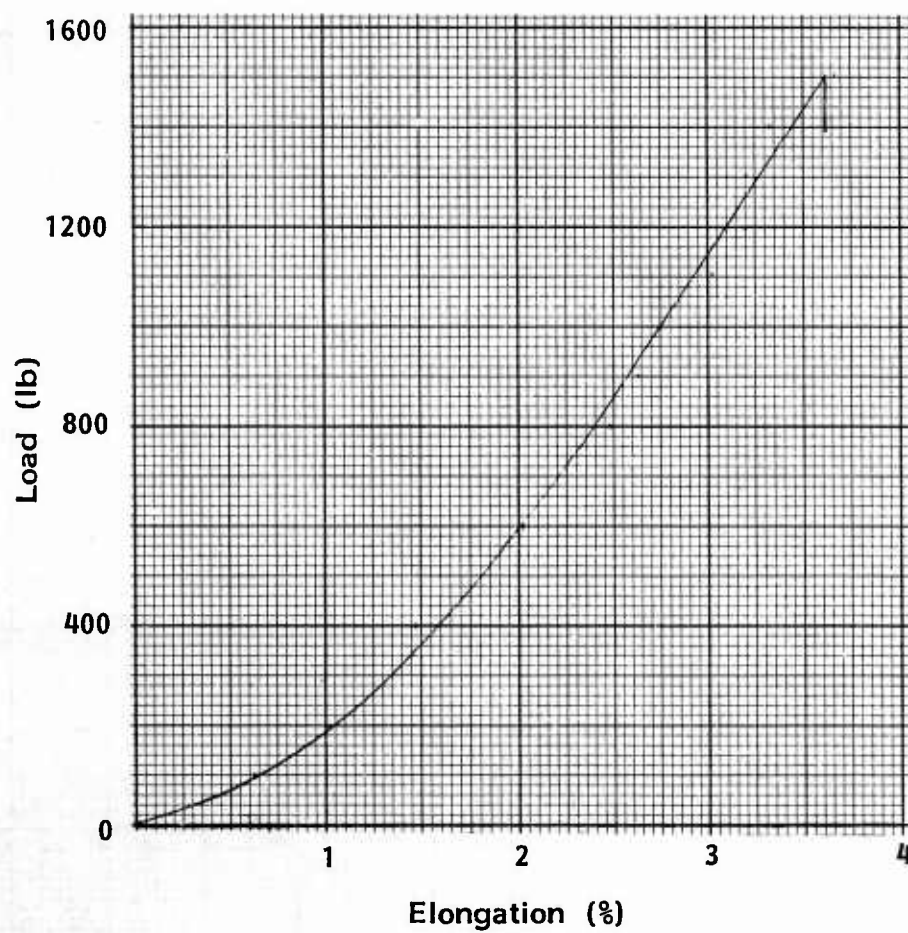
Figure 30. Average Load-Elongation Curve for 1/2-Inch
Wide Tubular Kevlar 29 Webbing, Type I
(FRL Sample No. 5034-90)
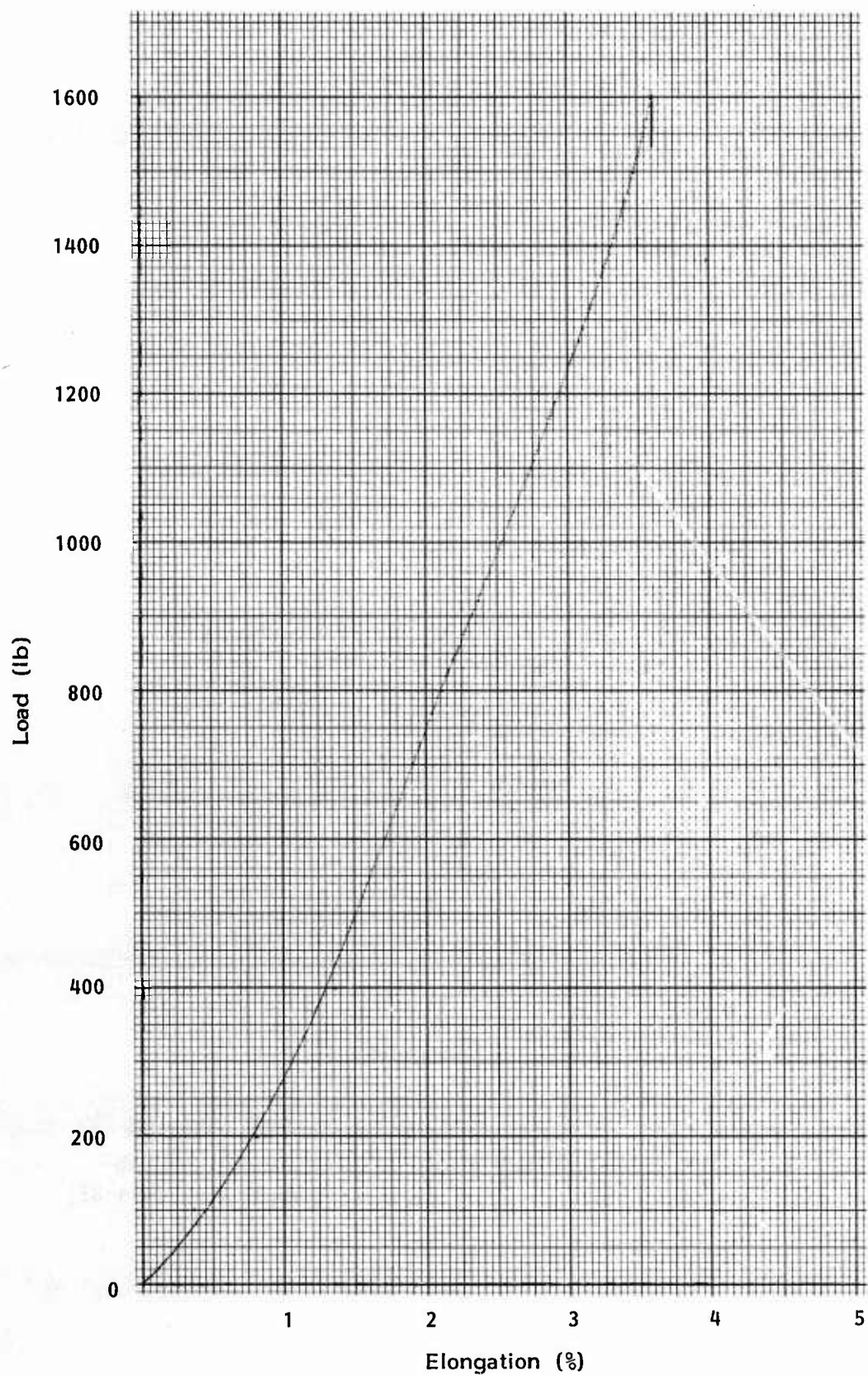
Figure 31. Average Load-Elongation Curve for 9/16-Inch Wide Tubular
Kevlar 29 Webbing, Type II (FRL Sample No. 5034-64)
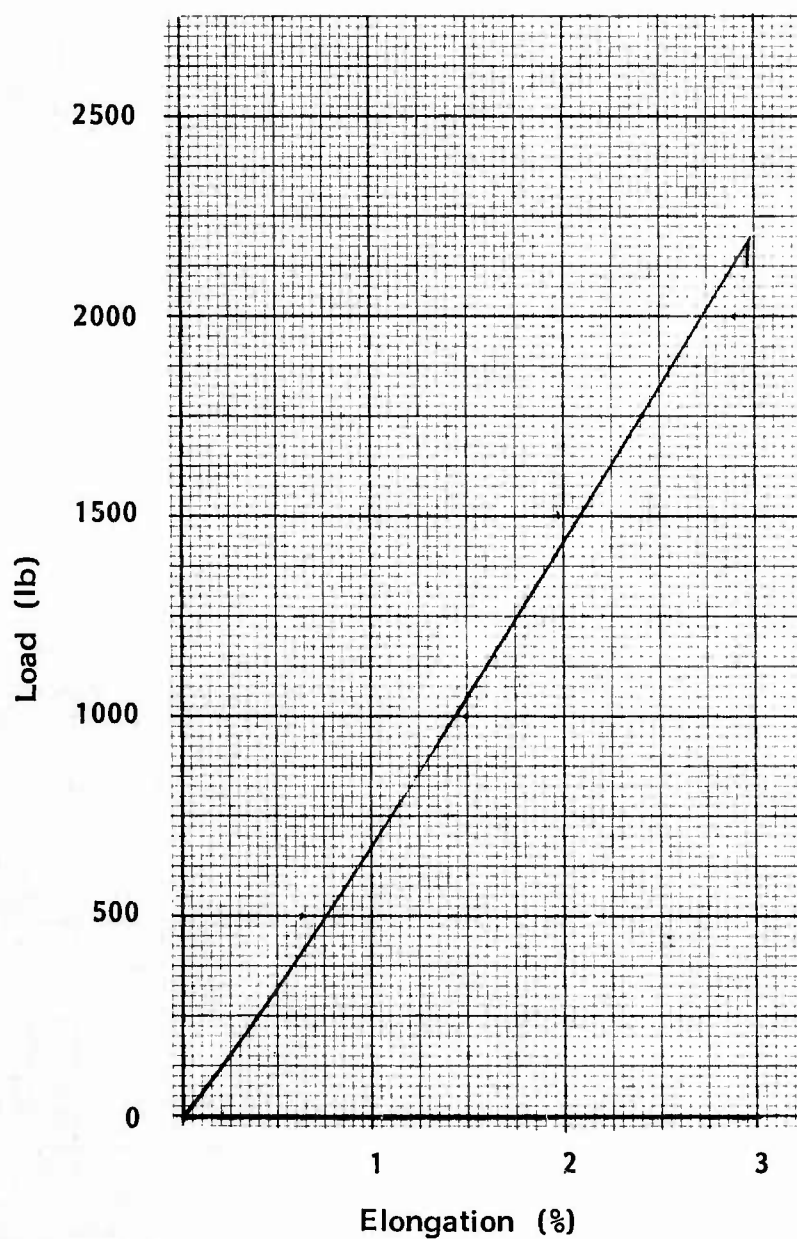
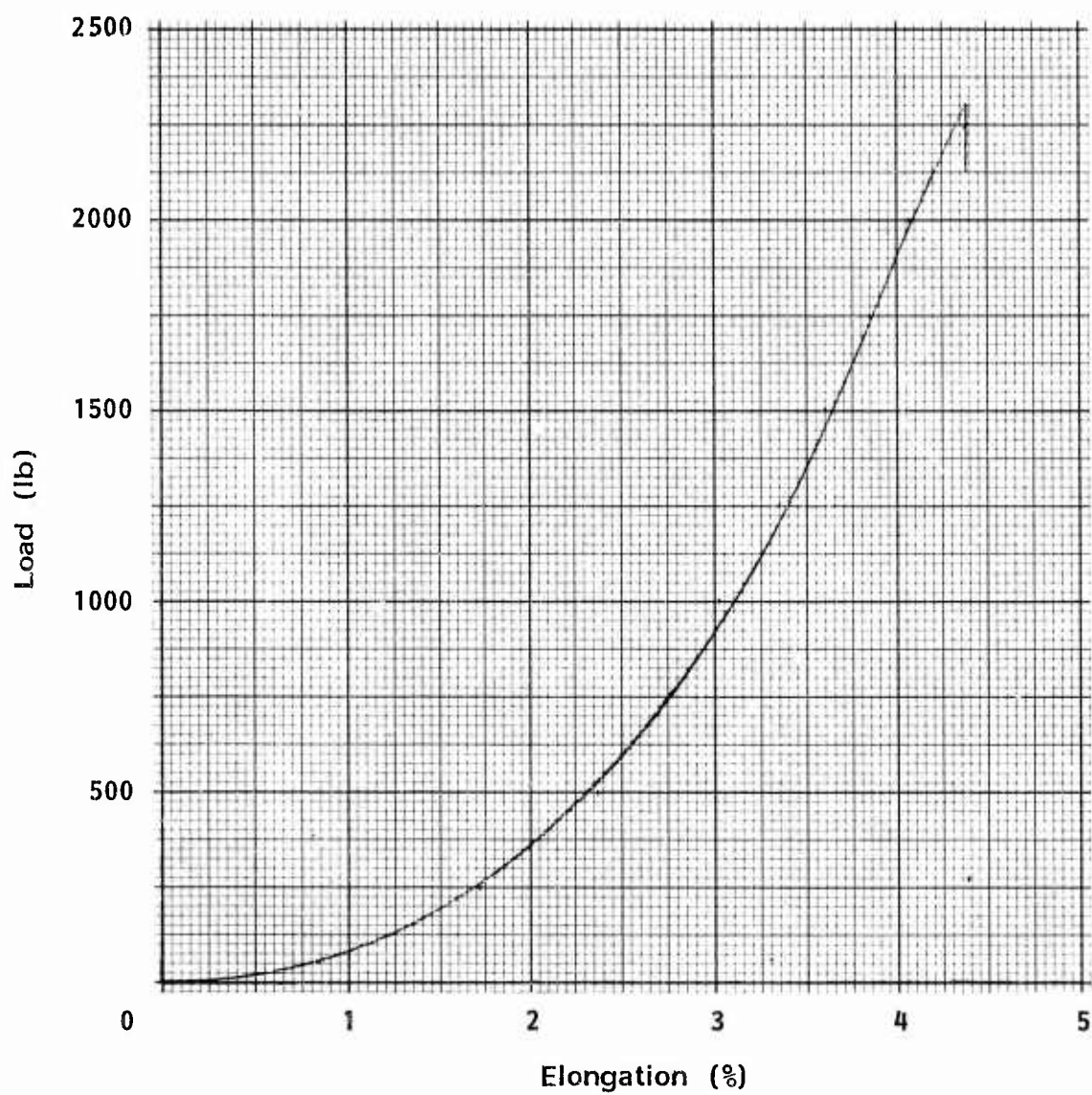Figure 32. Average Load-Elongation Diagram for
5/8-Inch Wide Tubular Kevlar 29 Web-
bing, Type III (FRL Sample No. 5034-36)
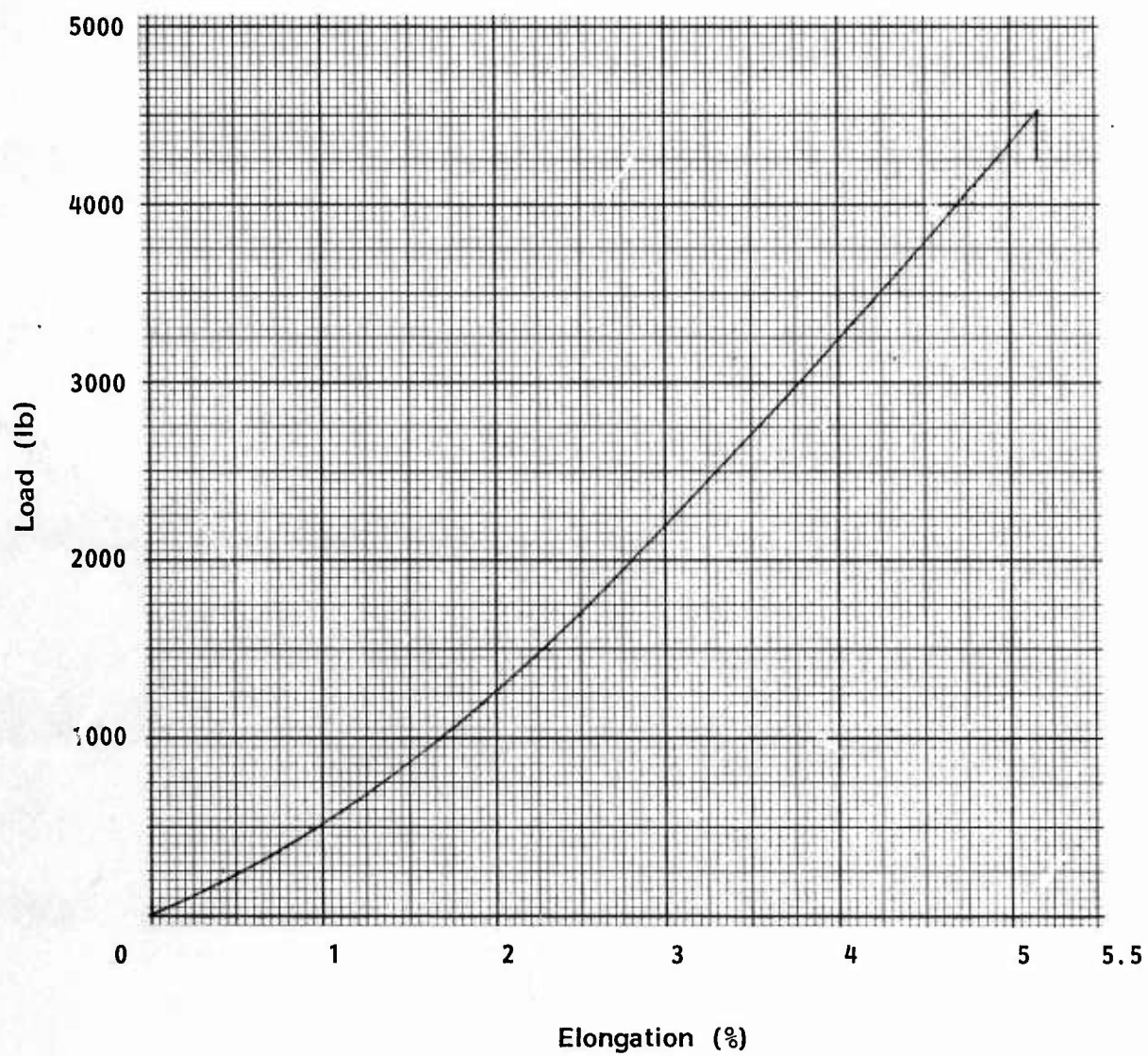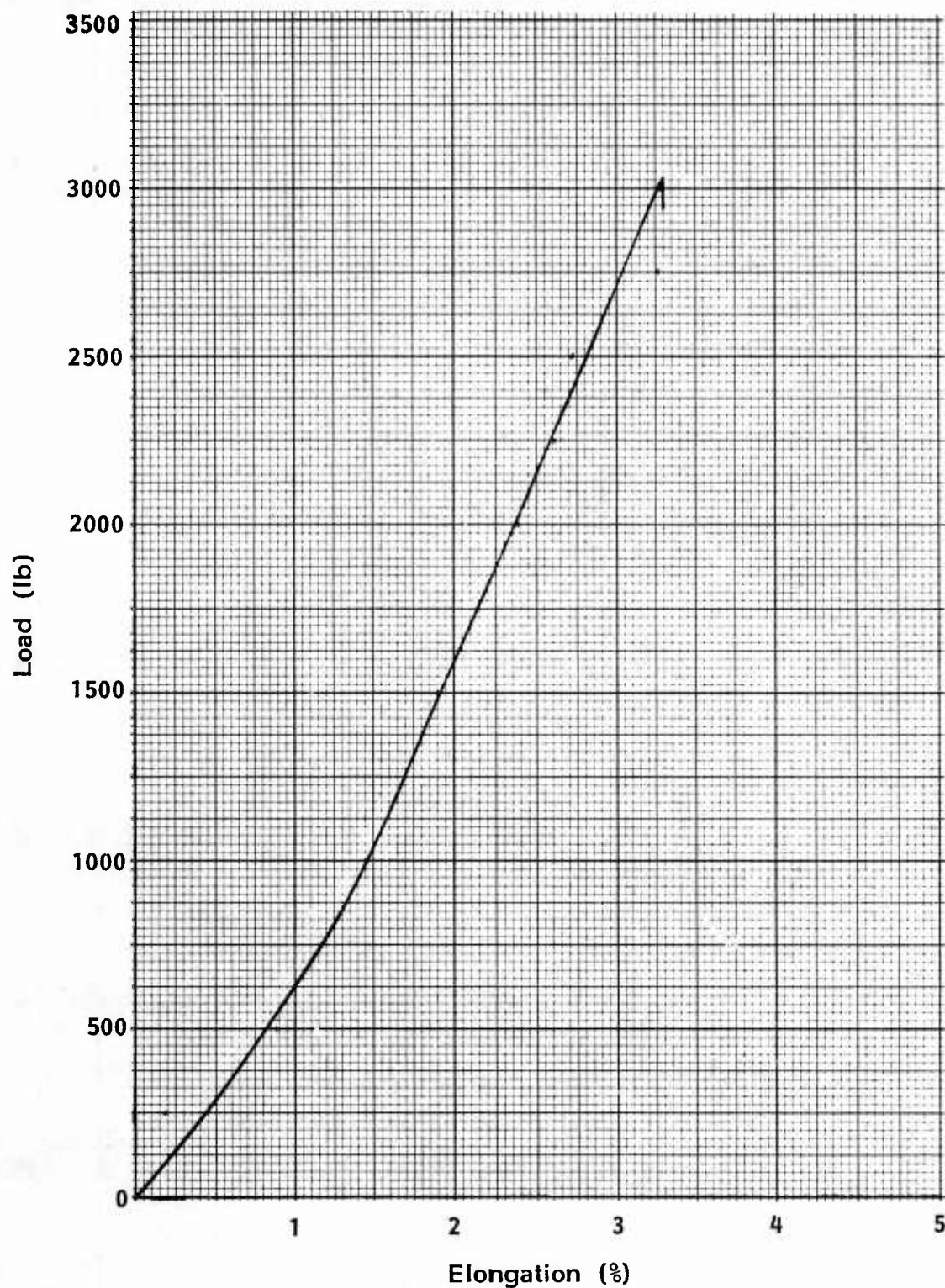
Figure 33. Average Load-Elongation Diagram for 3/4-Inch Wide
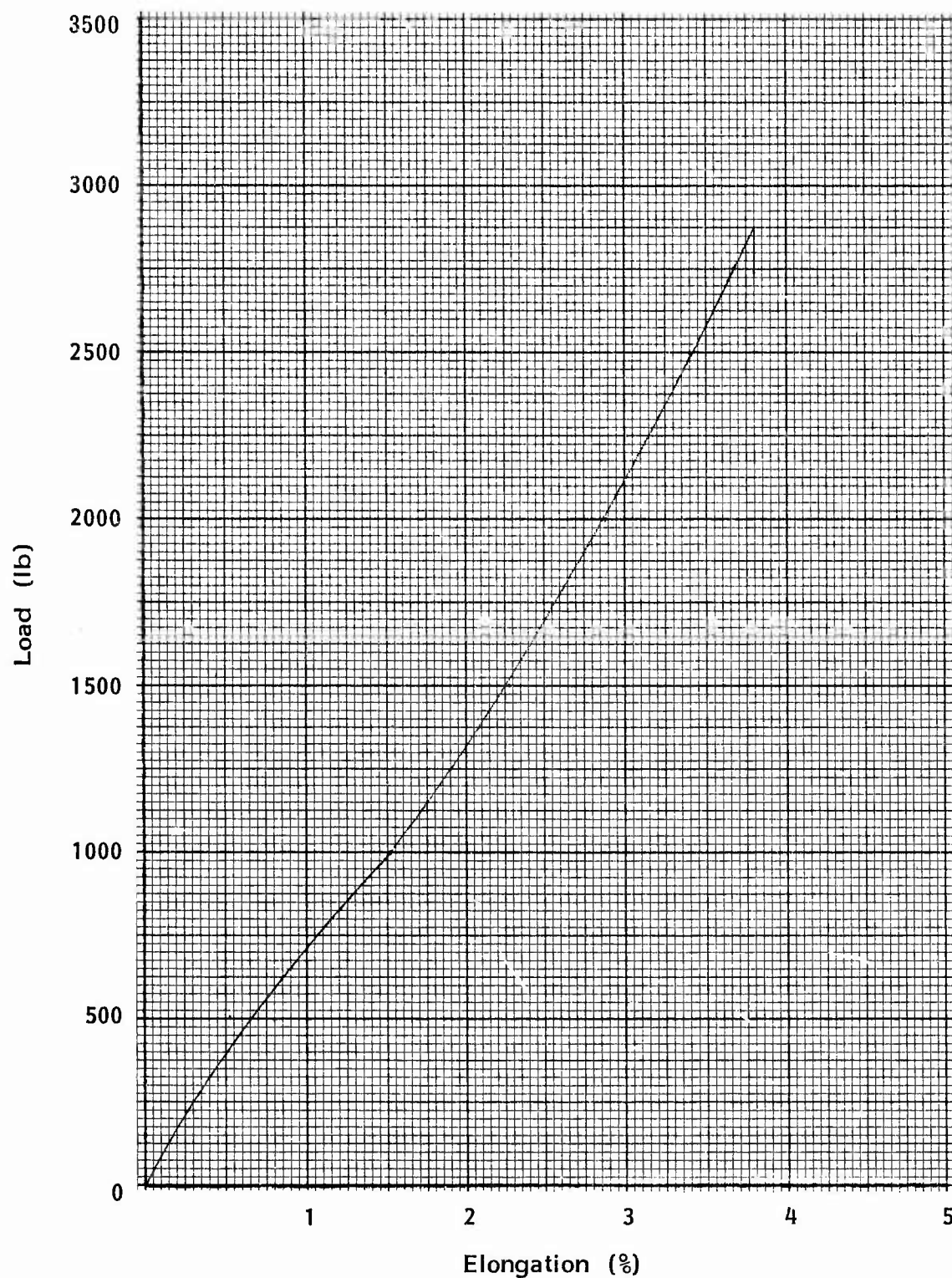   Tubular Kevlar 29 Webbing, Type IV (FRL Sample
           No. 5034-37)

51
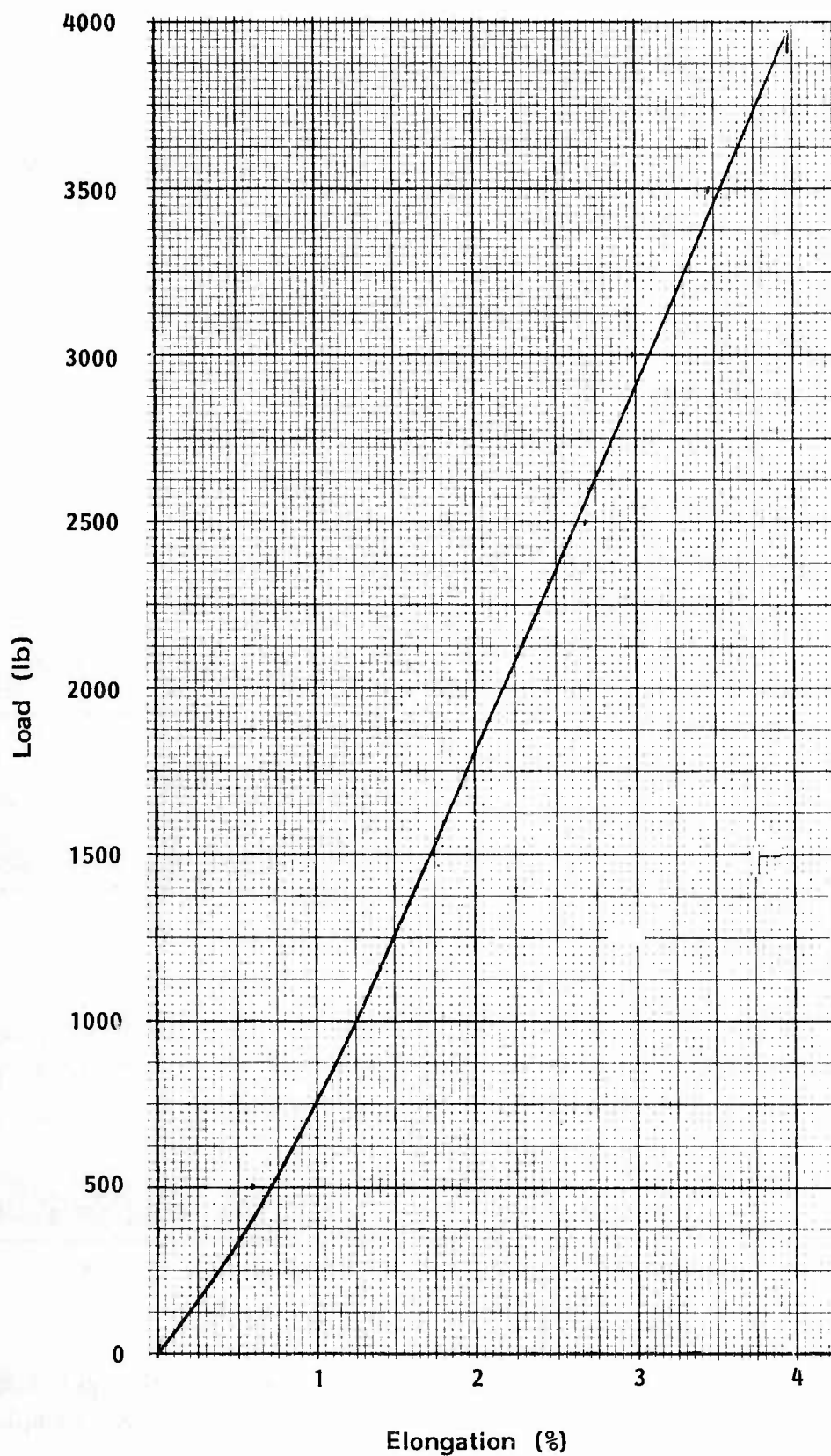
Figure 34. Average Load-Elongation Diagram for One-Inch Wide
Tubular Kevlar 29 Webbing, Type J (FRL Sample
No. 5034-35)

52

We have found that, although narrow fabrics can be woven successfully from an unsized Kevlar warp, the weaving of broad fabrics is improved significantly by the use of a size. Most of our weaving was done with warp yarns sized with 2% polyvinyl alcohol. Determination of the number of ends and picks per inch of a given yarn denier needed to obtain a prescribed air permeability, then, involved weaving a short length of some selected construction, removing it from the loom, scouring it, measuring the air permeability and then, if the permeability was not correct, going back to the loom to readjust the construction to get closer to the target value. If the permeability of the first sample is too low, it can be raised by decreasing the number of picks per inch, by increasing the filling yarn twist, or by changing the fabric weave. In other fibers, the air permeability of the fabric can be expected to respond to such constructional changes in a fairly predictable manner. In Kevlar, however, the relationship is less predictable, as is illustrated by the values given in Table 14.

In the first group of fabrics, the end and pick counts were changed systematically. Plain woven fabrics 87, 86, 85 and 84, for example, show the effect of reducing pick count at constant ends per inch from 58 to 45. This increased the air permeability, when the warp yarns still carried size, from 6.4 to 25.7 $ft^3/ft^2/min$, consistent with expectations. When the size was removed by scouring, however, the warp yarns flattened out to such an extent that the permeability was low (5.7 $ft^3/ft^2/min$) and, more importantly, virtually unaffected by this large reduction in picks per inch. When the ends per inch were reduced, as in fabrics 88A, B and C, so that the fabric was more open, a relatively small reduction in picks per inch from 48 to 44 and then to 40 had a significant effect on air permeability, even in the scoured state.

The effect of changes in yarn twist is illustrated in the next group of fabrics. In fabrics 77G and 77H the addition of 3 turns per inch of twist to the filling yarn only has significantly increased the permeability in the sized condition. Other examples are shown in the 79 series of fabrics, which also illustrates the influence of fabric weave. Note, however, that no measurements were made after removal of the warp size, which would be expected to show the behavior mentioned above, namely, that changes in filling yarn twist would have little if any influence on the permeability of a fabric with a tightly packed warp, but a significant influence when the warp yarns are not closely packed.

Weave changes have the expected results, which are that a reduction in interlacing density produces an increase in air permeability.

Only two broad fabrics were produced in any quantity in this program. One was a canopy fabric, the other a pack fabric. Their constructions and characteristics are given in Table 15. Load-elongation curves for warp and filling directions of the canopy fabric are given in Figure 35.

53

TABLE 14

EFFECT OF CONSTRUCTION ON THE AIR PERMEABILITY
OF KEVLAR BROAD WOVEN FABRICS

FRL Sample No. 5034-	Yarn Denier	Twist (tpi) Warp	Twist (tpi) Fill	Weave	Ends per Inch	Picks per Inch	Air Permeability* Sized	Air Permeability* Scoured	Warp Strength (lb/inch)	Weight (oz/yd²)
87	200	0	0	plain	60	58	6.4	5.6	460	3.2
86	200	0	0	plain	60	54	9.3	5.2	---	3.2
85	200	0	0	plain	60	50	11.4	4.7	460	3.0
84	200	0	0	plain	60	45	25.7	7.2	490	2.9
88C	200	0	0	plain	45	48	---	72.0	---	2.5
88B	200	0	0	plain	45	44	---	80.0	---	2.4
88A	200	0	0	plain	45	40	---	85.0	---	2.3
77G	400	0	0	plain	40	34	50	---	---	4.1
77H	400	0	3	plain	40	34	60	---	---	4.1
79B	100	0	0	1/3 twill	60	60	80	---	170	1.7
79C	100	0	5	1/3 twill	60	60	150	---	---	1.7
79A	100	0	0	2/2 twill	60	60	30	---	---	1.7
79E	100	0	2	2/2 twill	60	60	90	---	---	1.7
79D	100	0	5	2/2 twill	60	60	165	---	---	1.7
4B	200	0	0	plain	58	60	---	2	360	3.2
5	200	0	0	2/2 basket	59	59	---	18	400	3.2
6	200	0	0	2/2 twill	52	53	---	10	330	2.8
58	200	0	0	2/1 twill	54	54	---	75	---	3.1
7	200	0	0	3/1 twill	51	52	---	65	330	2.8
8	200	0	0	1/3 twill	51	51	---	60	320	2.8
10	200	0	0	4/4 twill	51	54	---	28	280	2.9
12	200	0	0	8 harness, 3 move satin	53	53	---	44	370	2.8
13	200	0	0	8 harness, 3 move satin	52	74	---	31	350	3.4
11	200	0	0	8 harness, 5 move satin	53	73	---	32	370	3.4

*Air Permeability, ft³/ft² at 0.5" water pressure differential.

TABLE 15

KEVLAR BROAD WOVEN FABRIC CONSTRUCTIONS

	Canopy Fabric 5034-60	Pack Fabric 5034-118
Yarn Denier		
Warp and Filling	200	200
Yarn Twist (tpi)		
Warp	5Z	0
Filling	0	0
Ends x Picks per Inch	55 x 54	60 x 43
Weight (oz/yd^2)	2.9	3.0
Thickness (inch) at		
0.02 psi	0.0076	---
0.1 psi	0.0059	---
Air Permeability (ft^3/ft^2/min at 0.5" water pressure differential)	67	6
Breaking Strength (lb/inch)		
Warp	360	---
Filling	340	---
Breaking Elongation (%)		
Warp	2.7	---
Filling	2.6	---
Rupture Energy (in. lb/in.)		
Warp	3.8	---
Filling	3.6	---
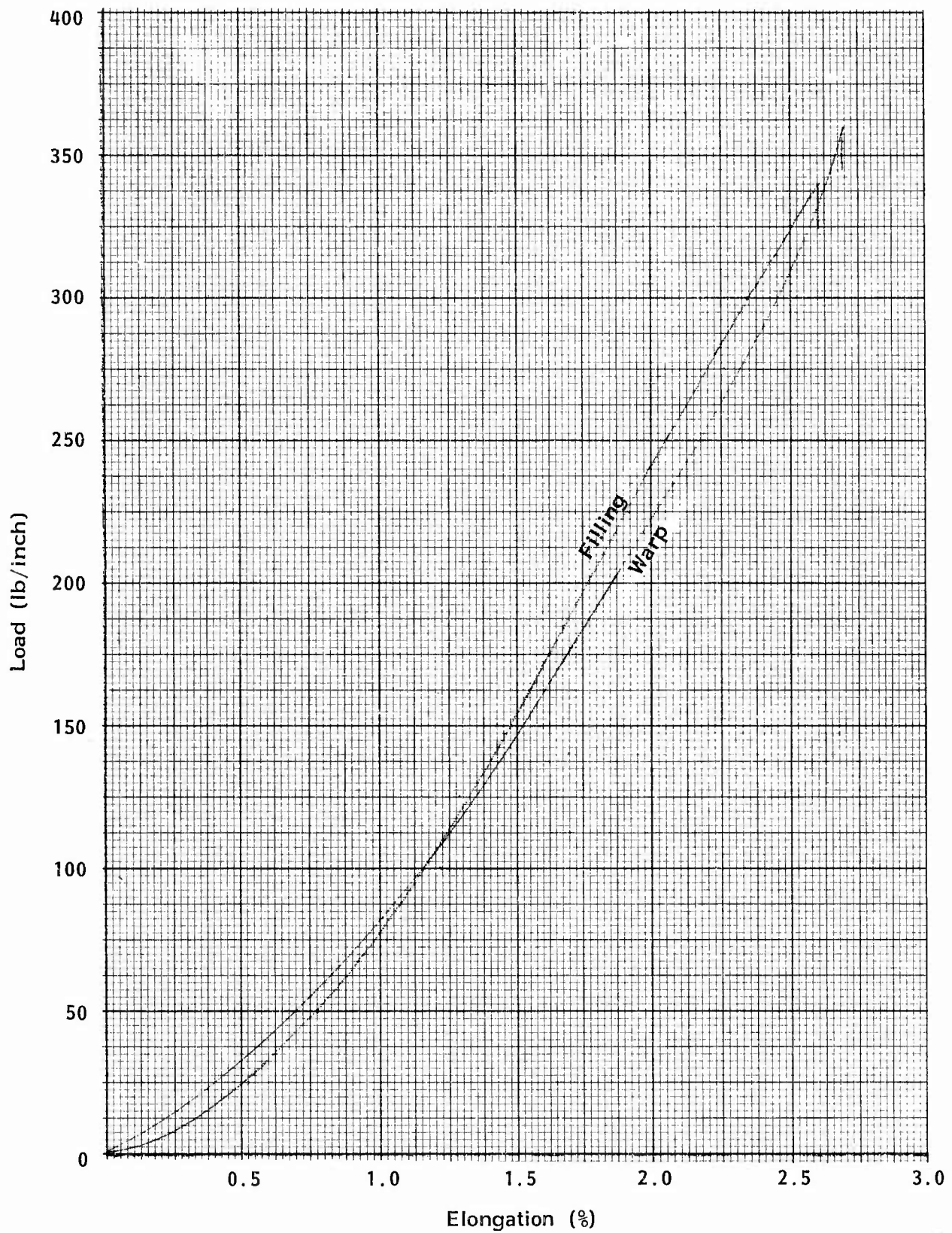
Figure 35. Load-Elongation Characteristics of Kevlar Canopy Fabric

VII. BRAIDED CORDS

Basic Structure

Braided cords used in nylon parachute systems may be either coreless (MIL-C-7515) or cored (MIL-C-5040). The latter contain a straight, central yarn assembly, the core, surrounded by a braided tube, the sheath. The coreless cords consist simply of a braided tube, corresponding in structure approximately to the sheath, without any central core. In order to obtain good strength translation efficiency in a cored braid, the elongation properties of core and sheath must be carefully matched. In a nylon cord, this is usually done by inserting a fairly high twist in the core yarn in order to give it a higher elongation to match the characteristics of the sheath. This is possible, within reasonable limits, because of the high elongation inherent in the nylon yarn itself.

In braids made from Kevlar yarns, which have extremely low elongation and in which the insertion of high levels of twist drastically reduces the strength, it was not possible to balance the elongation characteristics of a twisted core with those of a braided sheath. Thus, it did not seem feasible to make an efficient cored braid from Kevlar. All of the braids which were designed, therefore, were coreless.

Braid Construction

A braiding machine uses an even number of ends of yarn, half of which are wound around the structure in a clockwise direction, the other half in a counterclockwise direction. In order to balance torques and achieve a structure with no tendency to twist or kink, one set of yarns is twisted in a Z-direction, while the other set has an S-twist. Aside from the size of yarn used and the number of ends which are braided together (usually 8, 16, 24, 32, 64 or 96) the braid construction is determined by the relationship between the rate at which the braid is drawn off the machine and the speed of revolution of the yarn carriers in their circular track. This ratio (A/B) determines both the braid angle, which is the angle between the yarns and the axis of the braid, and the picks per inch, or the number of yarns intersected per inch by a line drawn parallel to the braid axis. As the size of the ratio increases, so does the braid angle and the picks per inch. Thus, a low ratio value implies an open, loose braid, and a high ratio a tight braid.

Experiments with seven different braid constructions gave relationships between the A/B ratio and the strength translation efficiency of the form illustrated in Figure 36, which is for a series of braids made from 1000 denier, 3-ply Kevlar yarn on a 16 carrier braider. The consistent decrease of strength translation efficiency with increasing A/B ratio is in part a geometric effect, and in part a true loss in yarn strength due to increasing yarn/yarn interactions within the structure. Thus, if strength were the sole criterion, we would choose the lowest possible ratio. In parachute applications, however, braid constructions must be tight enough to give good structural integrity, as well as providing for good strength in joints made by back-splicing. The final selection of braid construction, therefore, is the choice of the openest construction which will provide the desired integrity and spliceability.

57
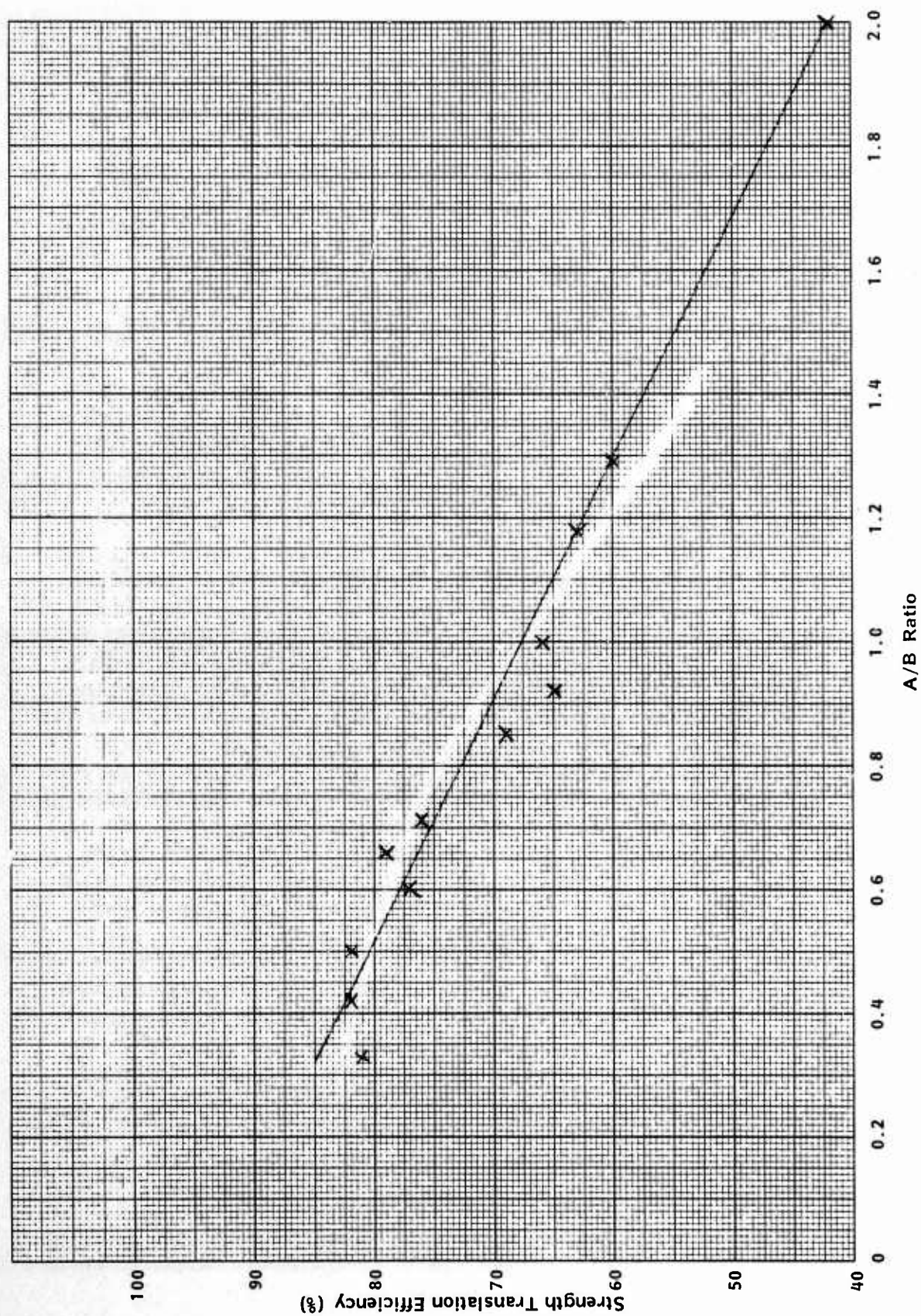
Figure 36. Relationship Between Strength Translation Efficiency and Construction for Kevlar Coreless Braided Cords

The final constructions chosen for the range of braids called for are given in Table 16. Strength translation efficiencies ranged from 60 to 96%, the weakest braids having the highest efficiencies.

Stress-Strain Behavior

Stress-strain curves for all of the braids listed in Table 15 are given in Figures 37 through 48.

VIII. SEWING THREADS

Choice of a suitable sewing thread for any application depends on thread diameter as well as strength. Because Kevlar threads can all be expected to have adequate strength, it was decided that the range of designs should be developed to duplicate, as closely as possible, the diameters of the corresponding nylon threads.

Using Federal Specification V-T-295 as a guide, nine Kevlar threads were designed to approximate the diameters of nylon threads size A, B, E, F, FF, 3-cord, 5-cord, 6-cord and 8-cord. Singles yarn deniers and twist levels were chosen to correspond as closely as possible to the nylon counterparts.

The resulting designs are given in Table 17, which also summarizes the results of measurements of tensile, knot and loop strengths and weight. The tensile strengths of the Kevlar threads average about 2-1/2 times that of their nylon counterparts, while the knot and loop efficiencies are only approximately one half those of the nylon threads. Thus, absolute knot and loop strengths of the Kevlar threads are only slightly higher than those of the corresponding nylon threads.

Sewability tests run at Wright-Patterson Air Force Base using all of these threads gave good results. Even without an added finish, good seams could be sewn using standard commercial equipment and techniques.

Subsequent use of some of these threads indicated that a good finish on the thread might aid in handling as well as in seam efficiency. A standard wax finish made little improvement, but it was found that application of as little as 1/2 to 1% of polyvinyl butyral to the thread gave better structural integrity, improved sewability and, in some cases, higher seam efficiencies. This finish is offered as an alternative in the tentative draft Military Specification for Kevlar sewing threads. It is applied by passing the thread through an impregnating bath containing 20% by weight of Butvar Dispersion BR (Monsanto Corporation, 50% solids in the product), followed by wiping over a soft felt and drying in a heated tube or over drying cylinders.

TABLE 16

CONSTRUCTION AND CHARACTERISTICS OF KEVLAR CORELESS BRAIDED CORDS

Draft Spec Type No.	FRL Sample No.	Diameter on Flat Width (inch)	Strength Mean (lb)	Range Low	Range High	Translation Efficiency (%)	Elong (%)	Weight (ft/lb)	Yarn den/ply/twist[1]	No. Carriers	Ends per Carrier	Total Ends	Picks[2] per Inch
I	21	0.017	40	37	41	92	3.7	15,000	200/1/5.0	4	1	4	9
II	22	0.026	80	78	81	91	4.2	7,200	200/1/5.0	8	1	8	18
III	39	0.050	155	150	160	96	4.0	3,600	200/1/5.0	16	1	16	23
IV	40	0.093	450	430	460	82	---	1,200	200/3/2.5	16	1	16	15
V	23	0.114	655	640	680	82	3.7	800	1000/1/4.0	16	1	16	13
VI	24	0.134	855	840	870	81	4.1	475	1500/1/3.0	16	1	16	11
VII	25	0.157	1220	1180	1240	77	4.2	375	1000/2/2.1	16	1	16	10
VIII	26	0.200	1705	1660	1750	75	4.1	225	1500/2/1.8	16	1	16	8
IX	28	0.240	2260	2200	2300	77	3.9	150	1500/3/1.0	16	1	16	7
X	29	0.347	4000	3700	4300	60	5.2	75	1500/6/1.0	16	1	16	6
XI	41	0.500	7190	6900	7500	72	3.7	55	1500/6/1.0	24	1	24	4

1. When a plied yarn is used, this is the value of the ply twist. Singles twist is always zero, or producer's twist. Half of the yarns in each cord are Z-twist, the other half S-twist.

2. All constructions are a 2 over, 2 under conventional stitch except Type I, which is a 1 up, 1 down basket or diamond.

60
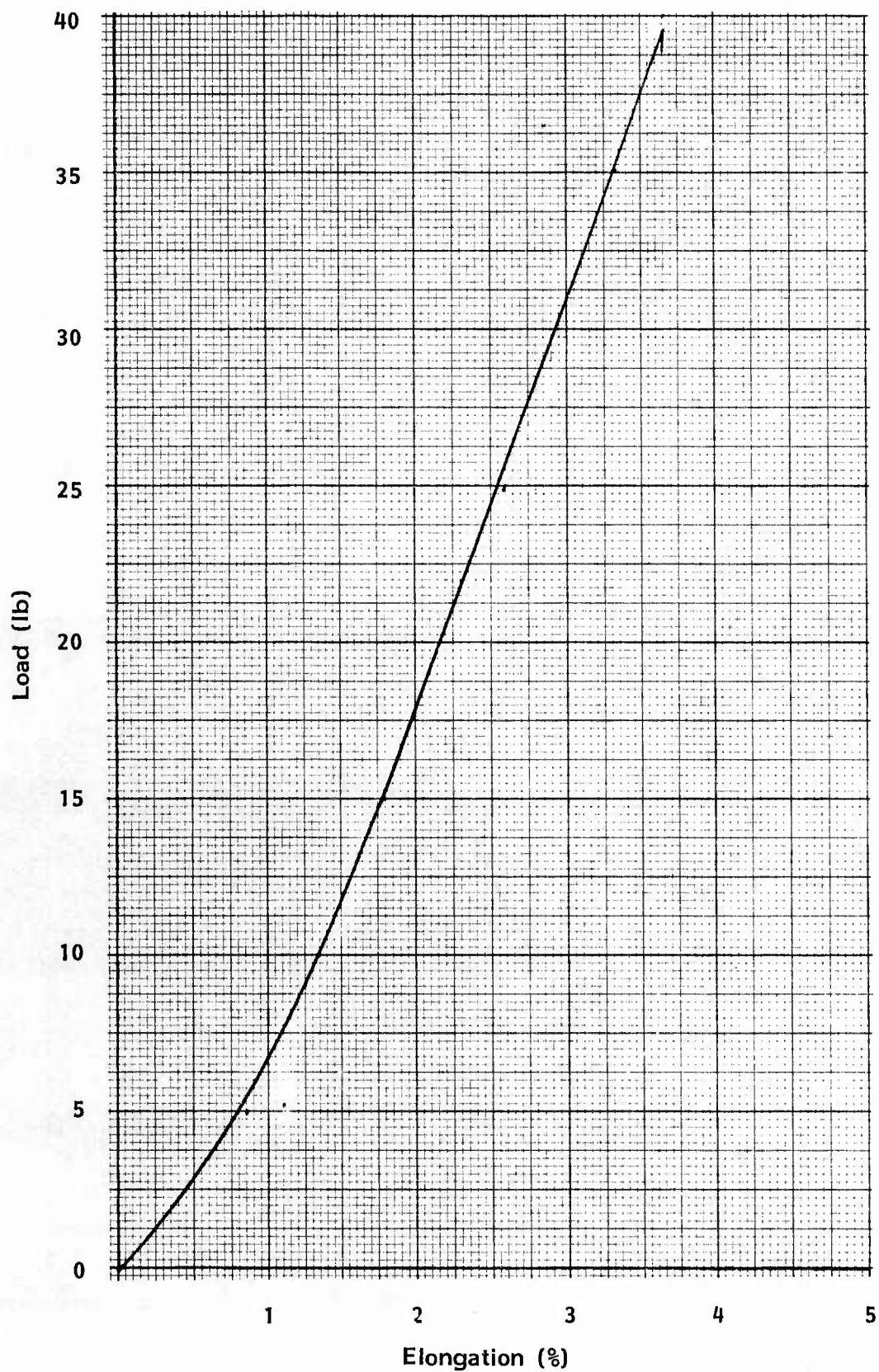
Figure 37. Average Load-Elongation Curve for Kevlar 29 Braided Cord, Type I (FRL Sample No. 5034-21)
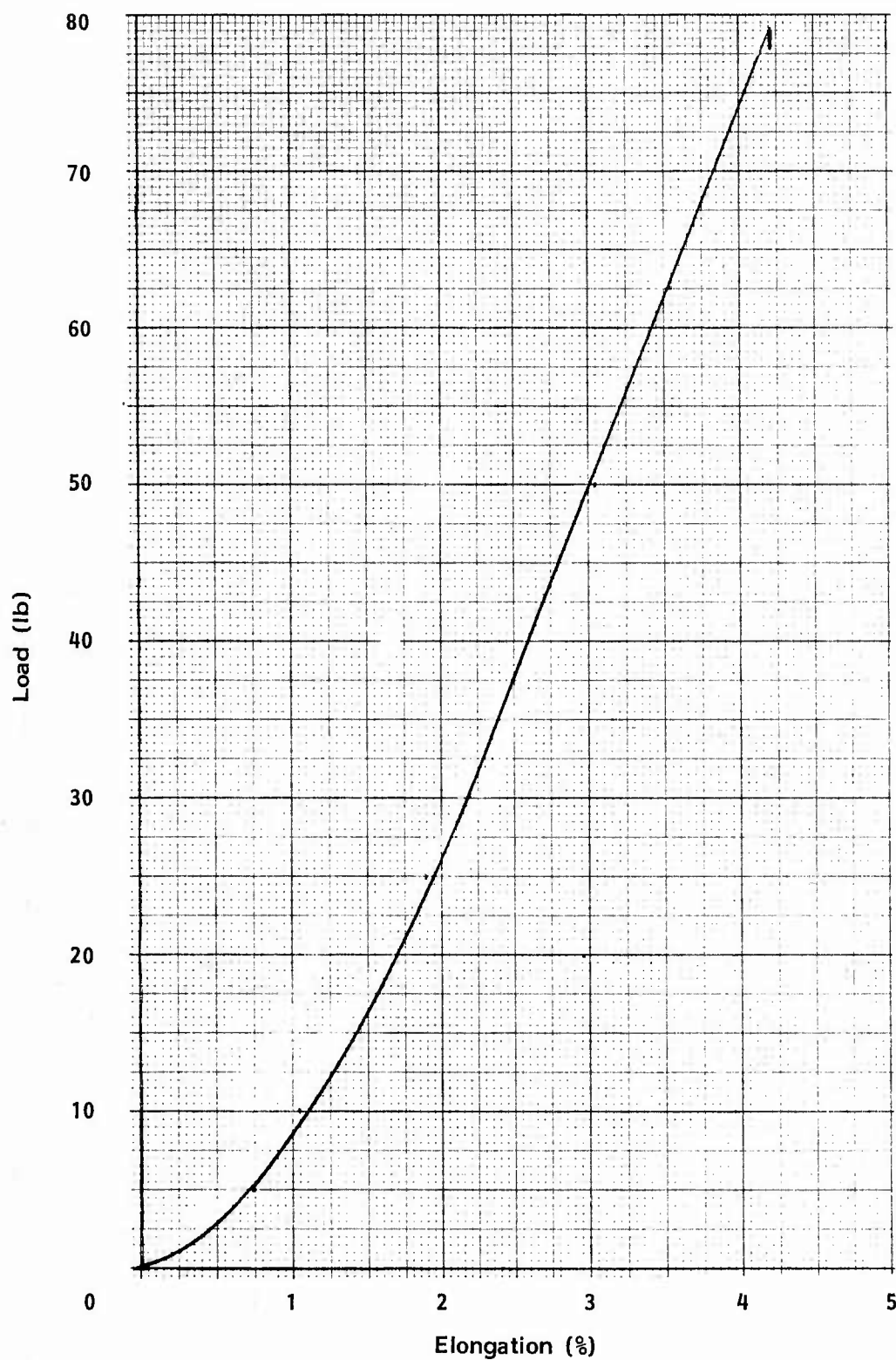
Figure 38. Average Load-Elongation Curve for Kevlar 29 Braided Cord,
Type II (FRL Sample No. 5034-22)
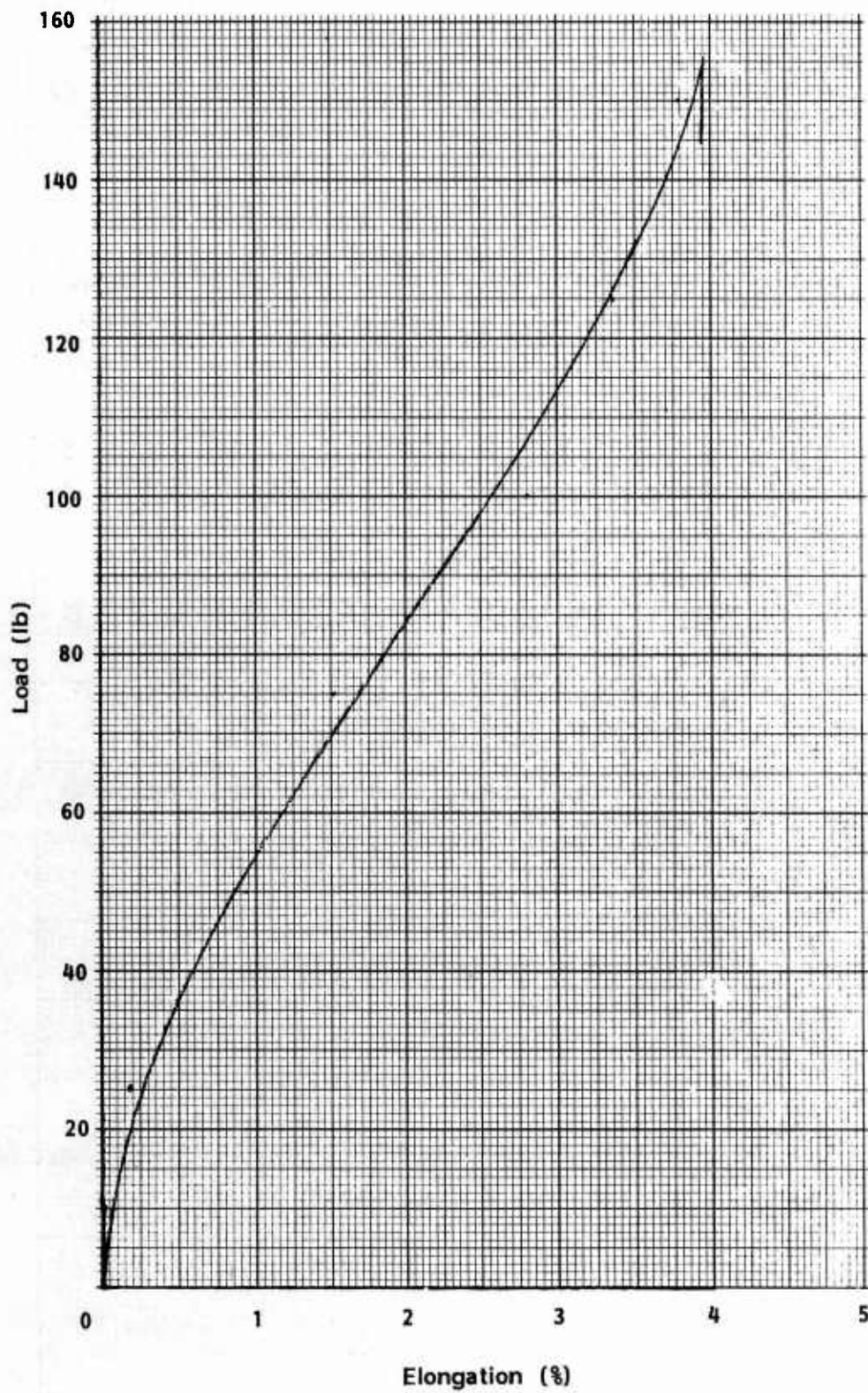
Figure 39. Average Load-Elongation Curve for Kevlar 29 Braided Cord,
Type III (FRL Sample No. 5034-39)
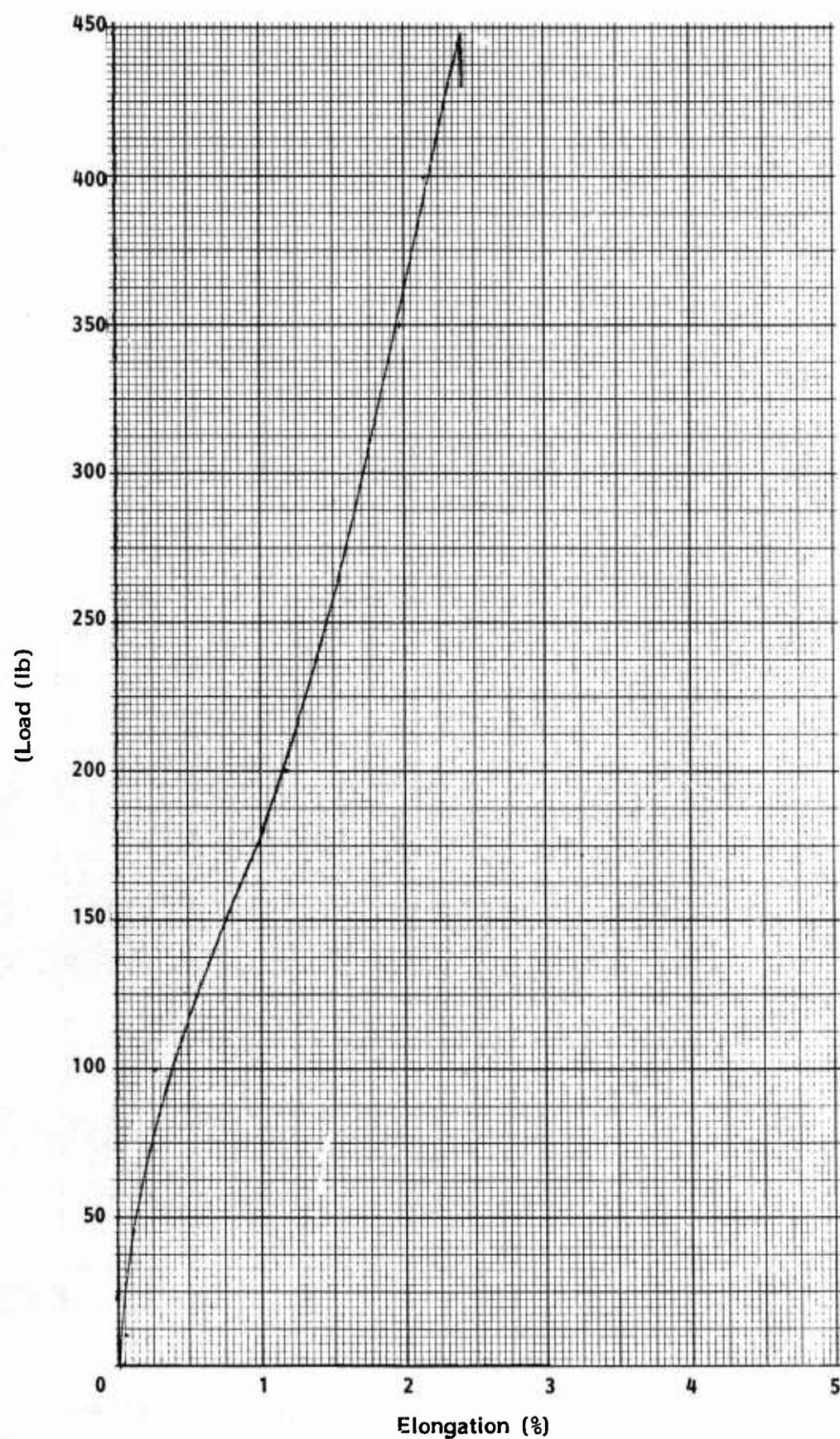
Figure 40. Average Load-Elongation Curve for Kevlar 29 Braided Cord,
Type IV (FRL Sample No. 5034-40)

64
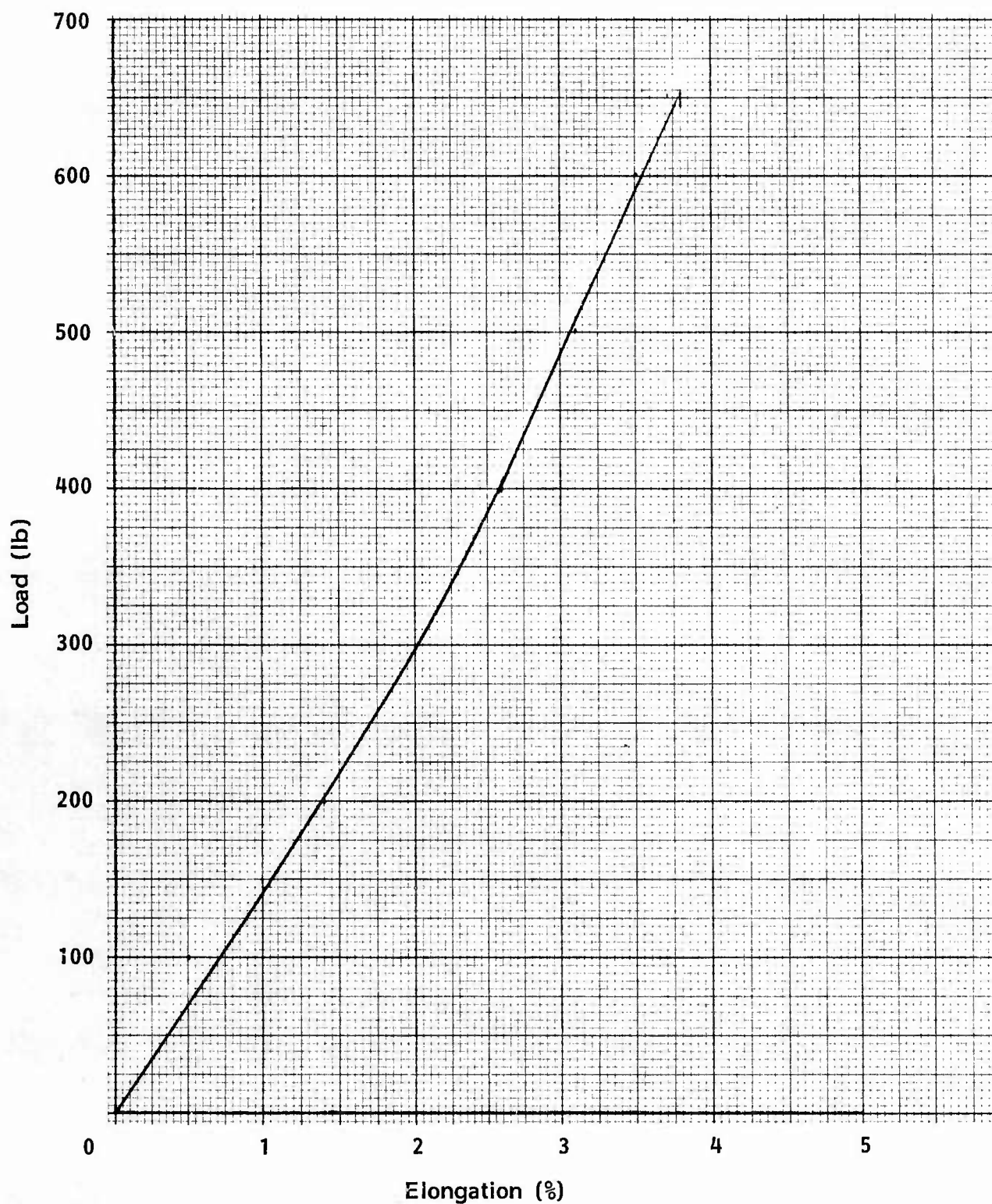
Figure 41.   Average Load-Elongation Curve for Kevlar 29 Braided Cord,
Type V (FRL Sample No. 5034-23)
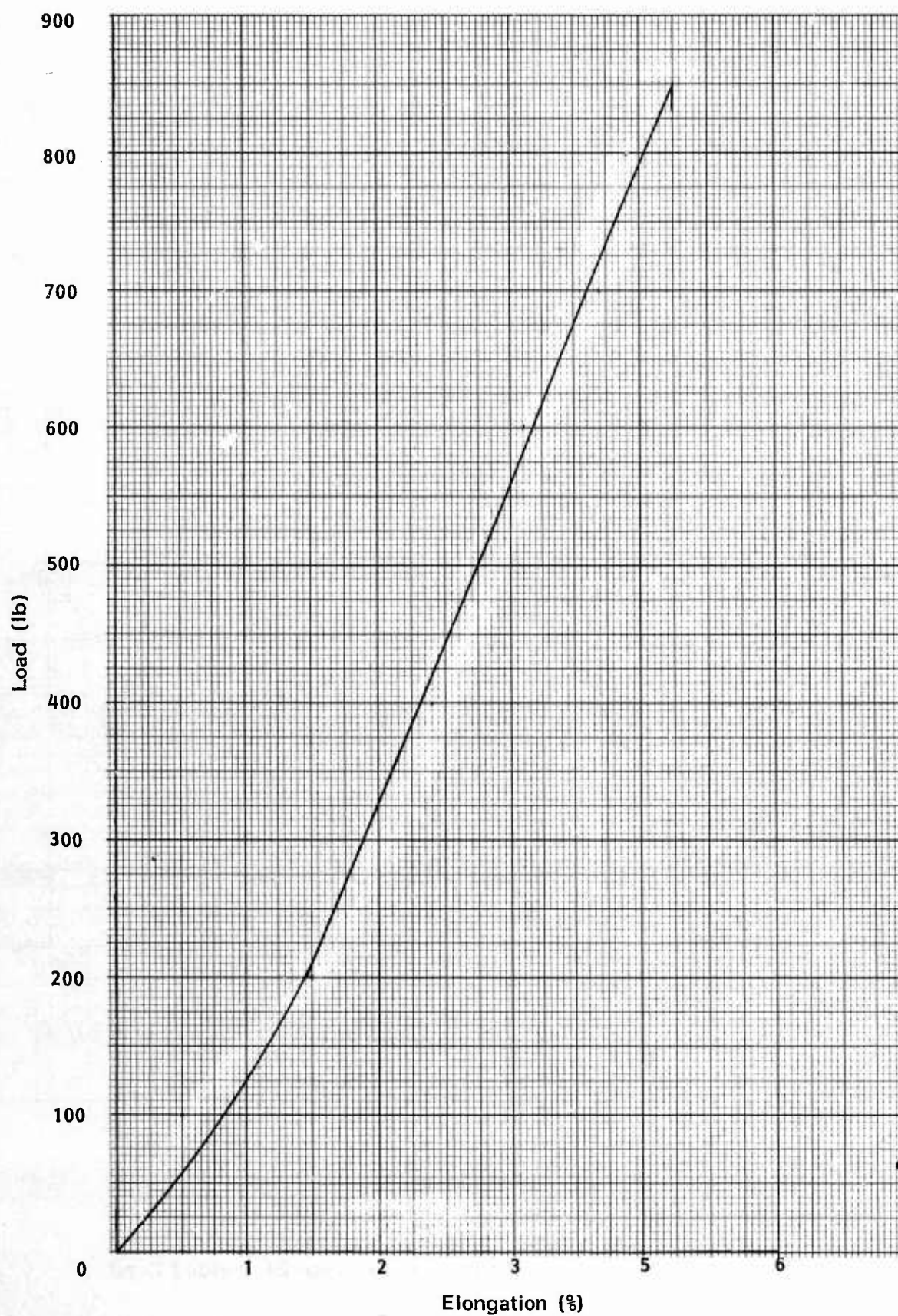
Figure 42. Average Load-Elongation Curve for Kevlar 29 Braided Cord,
Type VI (FRL Sample No. 5034-24)
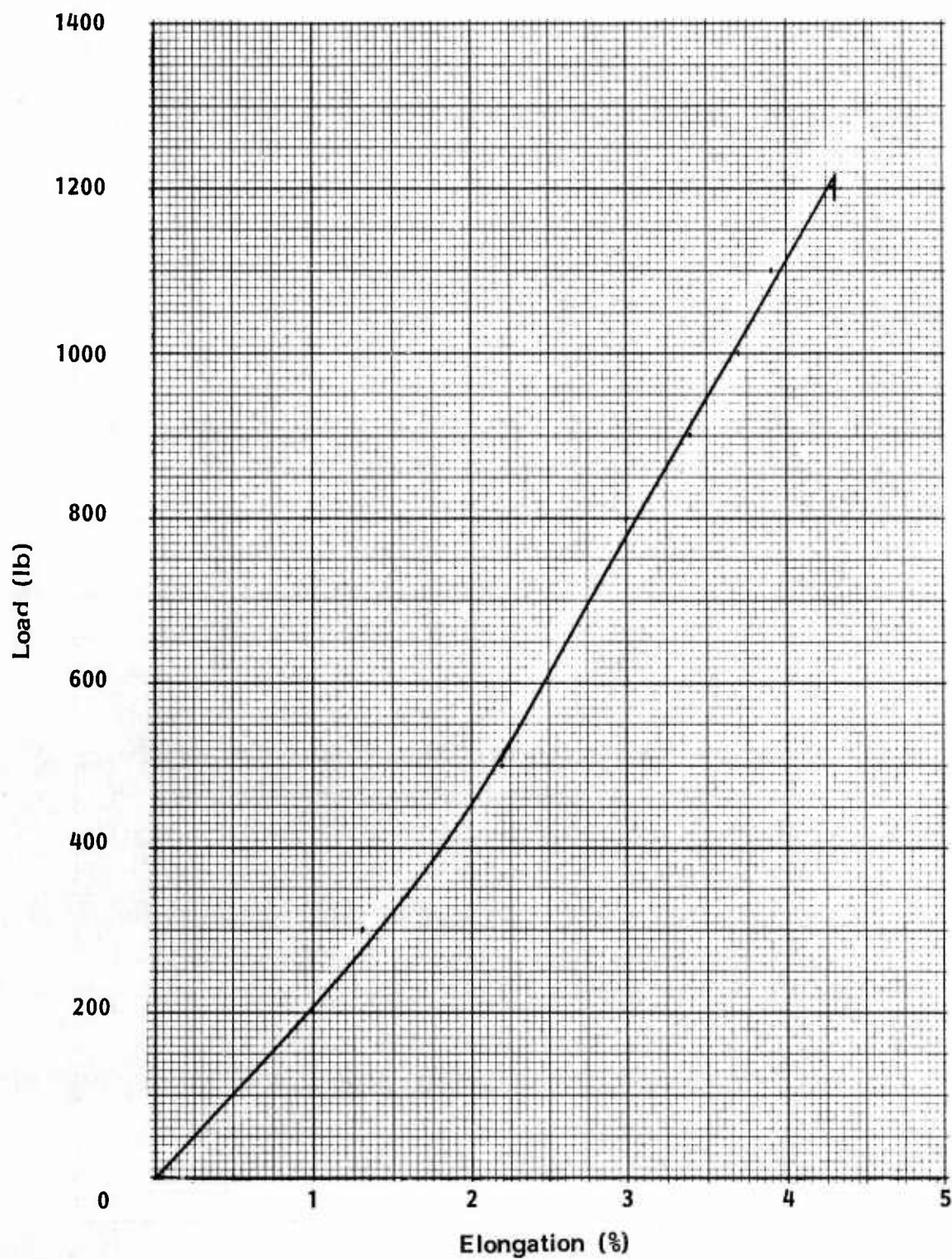
Figure 43. Average Load-Elongation Curve for Kevlar 29 Braided Cord,
Type VII (FRL Sample No. 5034-25)

67
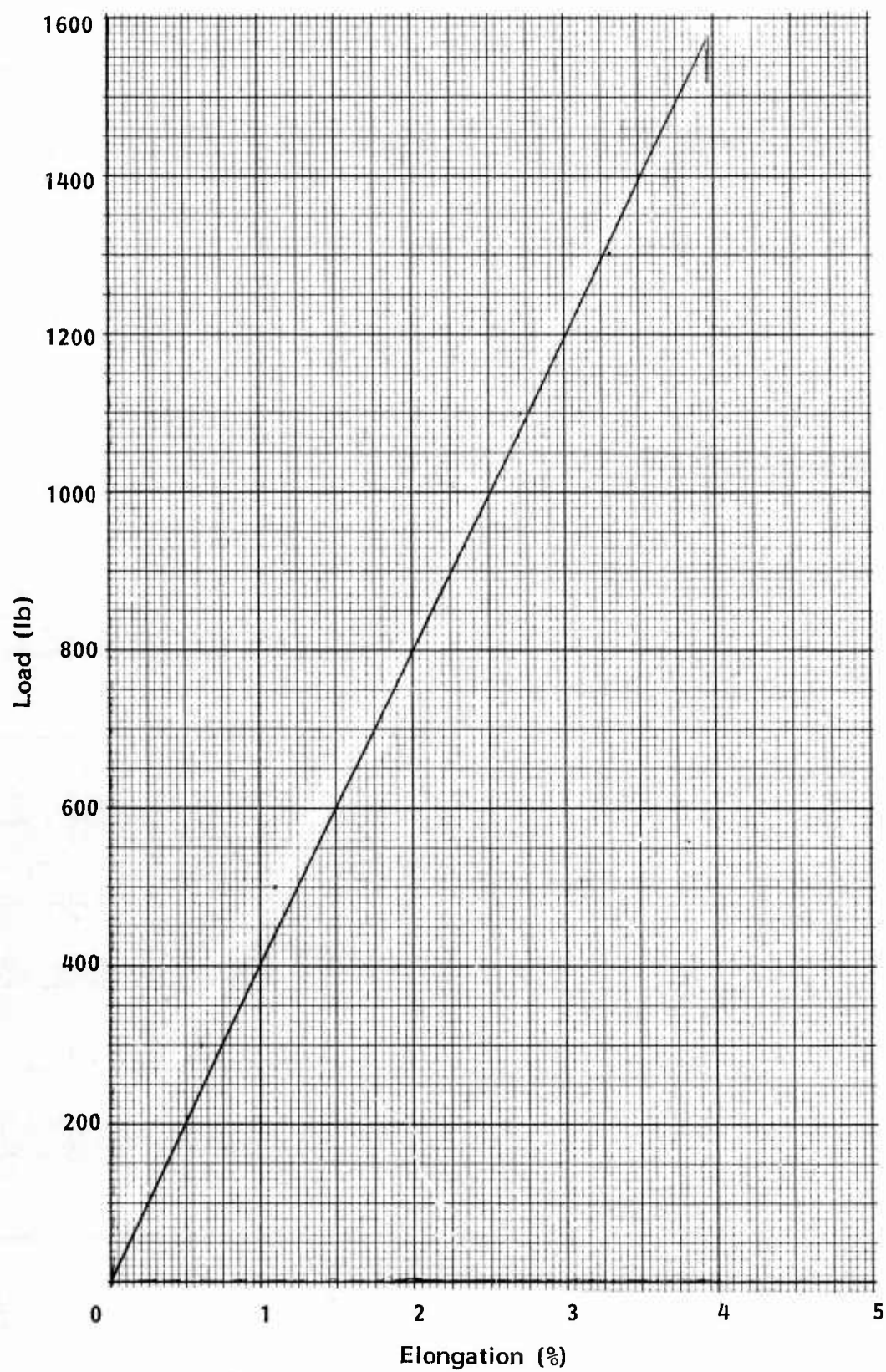
Figure 44. Average Load-Elongation Curve for Kevlar 29 Braided Cord, Type VIII (FRL Sample No. 5034-26)

68
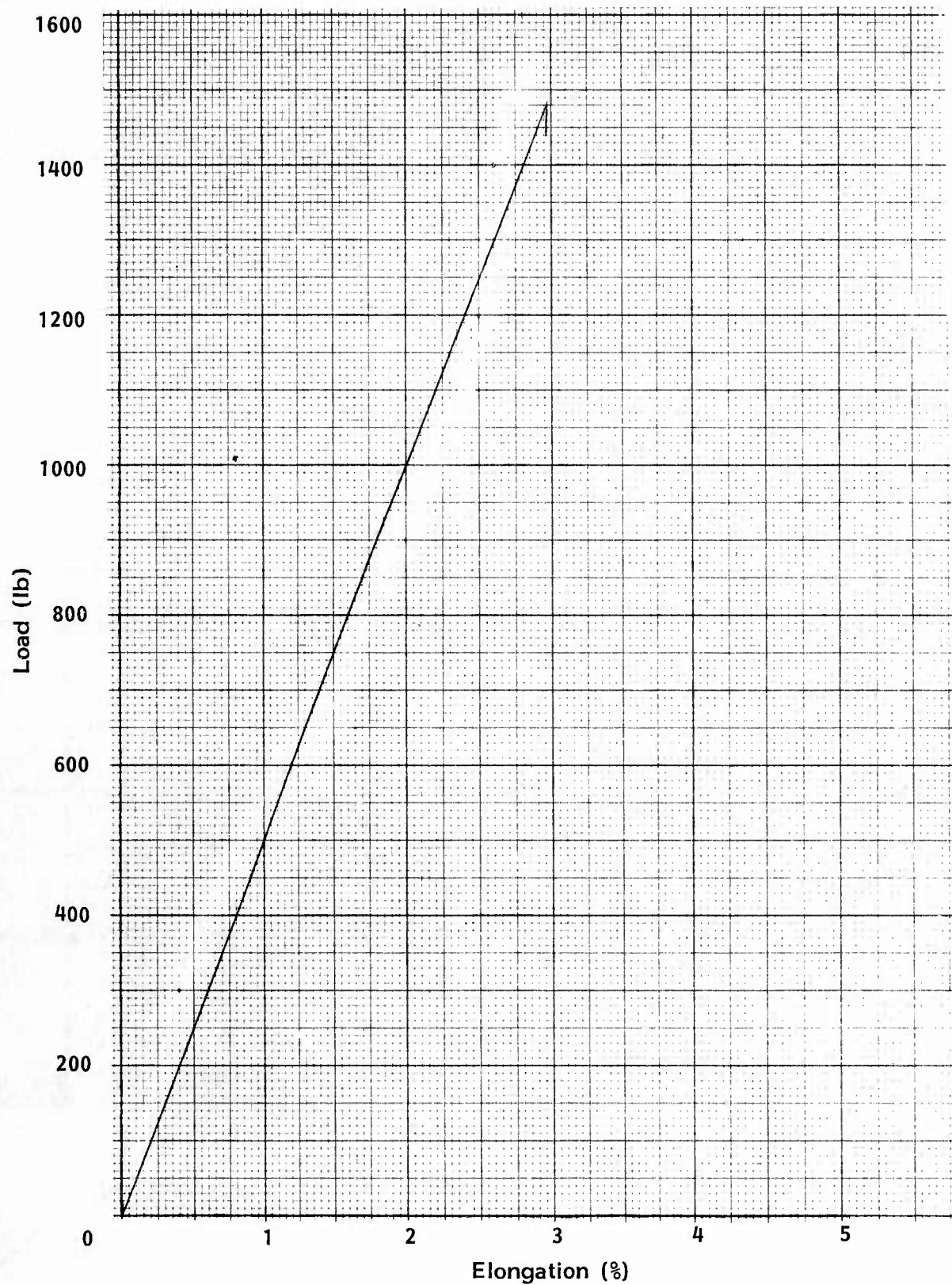
Figure 45.   Average Load-Elongation Curve for Kevlar 49 Braided Cord,
Type VIII (FRL Sample No. 5034-27)
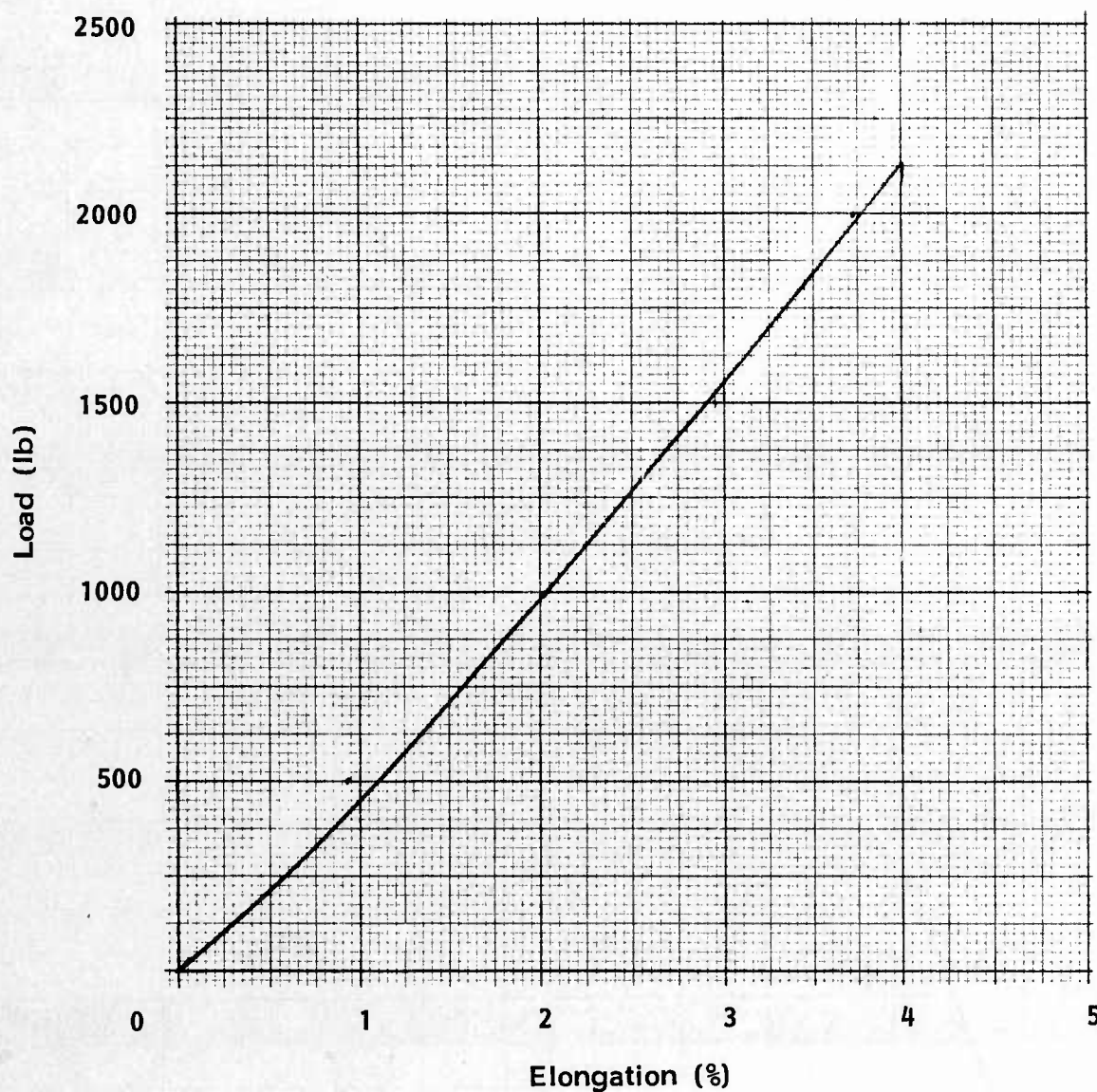
Figure 46.   Average Load-Elongation Curve for Kevlar 29 Braided Cord, Type IX (FRL Sample No. 5034-28)
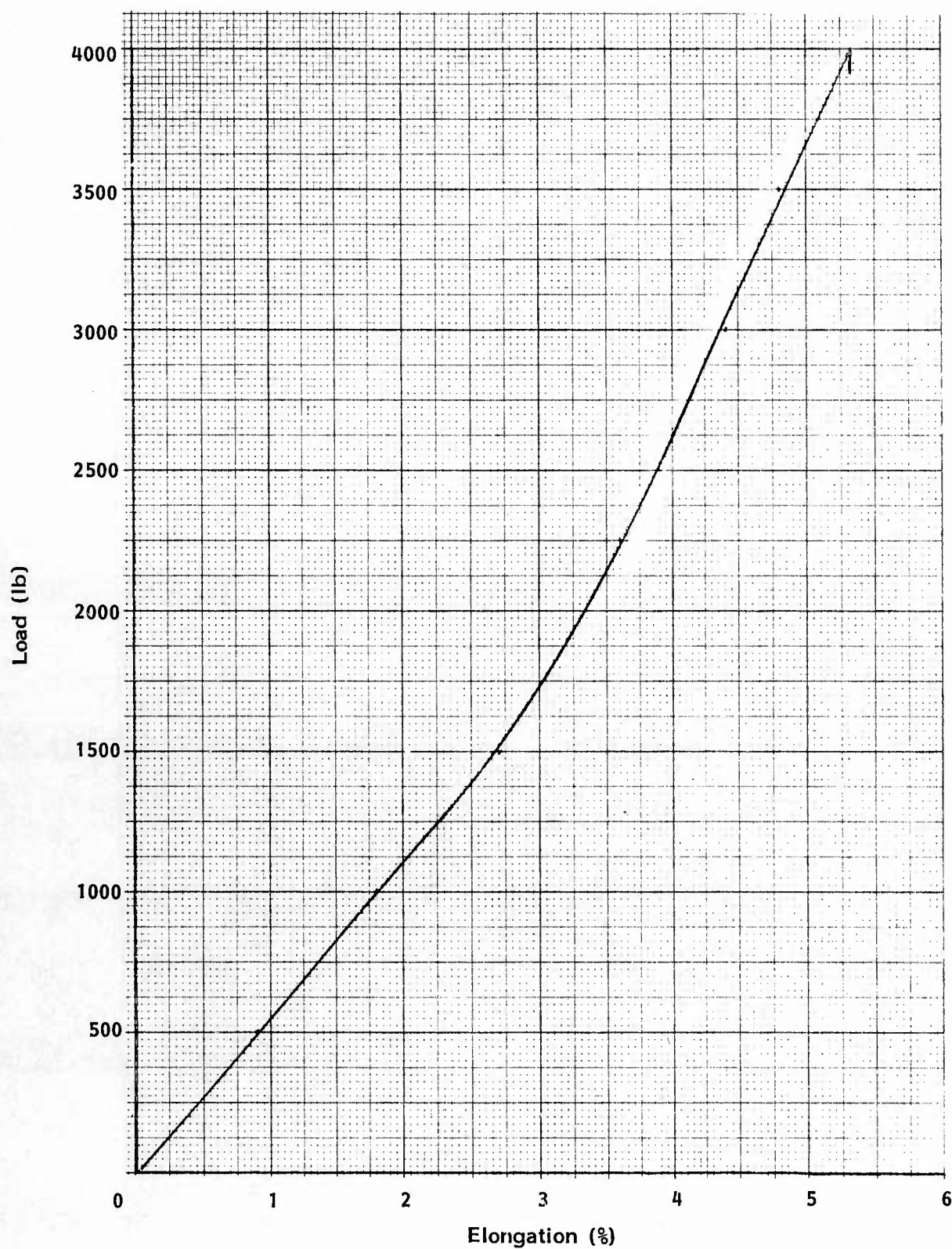
Figure 47.   Average Load-Elongation Curve for Kevlar 29 Braided Cord, Type XI
(FRL Sample No. 5034-29)

71
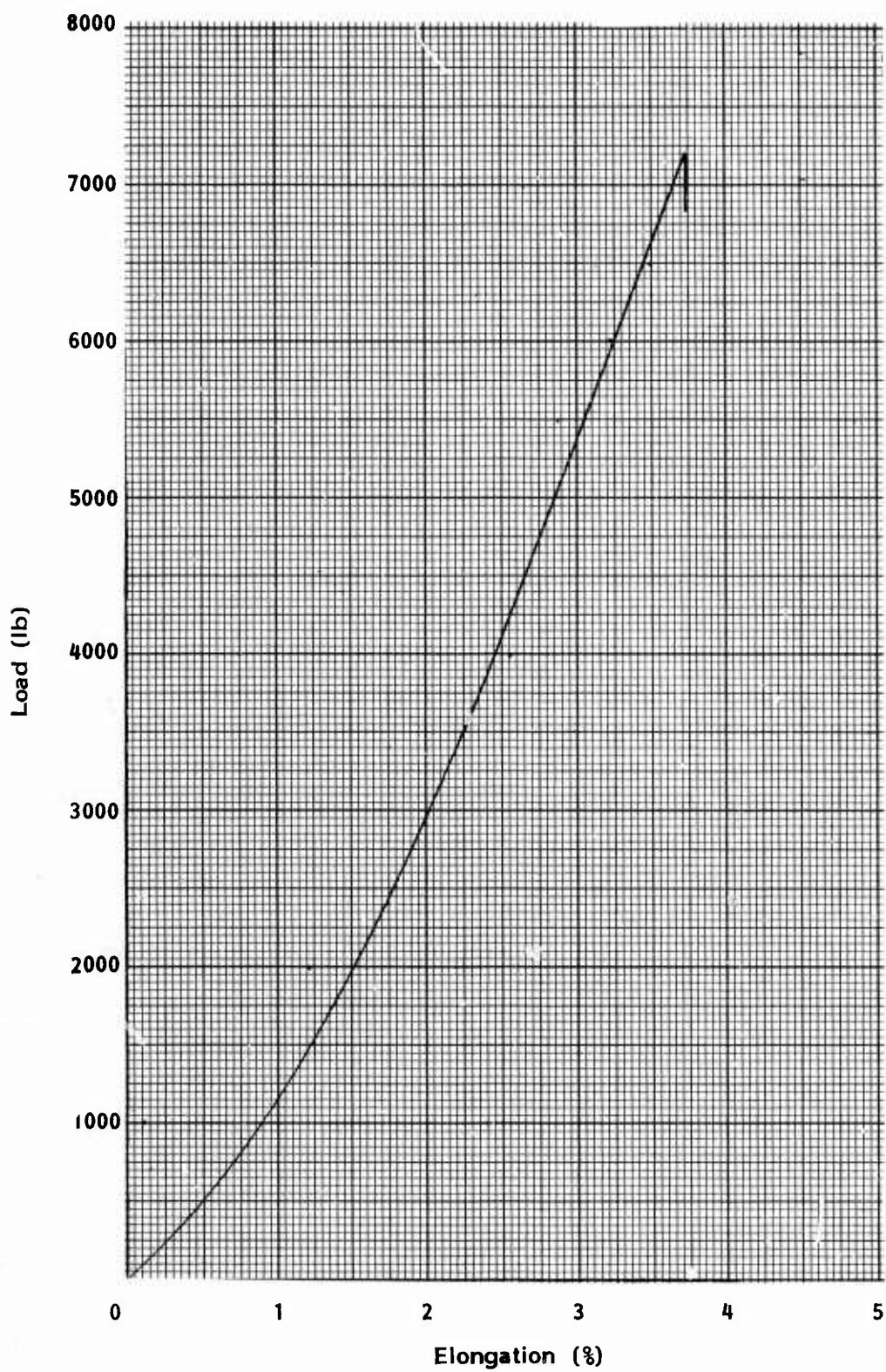
Figure 48. Average Load-Elongation Curve for Kevlar 29 Braided Cord, Type XJ (FRL Sample No. 5034-41)

TABLE 17

CONSTRUCTION AND CHARACTERISTICS
OF KEVLAR SEWING THREADS

Designation	Diameter (inch)	Strength (lb)	Knot Strength (lb)	Knot Efficiency (%)	Loop Strength (lb)	Loop Efficiency (%)	Weight (yd/lb)	Yarn Den/Ply	Twist (tpi) Singles	Twist (tpi) Ply
A	0.008	8	3.7	33	3.6	32	20,000	100/2	20S	10Z
B	0.013	16	7.1	33	7.0	32	10,000	200/2	12S	6Z
E	0.015	25	13.1	40	13.2	40	6,700	200/3	12S	6Z
F	0.017	35	16.5	37	16.8	38	5,000	200/4	10S	5Z
FF	0.021	60	23.4	36	26.7	41	3,350	400/3	8S	4Z
3-cord	0.025	80	37.2	40	48.4	52	2,100	400/5	10S	5Z
5-cord	0.036	150	66.1	39	88.8	53	1,050	1000/4	7S	3.5Z
6-cord	0.042	175	67.7	35	89.5	46	900	1500/3	6S	3Z
8-cord	0.054	225	113.4	45	151.6	61	550	1500/5	5S	2.5Z

IX.   COMPARISON OF KEVLAR 29 AND KEVLAR 49

One of the braids which had been made from Kevlar 29 was duplicated as closely as possible using Kevlar 49 yarn. This involved substituting a 1420 denier Kevlar 49 yarn for the 1500 denier Kevlar 29 yarn used in the braid designated as Type VIII, and leaving all other aspects of the construction the same. A comparison between the properties of the two yarns is shown in Table 18.

The construction and properties of the two braids are given in Table 19.

The braid made from Kevlar 49 had a lower strength than its Kevlar 29 counterpart because of its reduced total denier and the fact that Kevlar 49 yarn has a lower tenacity than Kevlar 29 yarn. The strength translation efficiency of Kevlar 49 was somewhat higher than that for Kevlar 29. Because of the basic difference in yarn characteristics, the Kevlar 49 braid had a lower rupture elongation than the Kevlar 29 braid.

The load-elongation properties of these braids are shown in curve 3 of Figures 49 and 50. These figures also show the change in load-elongation properties resulting from cyclic stress application. Each braid was loaded, and then unloaded cyclically ten times between zero and both 50 and 75% of its rated rupture value. After a tenth cycle the sample was broken and its new rupture load and extension measured. The behavior of the Kevlar 29 cord is shown in Figure 49, while the Kevlar 49 sample is shown in Figure 50.

The results reveal an increase in strength and decrease in extension for the Kevlar 29 after cycling to 50 and 75% of rupture load with the more significant change occurring at the 75% level. Kevlar 49 does not appear to be as markedly affected, perhaps due to its higher initial modulus and lower extensibility.

After 10 cycles of loading to 75% of the rupture load, the tensile characteristics of the two braids differ only slightly. They have the same rupture elongation (2%), but the Kevlar 29 braid retains its higher strength. Similar cycling experiments with Kevlar 29 400 denier yarns showed a similar change in tensile properties. These results are shown in Table 20, which also gives comparative data for Kevlar 49 400 denier yarn (not cycled).

A few results obtained for Kevlar 29 yarn subjected to as many as 26 cycles to 75% of its rupture strain showed that its modulus had risen to 820 gpd (no information about rupture tenacity or strain is available). It is apparent that such cycling causes the tensile properties of Kevlar 29 to approach those of Kevlar 49 in both yarn and braid. It is reasonable to assume that the same change would occur in narrow and broad woven fabrics, though no measurements were made on these materials. Kevlar 49 shows much less change in tensile properties as a result of load cycling, presumably because its original properties represent the ultimate which can be easily achieved in a fiber of this chemical structure.

TABLE 18

PROPERTIES OF ZERO TWIST 1500 DENIER KEVLAR 29 AND 1420 DENIER KEVLAR 49 YARNS

Material	Actual Denier	Rupture Tenacity (gpd)	Rupture Tenacity (10³ psi)	Initial Modulus (gpd)	Initial Modulus (10⁶ psi)	Rupture Elong (%)	Energy to Rupture (gpd)	Energy to Rupture (10³ psi)
Kevlar 29	1530	20.8	386	507	9.4	3.6	0.35	6.5
Kevlar 49	1516	16.6	308	715	13.3	2.4	0.19	3.5

TABLE 19

BRAIDS MADE FROM KEVLAR 29 AND KEVLAR 49 YARNS

Material	FRL Sample No.	Strength (lb)	Strength Translation Efficiency (%)	Elongation (%)	Weight (ft/lb)	Yarn den/ply/twist[1]	No. Carriers	Ends per Carrier	Total Ends	Picks per Inch
Kevlar 29	26	1705	75	4.1	225	1500/2/1.8	16	1	16	8
Kevlar 49	27	1450	82	2.7	250	1420/2/1.8	16	1	16	8

1. This is the ply twist. Singles twist is producer's, or nominally zero. Half the yarns are Z-twist, the other half S-twist.

TABLE 20

EFFECT OF LOAD CYCLING ON THE TENSILE PROPERTIES OF KEVLAR 29 YARN

Material	Actual Denier	Strain Rate (%/min)	Strain Level % of Rupture Strain	No. Cycles	Unrecovered Strain (%)	Rupture Tenacity (gpd)	Rupture Strain (%)	Initial Modulus (gpd)
Kevlar 29	414	10	rupture	--	----	25.2	3.3	660
	414	10	75	6	0.41[1]	22.1	2.6	770
Kevlar 49	410	10	rupture	--	----	18.5	2.2	840

1. After 10 minutes relaxation.

75
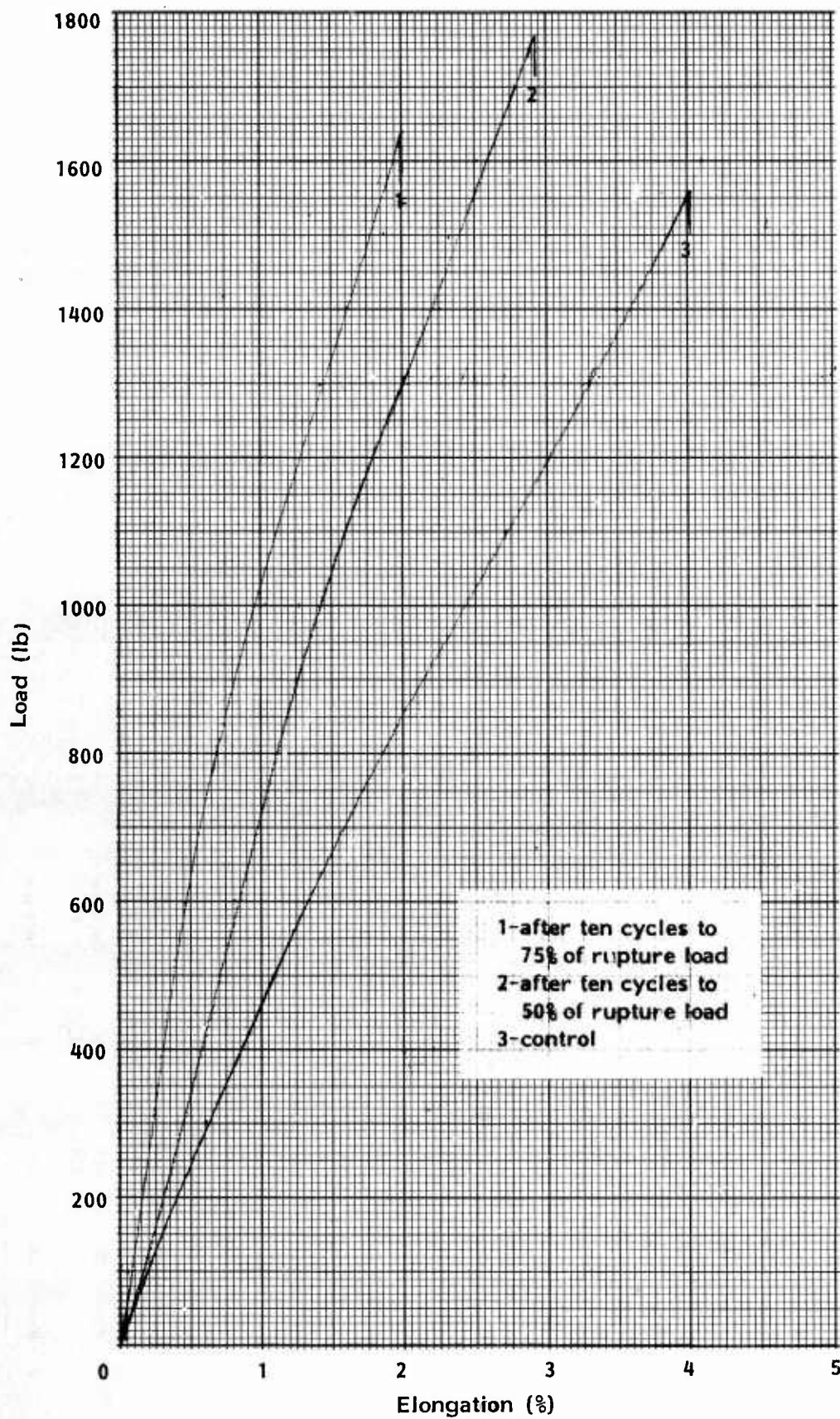
Figure 49.   Load-Elongation Curves of Kevlar 29 Braided Cord After
Cyclical Loading (FRL Sample No. 5034-26)

76
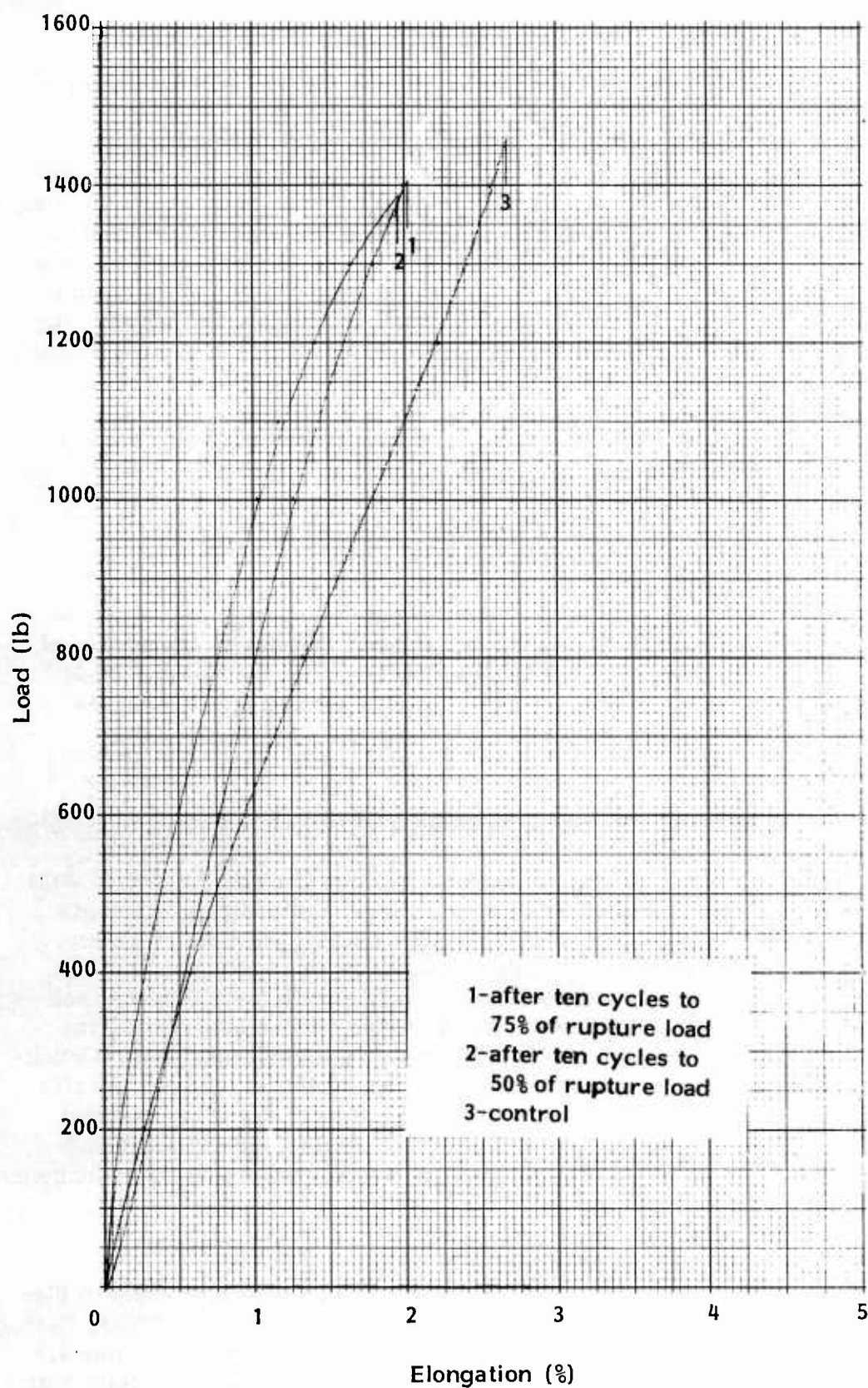
Figure 50. Load-Elongation Curves of Kevlar 49 Braided Cord
After Cyclical Loading (FRL Sample No. 5034-27)

77

X.   COMPARATIVE WEIGHTS OF KEVLAR AND NYLON WOVEN FABRICS

Initial interest in the use of Kevlar in parachute systems was the poten-
tial for weight reduction, because of Kevlar's high strength per unit weight.
The structures described in this report made it possible to determine the magni-
tude of this weight-saving in narrow fabrics. Figure 51 shows the relation-
ship between weight and strength for many of the Kevlar fabrics which were
developed, and for similar nylon fabrics for which the values were taken from
military specifications. Over the whole range of strengths represented, the
ratio of the weight of nylon fabrics to that of Kevlar fabrics of corresponding
strength is 3 or more.

Considering the fact that a significant part of the weight of a parachute
system is in the hardware, which would be the same whether the fabrics were
made from nylon or Kevlar, one could confidently expect to produce Kevlar
parachute systems at half the weight of a corresponding nylon system. Recent
experience has shown this to be correct.

Since weight and bulk are related through the specific gravity of the
fiber (1.14 for nylon, 1.45 for Kevlar) this means that Kevlar parachutes of
the same size and strength as their nylon counterparts could be packed in
almost one-half the space, or alternately a much larger Kevlar parachute
could be packed in the same space.

XI.   IMPACT STUDIES OF KEVLAR STRUCTURES

Approximately 15 years ago, under Air Force Contract AF33(616)-6321,
FRL designed and constructed a device capable of rupturing high strength
parachute components of up to 10,000 pounds breaking strength at impact
speeds between 200 and 700 feet per second. This device has been used in
the past to determine the impact behavior of textile structures in use or con-
templated for use by the Air Force. It has proven helpful in assessing the
potential value of commercial and experimentally produced materials, particu-
larly with regard to their energy-absorbing capabilities at high strain rates.
As part of the on-going Kevlar development program it was suggested that
the high strain rate response of webbings made from this new fiber be mea-
sured in order to determine their effectiveness under impact loading conditions.

The Measuring System

The impact tester as originally designed is shown schematically in Fig-
ure 52. The specimen to be impacted is folded in the shape of a "V" and fastened
to the rear of Pendulum No. 1. A missile whose mass can be varied from 0.5
to 10 pounds is propelled from a helium operated gun, through an opening in
the first pendulum, striking and rupturing the sample. The deflection of
Pendulum No. 1 resulting from the impact can be measured. After breaking
the specimen, the projectile enters and is contained in Pendulum No. 2. The
deflection of this pendulum can also be recorded.
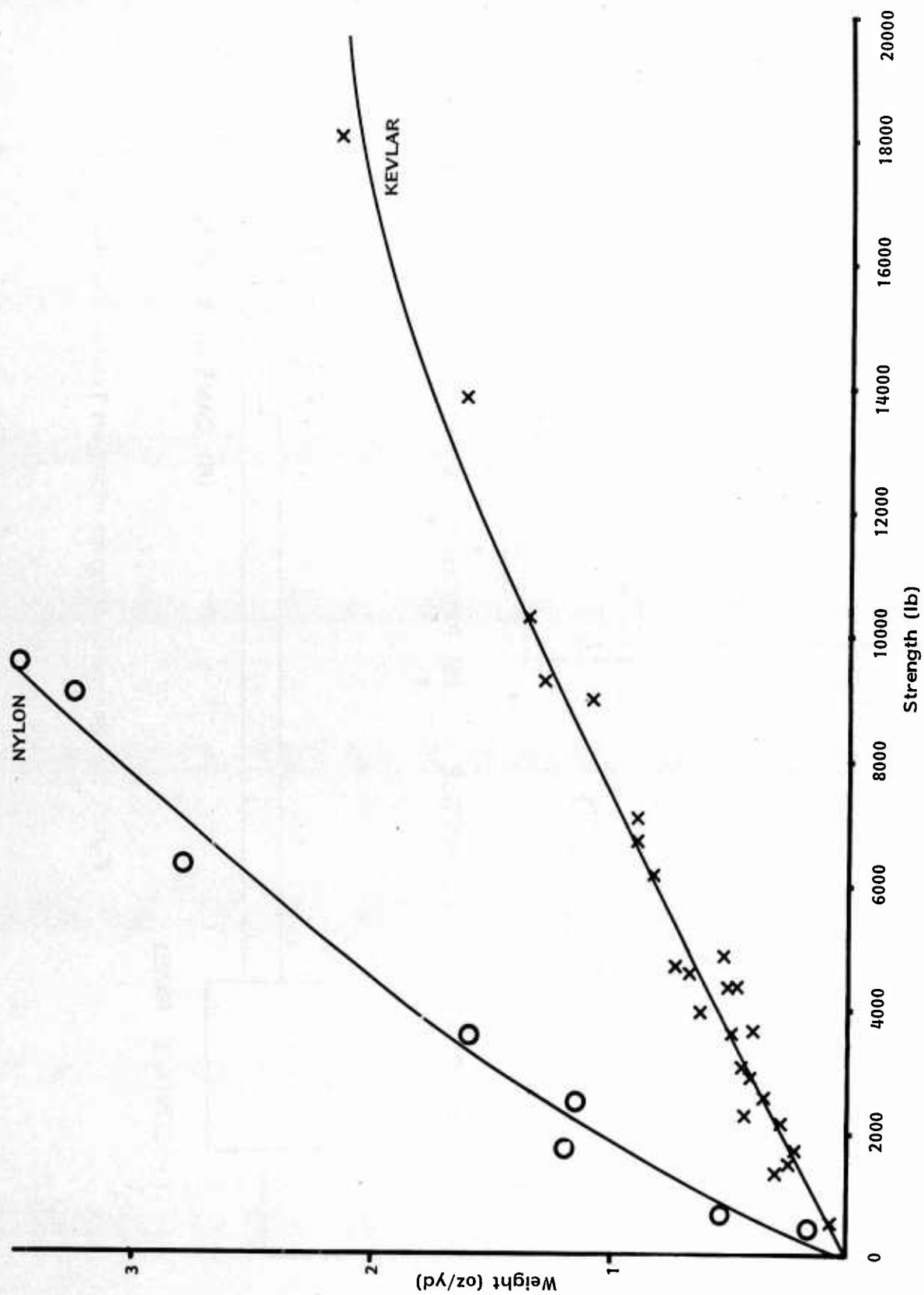
Figure 51. Strength : Weight Relationships for Nylon and Kevlar Narrow Fabric

(1) GAS GUN   (2) MISSILE   (3) PENDULUM NO. 1   (4) PENDULUM NO. 2

(5) DEFLECTION DEVICES

SPECIMEN

(6) CAMERA & LIGHT

(7) CONTROL PANEL
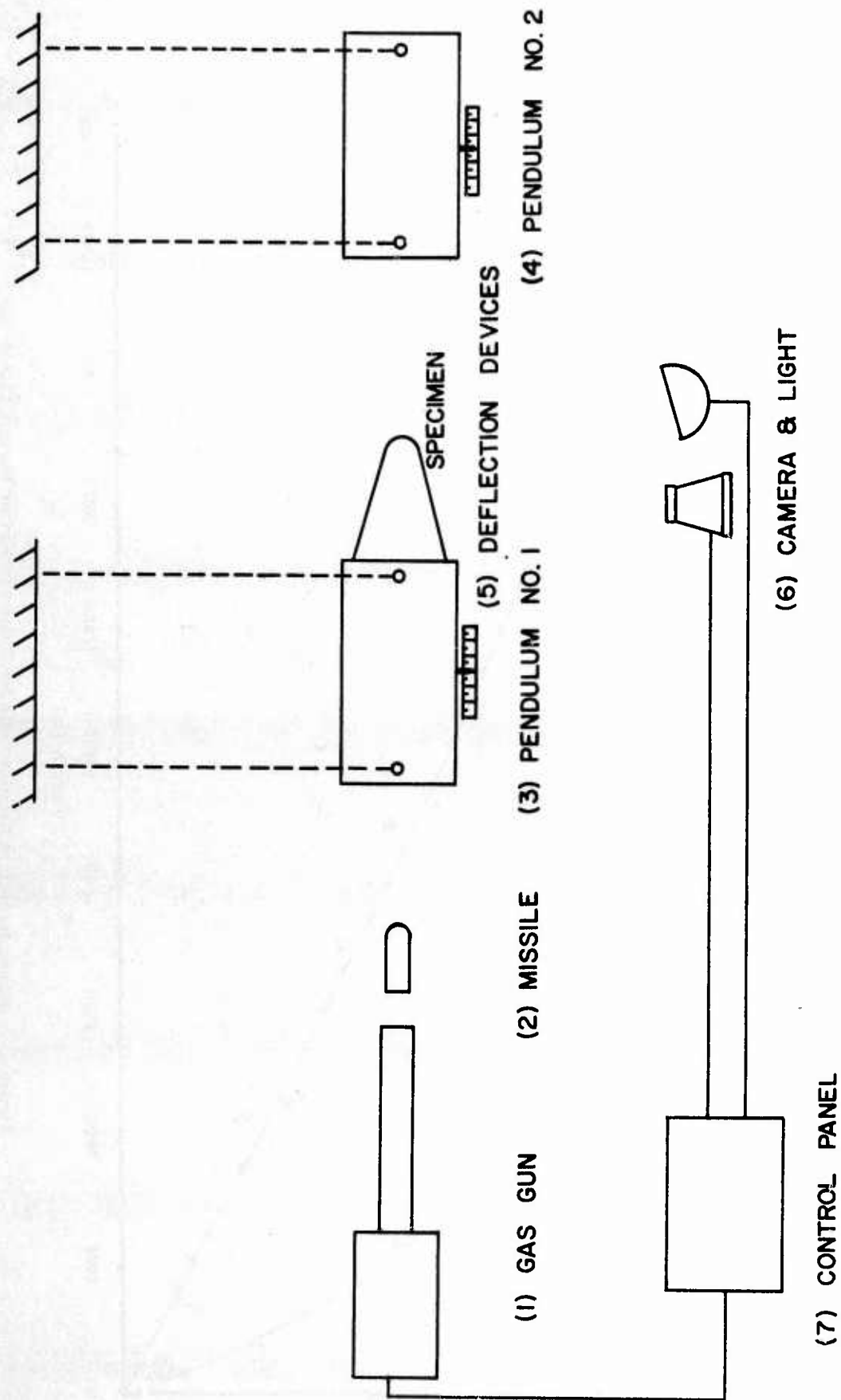
Figure 52.   Schematic Diagram of Impact Testing Machine

Knowing the period and displacement of the second pendulum, the residual velocity of the missile can be calculated. Similarly, knowing the period and displacement of the first pendulum, the loss in missile velocity as a result of specimen rupture can be determined. Having measured the residual velocity and the velocity loss, it is possible to determine the striking velocity from a summation of the two known quantities. Impact energy absorption by the specimen can then be calculated knowing the mass of the missile and its initial and final velocities.

$$E = 1/2 \, m \, (V_S^2 - V_R^2)$$

where

     E is the total energy absorbed in rupturing the specimen

     m is the mass of the projectile

     V_S is the projectile striking velocity

     V_R is the projectile residual velocity.

In addition, in much of the past work a high speed multiple flash lamp (up to 25 flashes per 10 microseconds) illuminated the event and recorded it as multiple exposure on one sheet of 4 x 5 inch photographic film. It was intended that the multiple images be used to provide information on projectile deceleration and specimen extension during impact. While much useful information was obtained from this technique, it was apparent that the measurement of precise forces and extensions was very difficult and time-consuming.

During the mid-1960s Beckman-Whitley Corp. introduced a camera, Dynafax Model 350. This camera, a rotating drum type, uses a strip of 35 mm film, approximately 34 inches long, fastened to a rotating drum together with a rotating octagonal mirror to accomplish image separation. The rotational speed of the mirror establishes the rate at which photographs of an event are taken. For example, up to 224 pictures can be taken with an exposure time of each as short as 0.75 microsecond, and constant time between successive exposures as short as 28.6 microseconds. This means that at projectile speeds of 200 feet per second, the position of the missile can be recorded approximately every 1/16 inch during its travel over a one-foot distance. With this capability it is felt that more precise measurement of force (via missile deceleration) and specimen extension can be made.

The Model 350 Dynafax camera is currently marketed by the Cordin Co., Salt Lake City, Utah, and through a leasing arrangement was installed at FRL on a temporary basis so that its capabilities could be determined in conjunction with the Impact Test Machine. Figure 53 is a photograph of the camera and Figure 54 is its optical schematic.

Referring to Figure 54, an image is formed at the mask (2) by the objective lens (1). Light then passes through the field lens (3) to the entrance relay mirror (6). The mirror directs the light through the entrance relay lens (7)
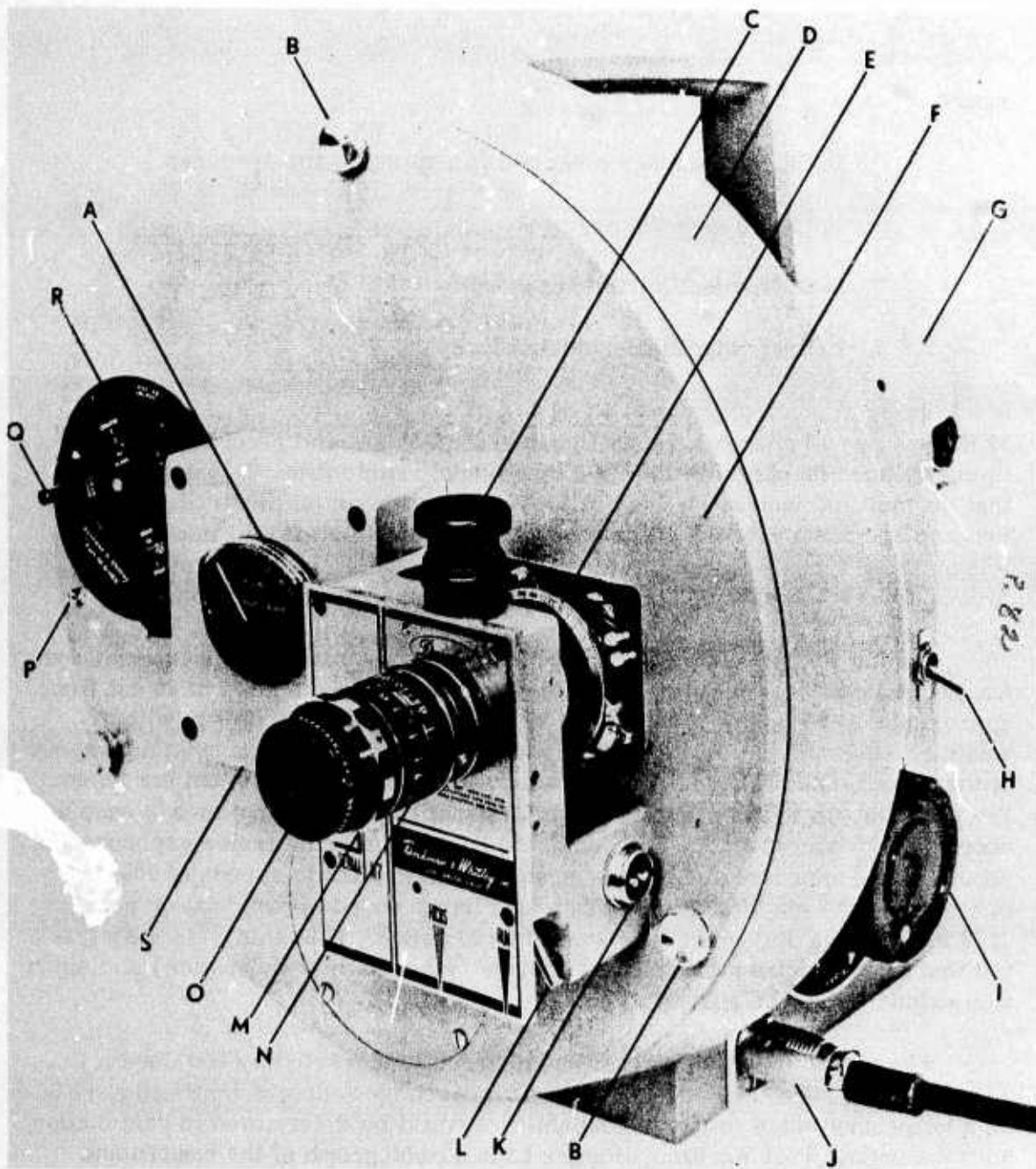
MODEL 350

Figure 53. High Speed Framing Camera
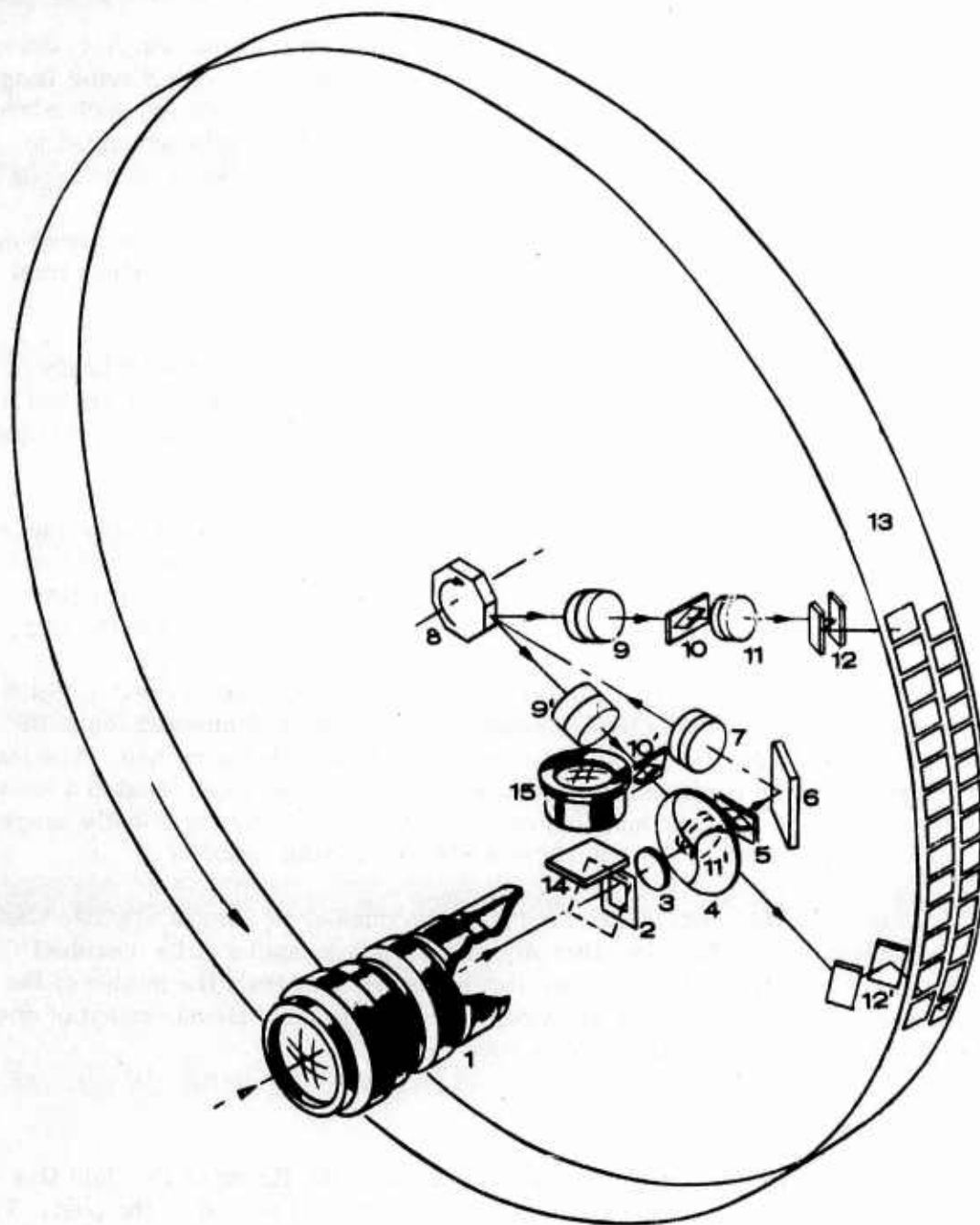
82

1. Objective Lens
2. Mask
3. Field Lens
4. Capping Shutter
5. Entrance Diamond Stop
6. Entrance Relay Mirror
7. Entrance Relay Lens
8. Rotating Mirror
9. Collimating Relay Lens
10. Exit Diamond Stop
11. Imaging Relay Lens
12. Exit Relay Mirrors
13. Film
14. Focusing Mirror and Ground Glass
15. Focusing Eyepiece

Figure 54. Optical Schematic of Model 350 Dynafax Camera

and onto the rotating mirror face (8). Immediately after reflection from the rotating mirror face the light beam forms a second image. This is a moving image because of the mirror's rotation. As the octagonal mirror rotates, each mirror face, in turn, presents the reflected image to two optical paths arranged to receive it through lenses (9) and (9').

The first path is through the collimating relay lens (9) and the imaging relay lens (11), and then through the exit relay mirrors (12) to form a final image on the front half of the film (13).

When the rotating mirror turns 22-1/2° farther, the reflected image is swept across the second optical path. This path is similar to the first, but it places its final image on the rear half of the film. Optical elements in this path are indicated by primed numbers (9', 10', 11', 12').

In each path the final image of the film plane is a moving image, due to the effect of the rotating mirror (8). However, the image moves in the same direction and at the same speed as the film, which is riding in the rotating drum of the camera. As a result the image is stationary relative to the film.

A variable-duration, high-intensity single flash lamp is used to illuminate the event. The flash duration can be varied between one and ten milliseconds depending upon the speed of the event being photographed. The lamp is triggered as the projectile passes through an infrared beam located a known distance ahead of the specimen, in order to provide a series of missile images prior to impact and thereby establish a missile striking velocity.

The flash duration is adjusted so that a number of images are also shown after the specimen is broken, thereby providing a measure of the residual velocity. These two velocities can also be determined from the motion of the two pendulums, thus allowing for an independent mechanical measurement of energy absorption by the specimen as described earler.

Experimental Procedure

The operational procedures associated with the firing of the Cold Gas Gun Impact Tester are essentially unchanged from those employed in the past. The tester is located in a separate area of the laboratory and all firings are performed from a console located in an adjacent room. The major change is that the Dynafax camera and light source have been substituted for the EG&G Multimicroflash and still camera. All tests are conducted with the room lights extinguished and the Dynafax camera shutter opened so that when the missile triggers the light, the event is captured on film.

The camera is brought up to the desired framing rate several minutes before the firing of the missile. The precise rate is checked with an oscilloscope by measuring the rotational speed of the octagonal mirror.

The mirror drive assembly contains a small induction coil built into its housing. A permanent magnet attached to the mirror drive shaft passes close

to this coil on every revolution of the mirror, inducing a pulse of current in the coil. This current is used to operate a built-in electronic tachometer which is graduated to read in pictures per second. However, this measurement is made more precisely by using a measurement oscilloscope.

Once the framing rate stabilizes, the room lights are extinguished, the shutter opened and the missile fired. The lamp is triggered and the event recorded. The camera shutter is then closed, the room lights turned on and the measurements of pendulum displacements made. The strip of film is removed from the camera and developed in the normal manner. Depending upon the framing rate selected, up to 224 images, each approximately 11 mm wide, can be obtained on this one film strip. Figure 55 illustrates the type of negative obtained. Either or both rows of negatives can be enlarged to make a series of photographic prints from which the measurements of missile displacement and specimen extension are made.

Data Reduction

Force-strain diagrams for Type XVII nylon webbing tested at an impact speed of 250 fps were derived solely from data recorded on high speed motion picture film during each test. Extraction of the essential data from the film record of a test required numerous measurements of missile displacement and gauge distance made with great precision. Force was determined at a given instant from the product of missile mass and missile deceleration. Since the second derivative of displacement with respect to time is deceleration, missile displacements were measured as accurately as possible at a number of equally-spaced intervals. Strain values could be obtained more directly by comparison of photographed gauge distances on a stressed specimen with the corresponding distance measured and recorded before the onset of loading. Although the data reduction technique has perhaps not yet been optimized, it has yielded, in its present state of evolvement, a very satisfactory set of force-strain diagrams for the nylon webbing tested.

Photographs similar to the one shown in Figure 56 were printed from each of approximately sixty frames of the motion picture film exposed at 0.1 millisecond intervals during a single test. The separation of two pairs of gauge marks painted on the specimen was determined at each interval. Using dividers, gauge distances were transferred from the photograph to the upper portion of a worksheet similar to the one shown in Figure 57. Thus, the scale of distances shown on the work sheet is that of the printed photographs, 4/10 actual size. Strain ordinates in the force-strain diagram eventually derived were obtained directly from the gauge distance-frame number diagram plotted on the worksheet. The diagram on the lower portion of the worksheet, a plot of missile displacement versus frame number, was also determined by transferring distances directly from the photographs with dividers and eventually became the basic element in the procedure followed to determine force values. Initial attempts to accurately determine the second derivative of missile displacement at a reasonable number of time intervals were not wholly successful. Using measured displacement values, tables of finite differences were made for several sets of test results, but in every case, values of the second difference were

Figure 55. A Contact Print Showing the Actual Size of Each Film Frame Obtained with the Model 350 Dynafax High Speed Camera
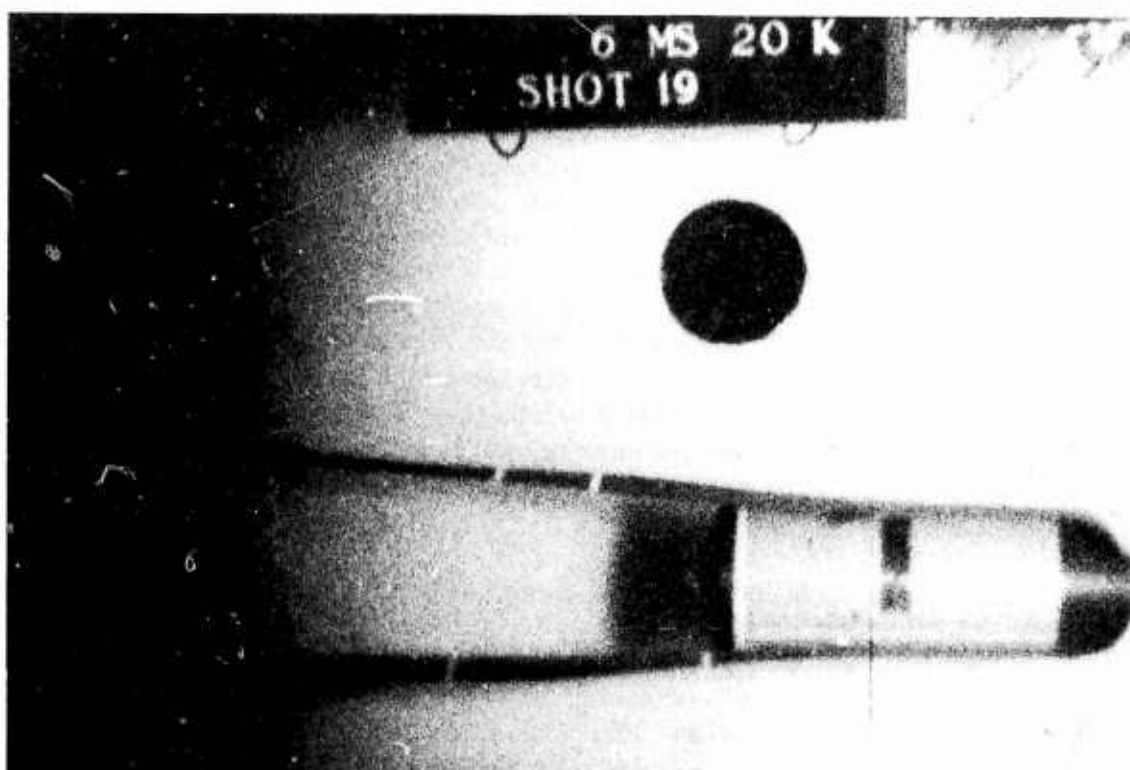
Figure 56. A photograph typical of the many recorded during each impact test with the Model 350 Dynafax High Speed Camera. This enlargement is ~0.3X actual size and 17X the size of the film image.
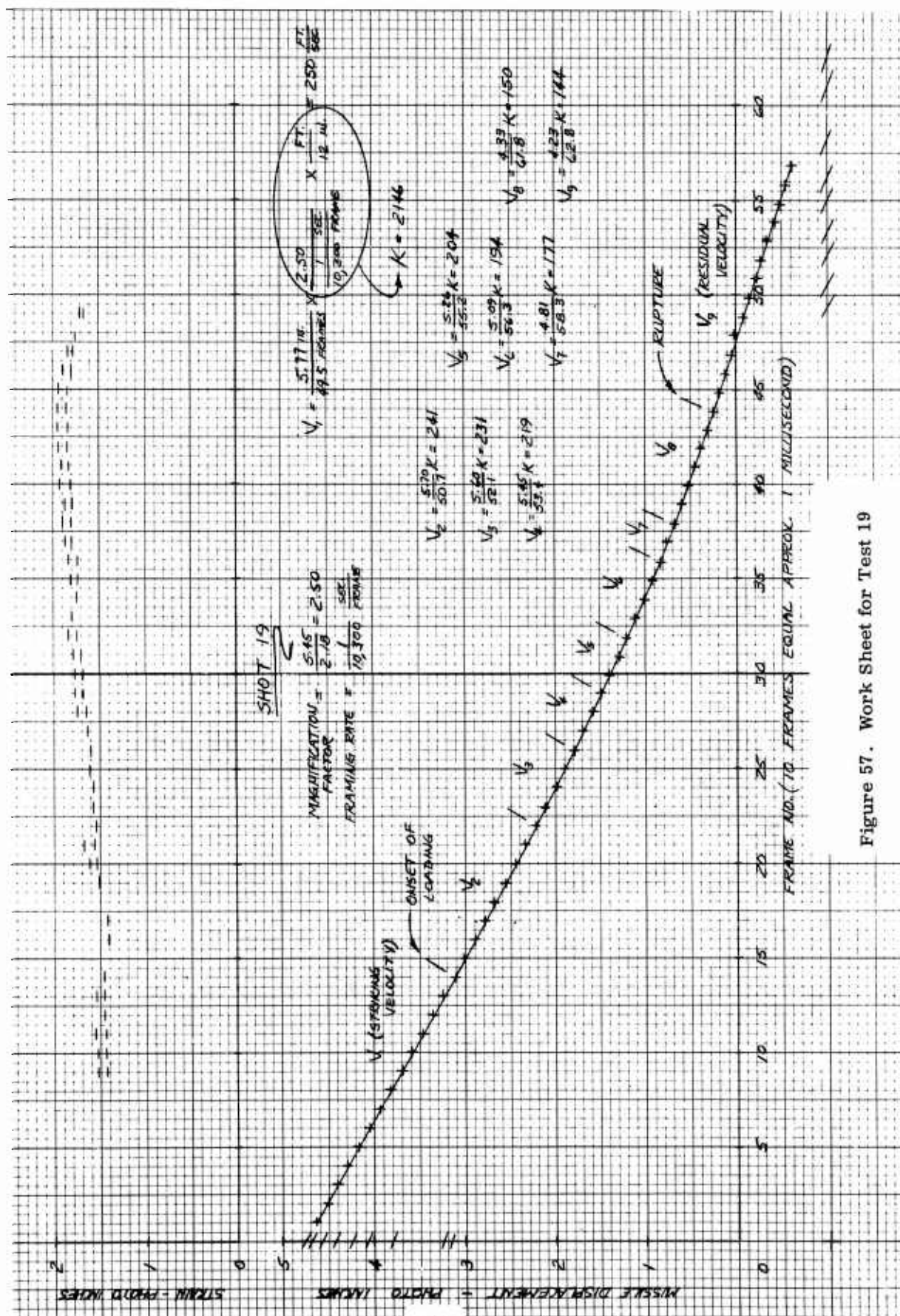
Figure 57. Work Sheet for Test 19

87

generally equal to zero. Theoretically, this indicates a constant velocity (zero deceleration) state, but here it was a consequence of the minimum attainable reading error being large in comparison to the differences obtained and indicated only the futility of the approach. At this point, two changes in technique were implemented that together made the determination of forces by double differentiation of the displacement-time curve viable. First, a missile lighter than that which would normally be employed was substituted and the three tests were repeated. To maintain the same energy transfer from missile to test specimen, the lighter missile must be slowed a greater amount, resulting in potentially greater accuracy when velocity differences are taken. This second set of data was then differentiated graphically, as shown on the worksheet in Figure 57. Notice that a series of straight lines was drawn through data points on the missile displacement-frame number diagram; except for time intervals before and after impact, this is an idealization, since a linear displacement-time diagram indicates constant velocity. The slopes of the linear segments were measured to determine average missile velocity for each of the nine intervals shown. The second derivative, deceleration, was obtained by dividing the velocity change from segment to segment by the time interval represented by the graphical distance from the midpoint of one segment to the midpoint of the next. For example, the deceleration from V_2 to V_3 equals V_2 minus V_3 divided by the time interval represented by six camera frames, 0.6 millisecond. In this example, deceleration was determined at eight intervals, so that, after multiplying each deceleration by the missile mass, eight data points representing force were available for the desired force-strain diagram. The actual forces calculated were divided in half since they represent forces distributed equally on both legs of the "V"-shaped specimen.

After force and strain ordinates had been determined with aid of the worksheet, they were plotted against time as shown in Figure 58. The data point scatter evident in this diagram is a clear illustration of the limitations encountered in this technique. However, by drawing force-time and strain-time curves through the midpoint of the scatter at each time interval, average force and strain relationships are defined with far greater accuracy than has been previously possible for high strength members subjected to impact loading. The force-strain diagram for Shot 19, shown in Figure 59, was obtained directly from information shown in Figure 58 by plotting average force versus average strain at ten time intervals. Force-strain diagrams for Shots 15 and 16, also presented in Figure 59, were obtained in a like manner.

Discussion of Results

Inspection of Figure 59 shows excellent agreement among the first three force-strain diagrams derived using the newly developed photographic technique. The validity of the diagrams was verified by comparison with related data obtained through pendulum deflection measurements. As described previously, the established ballistic pendulum technique yields an accurate measure of rupture energy which is completely independent of the photographic method. Thus, by employing both techniques simultaneously, and measuring the area under the photographically-obtained force-strain curves, two independent measures of rupture energy can be compared to provide sound verification.

88
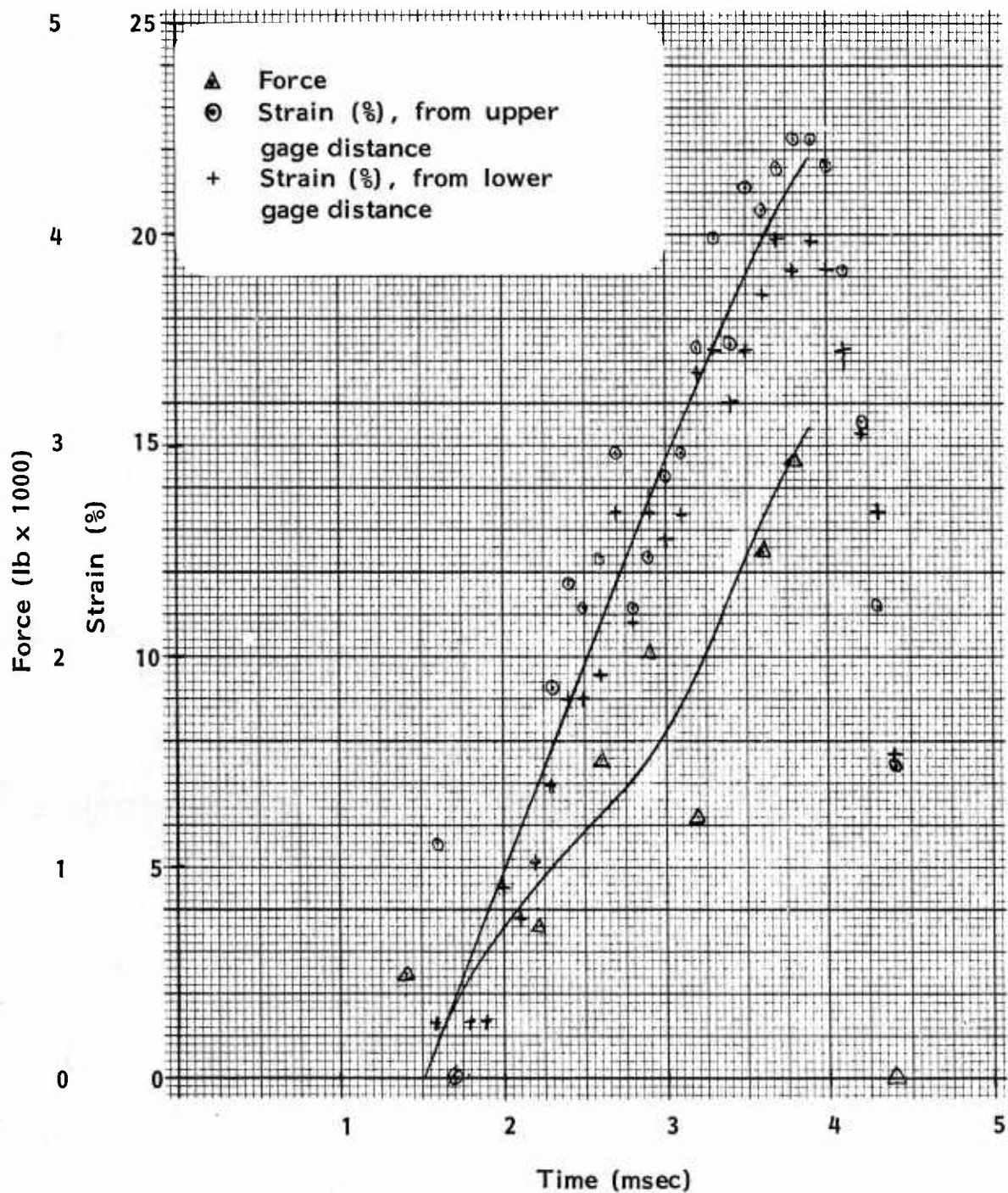
Figure 58. Force and Strain versus Time, Measured During a Tensile Test of One-Inch Wide Nylon Webbing, Type XVII, Impacted at 240 fps
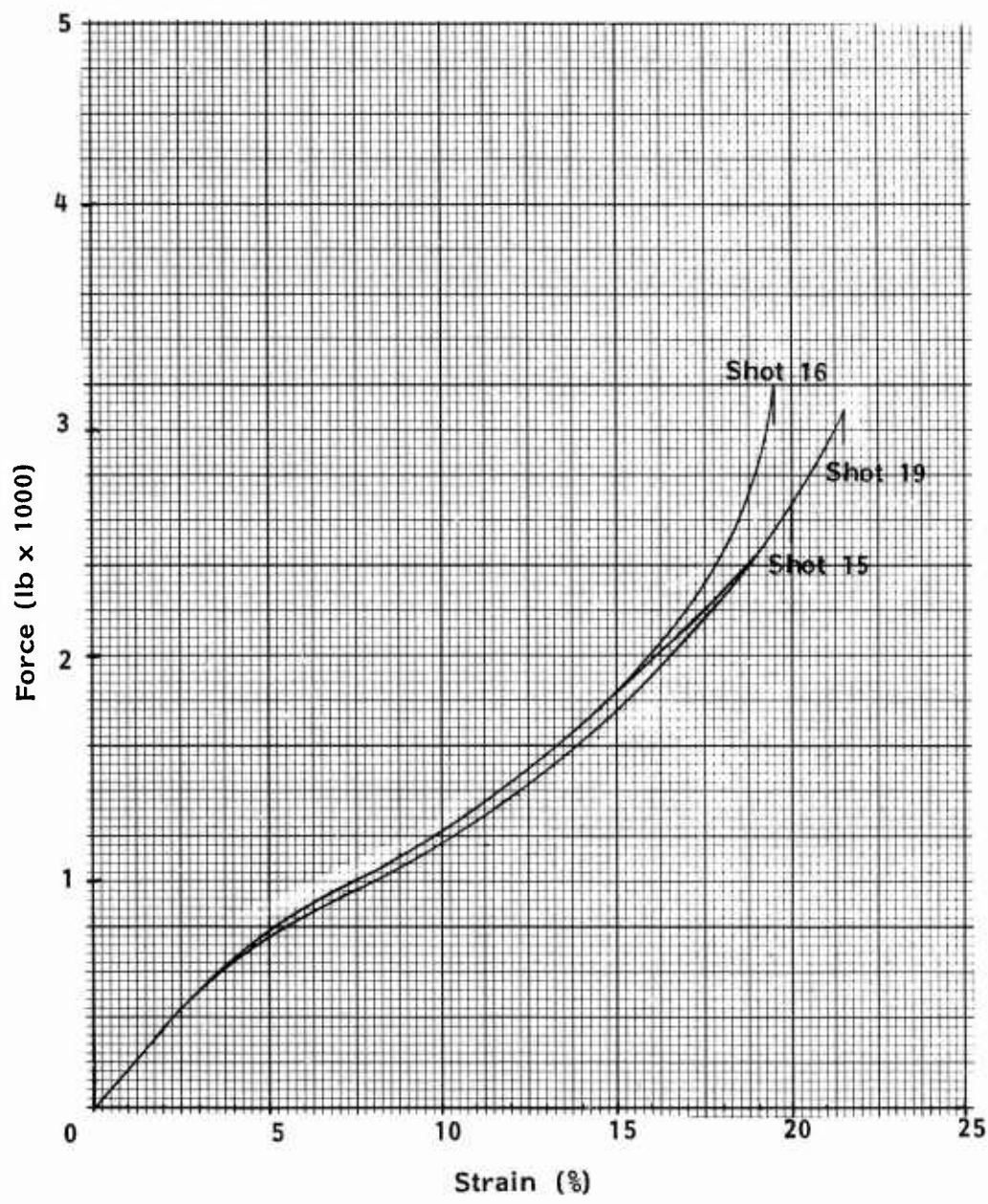
Figure 59.   Force-Strain Diagrams for One-Inch Wide Nylon Webbing,
Type XVII, Tensile Tested at an Impact Velocity of 240 fps

This comparison, readily seen in Table 21, shows that agreement between data obtained by the two methods is extremely good. Energies obtained photographically differ by no more than 11% from those obtained using ballistic pendulums.

TABLE 21

SUMMARY OF TENSILE DATA OBTAINED FOR
ONE-INCH WIDE, TYPE XVII NYLON WEBBING

Tested at an Initial Strain Rate of ~8500%/Sec				Tested at a Strain Rate of ~8%/Min		
Rupture Force (lbs)	Rupture Strain (%)	Rupture Energy ft-lb/ft) from		Rupture Force (lbs)	Rupture Strain (%)	Rupture Energy (ft-lb/ft)
		Photographs	Pendulums			
2640	20	260	290	3580	27.6	---
3180	19	295	299	3595	27.5	---
3100	22	248	276	3590	27.0	---
				3625	27.8	---
				3600	27.4	---
2970	20	268	288	3600	27.4	391 Avg

The effect of impact loading upon the force-strain characteristics of the Type XVII nylon webbing tested is evident in Figure 60, in which two force-strain diagrams are presented. The first is typical of the three diagrams obtained through impact testing at an initial strain rate of ~8500%/minute using an Instron Tensile Tester. Precise strain rates are not reported because capstan jaws were used and actual specimen lengths are difficult to determine. Further complicating strain rate reporting is 1) the probability that the stressed specimen length varies significantly during an impact test and, 2) the fact that the missile velocity continuously decreases as kinetic energy is transferred to the test specimen. The differences apparent between the diagrams in Figure 60 are typical of similar comparisons that have been made of nylon tapes at high and low strain rates using the FRL/ AFML piston-driven tensile tester.* Now, as in the past, a greater initial modulus at the high strain rate is perhaps the most significant difference between diagrams. Beyond the initial portion, both force-strain diagrams are similar in shape, although the high strain rate test terminates with specimen failure at lower levels of force and strain.

---

*Mechanical Properties of High-Temperature Fibrous Structural Materials, Part III, High-Speed, High-Temperature Tensile Tester. AFML-TR-67-267, Part III, Sebring, Freeston, Platt and Coskren.
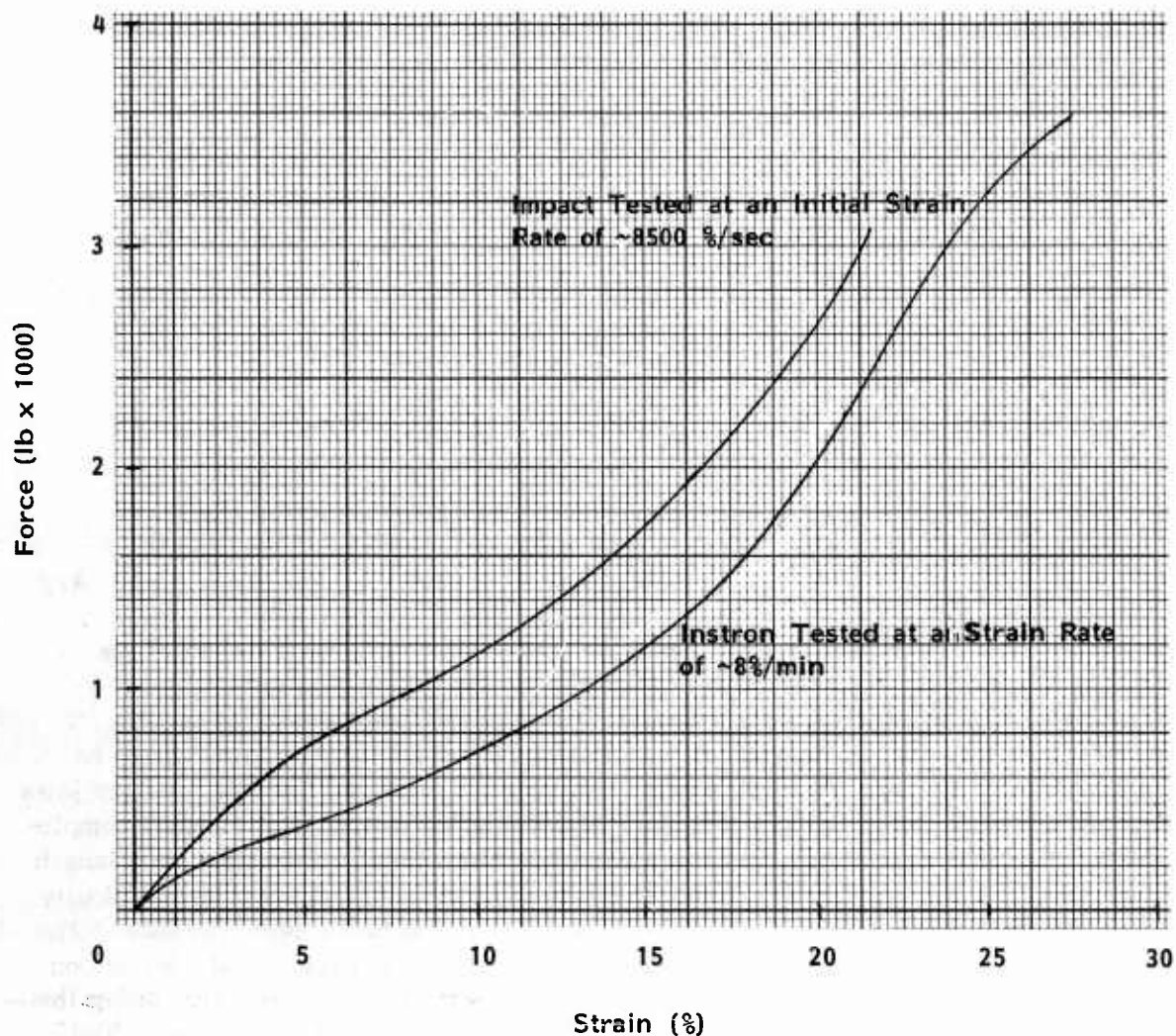
Figure 60. Typical Force-Strain Diagrams for One Inch Wide Nylon Webbing
Type XVII, Tensile Tested at Two Widely Differing Strain Rates.

Laboratory Modifications to the Photographic Method for the
Testing of Kevlar Structures

A one-inch wide, 9000-lb Kevlar webbing, FRL Sample No. 5034-93, was
selected for impact testing using the cold gas gun and the photographic method
for obtaining force-strain diagrams. At the outset, an unexpected problem
arose that is apparently unique to Kevlar. The gas blast that preceded the
missile as it left the muzzle of the gun (see Figure 61) disturbed the V-shaped
specimen to such a degree that full, square contact between missile and speci-
men could not always be obtained; several partial breaks and complete misses
occurred. In addition, specimen flutter caused by gas blast frequently broke
the infrared beam that is normally interrupted only by the missile, resulting in
erratic triggering of the flash lamp and subsequent failure to record the 3 milli-
second impact event photographically. Although specimen flutter has been fre-
quently observed during impact testing of other materials, its magnitude has
never been great enough to be of consequence. The extreme flutter observed
with Kevlar was presumed to be related to its high tensile stiffness, although
this phenomenon is not completely understood. Eventually, the difficulties
presented by specimen flutter were avoided by making several changes in the
test procedure. The location of the apex of the V, the point of impact, was more
rigidly fixed by tying it with a network of light tire cord yarn (seen in Figure 61)
and shoulders were added to the missile nose to prevent the specimen from slip-
ping off before it was tensioned. The shoulders did not change the nature of
the contact area in any way; they merely aided specimen-missile alignment just
prior to impact. After these changes were made, the infrared beam, located
about four inches from the apex of the V, was still being interrupted prematurely
as the specimen legs were moved by the gas blast. This prompted a decision to
improve a long-standing deficiency in the cold gas gun apparatus and to solve
the immediate difficulty by adding an adjustable delay unit to the triggering cir-
cuit for the flash lamp. The delay unit made it possible to move the infrared
beam to a point more than two feet ahead of the apex where the width of the V
was six inches and specimen-light beam intereference was thus eliminated.
The linearly adjustable delay unit also made possible small, precise changes in
flash lamp timing and improved the efficiency of the test procedure considerably.

Data Reduction

Photographic records of three 150 fps impact tests of one-inch wide, 9000-
lb Kevlar webbing, FRL Sample No. 5034-93, were obtained. The graphical
analysis method discussed above was applied without modification using a set
of fifty 8 x 10 inch photographs for each test.

Upon completion of the graphical analysis, diagrams showing both force
and strain as a function of time were plotted for each test. One of these is shown
in Figure 62. Notice that the data points in the strain-time diagram form several
steps, or regions where the measured strain remains unchanged for relatively
long time intervals. Steps like these, some of longer duration than those seen
in Figure 62, occurred in diagrams obtained for the other two tests and led to
the inevitable conclusions that the precision of the strain measuring system is
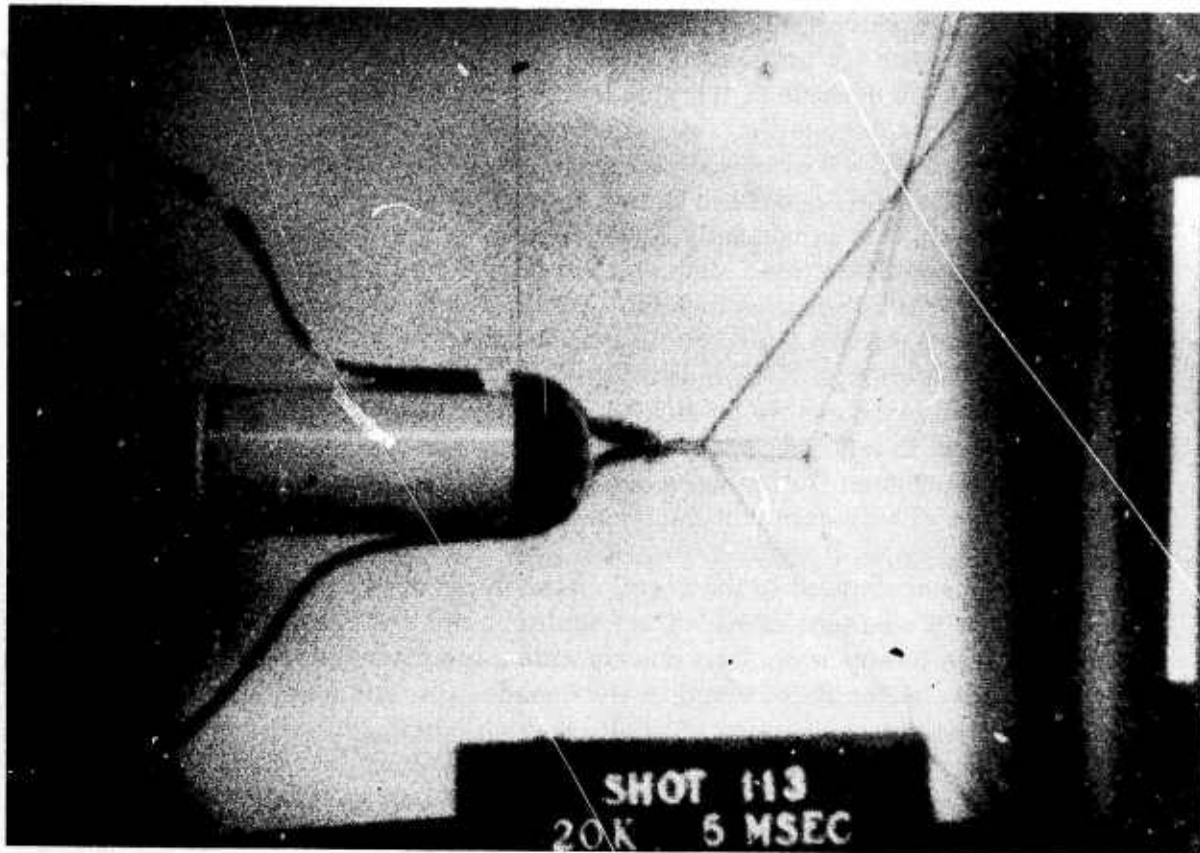
Figure 61.   A photograph typical of the many recorded during each impact
test. In this frame, the missile has not yet begun to strain the
Kevlar webbing.
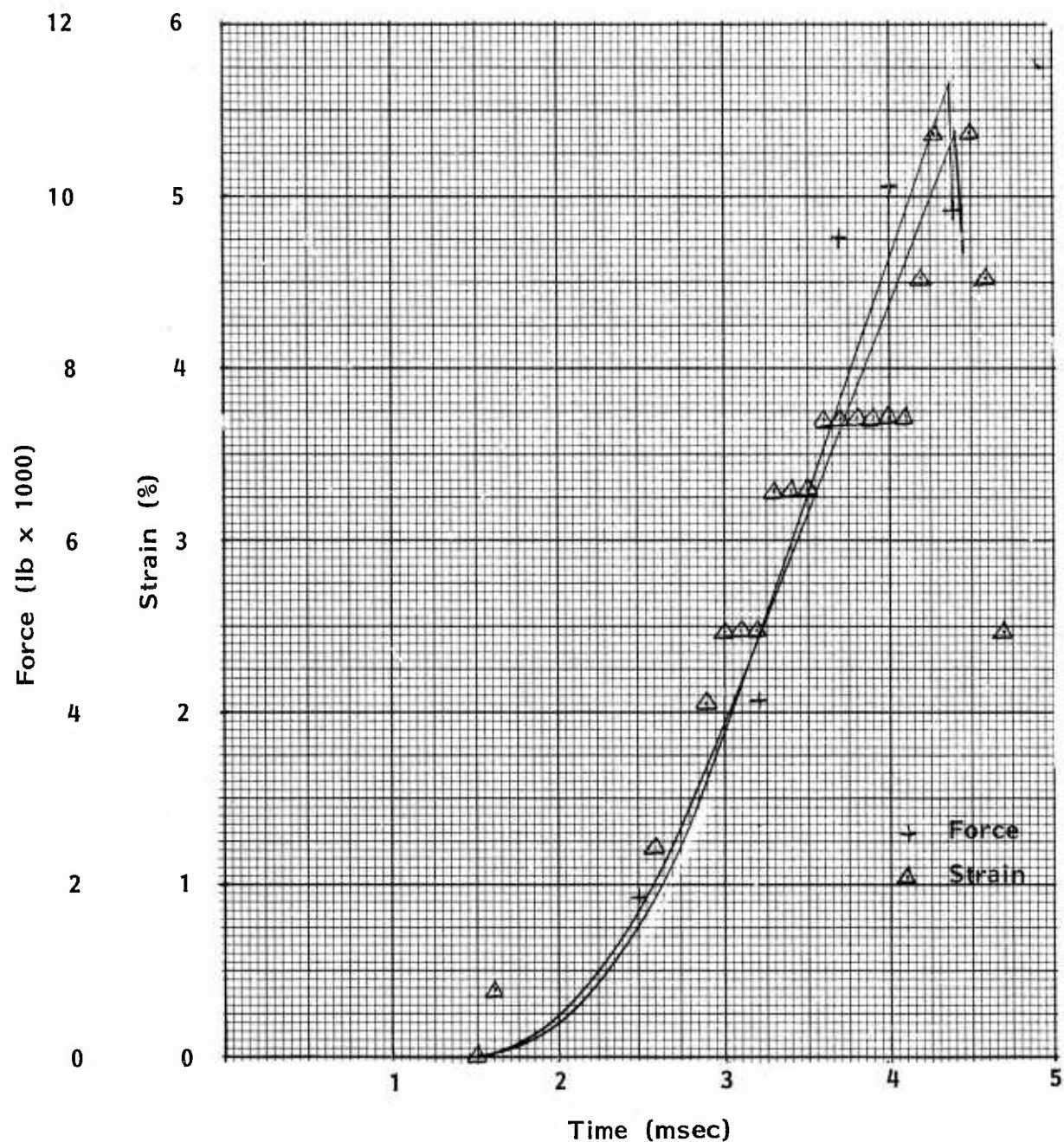
Figure 62. Force and Strain versus Time for a Tensile Test of One-Inch Wide
Kevlar 29 Webbing, FRL Sample No. 5034-93, Impacted at 150 fps.
The strain rate was approximately 3300%/sec.

not quite great enough to measure the small incremental changes in strain that occur in Kevlar structures. The precision of the system used is great enough, however, to accurately measured rupture strain and to permit a reasonable approximation of the force-strain curve to be drawn. For the three tests analyzed, rupture strains of 5.5, 5.1, and 5.4% were obtained. An approximate force-strain diagram, plotted directly from data shown in Figure 62, is presented in Figure 63. Fortunately, the validity of this diagram can be verified by a method that is both convenient and reliable: the comparison of the rupture energy value obtained by measuring the area under the curve with that obtained by the ballistic pendulum method. Using a planimeter to measure the area under the force-strain diagram, the rupture energy was found to be 299 ft-lb/ft. This is in good agreement with the value of 324 ft-lb/ft determined by the ballistic pendulum method.

Discussion of Results

Effective energy absorption comparisons require that the total rupture energy recorded in each test be normalized on a basis of specimen length or weight. However, since capstan jaws must be used to grip high strength webbings of the type under study, the actual energy absorbing length is not clearly defined. Previous work with nylon webbing has shown that approximately two thirds of the material wrapped on the capstans used should be included in the gauge length. Although some evidence exists that suggests an appropriate factor for Kevlar might include more of the capstan wrap, the two thirds factor will be used for both nylon and Kevlar until the subject can be studied fully.

During the course of the development work required to apply the photographic method to Kevlar, ten rupture energy determinations were made for a 9000 lb Kevlar webbing (FRL Sample No. 5034-93) using the ballistic pendulum technique. The rupture energy values obtained, listed individually in Table 22, provide essential data for Table 23, which shows the effect of strain rate on nylon and Kevlar 29 webbings of approximately equal strength. Rupture energy data for two nylon and two Kevlar webbings are included in Table 23. Also presented, wherever possible, are rupture force and strain values, including those obtained by the photographic method at high strain rates. Perhaps the most significant finding reported in Table 23 is the great <u>increase</u> in rupture energy measured for Kevlar webbings when the strain rate is increased to several thousand percent per second: for the 9000 lb webbing, the rupture energy increase is 75%, and for the 4000 lb tubular structure, the increase is 42%. For both nylon webbings, however, a <u>decrease</u> in rupture energy accompanies the increase in strain rate.

Conclusions and Recommendations

In assessing the impact performance of potential parachute load line materials, tensile rupture energy is perhaps the single most important parameter. Other basic considerations are the impact tensile modulus, rupture strain, rupture force and the weight of the structure. Although impact rupture energy has been a measurable quantity for some time, impact modulus, rupture strain,

96
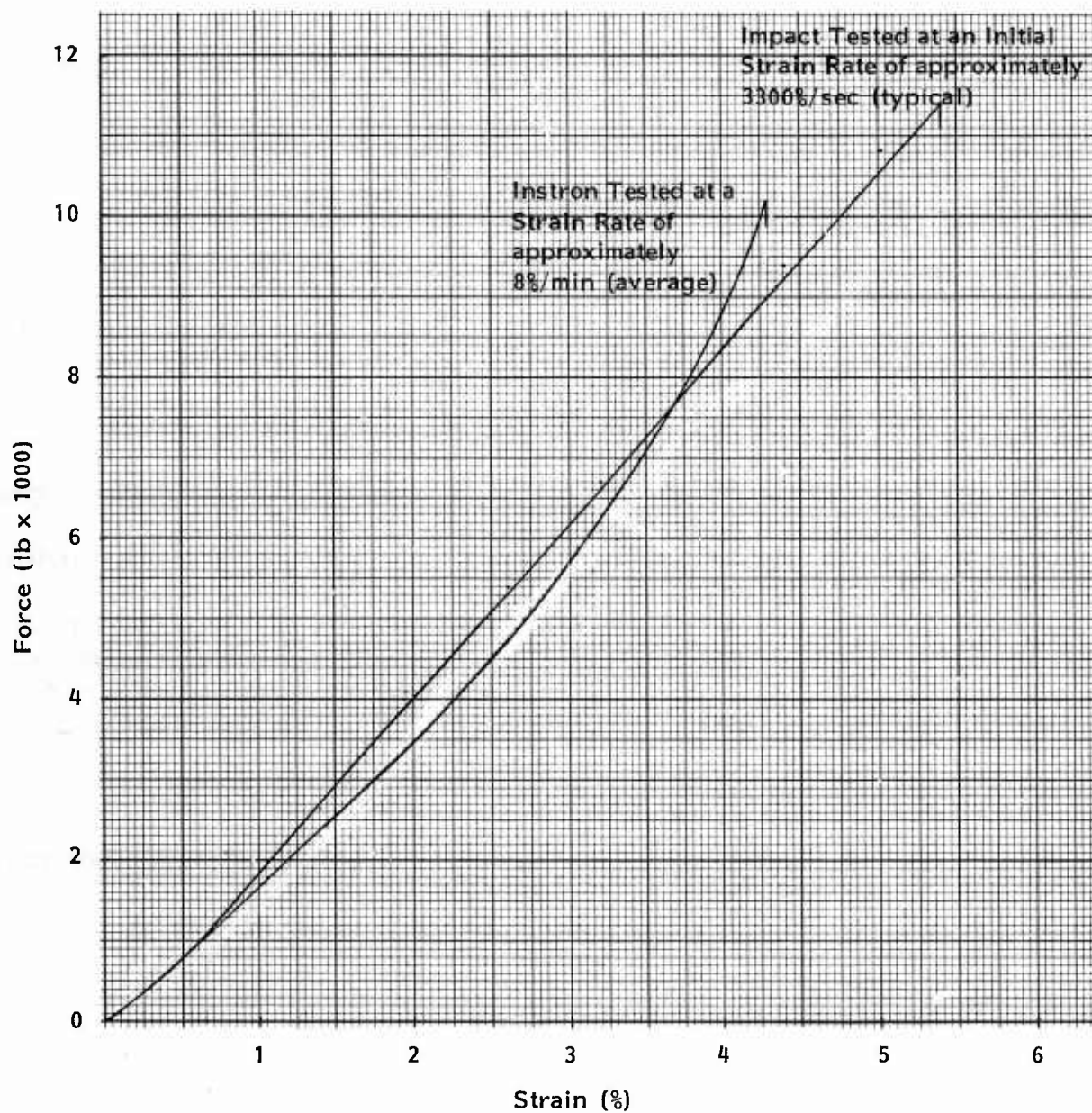
Figure 63. Force-Strain Diagrams for One-Inch Wide Kevlar 29 Webbing, FRL Sample No. 5034-93, Tenside Tested at Two Widely Differing Strain Rates

TABLE 22

RUPTURE ENERGY OF ONE-INCH WIDE, 9000 LB
KEVLAR WEBBING (FRL No. 5034-93) TENSILE TESTED AT
AN IMPACT VELOCITY OF 150 FT/SEC

Shot No.	Gage Length* (ft)	Approx Strain Rate (%/sec)	Rupture Energy (ft-lb/ft)	(ft-lb/lb)	Description of Break
96	9.14	3300	273		Complete at apex except for 5 warp yarns
100	5.22	5750	363		Complete at apex
102	5.22	5750	326		Complete at apex except for 6 warp yarns
103	5.22	5750	342		Complete at apex
104	5.22	5750	352		Complete at both capstans
106	9.22	3250	307		Complete at one capstan
108	8.88	3400	278		Complete at one capstan and partial at apex
109	8.88	3400	276		Complete at apex
113	9.05	3300	289		Complete at apex
114	9.05	3300	324		Complete at one capstan
Average			313	10,990	
Standard Deviation			33		
Coefficient of Variation (%)			11		

*Includes both sides of V and two thirds of material wrapped on capstan jaws.

TABLE 23

THE EFFECT OF STRAIN RATE ON
THE RUPTURE ENERGY OF NYLON AND KEVLAR 29 WEBBINGS
OF APPROXIMATELY EQUAL TENSILE STRENGTH

Material	Approx Strain Rate	Rupture Energy		Rupture Force (lb)	Rupture Strain (%)	Change in Rupture Energy at High Strain Rate (%)
		(ft-lb/ft)	(ft-lb/lb)			
Kevlar webbing 1" wide, 9000	8%/min	180	6,320	10,260	4.3	
lb nominal strength, FRL No. 5034-93	3250 to 5750 %/sec	313	10,990	11,460	5.3	+75
Nylon webbing 1" wide, 9000	8%/min	487	9.510	7,225	19.0	
lb nominal strength	5750 %/sec*	403	7,870	--	--	-17
Kevlar webbing 1" wide, tubular	8%/min	72	5,620	3,950	4.0	
3500 lb nominal FRL No. 5034-35	8500	102	7,960	--	--	+42
Nylon webbing, 1" wide, 2500	8%/min	391	20,490	3,600	27.0	
lb nominal Type XVII	8500	288	15,090	2,970	20.0	-26

and force values have not been available to the designer. However, the recently developed photographic technique yields all of this information in the form of a complete force-strain diagram and it has now been successfully applied to a Kevlar structure having a rupture strain of only 5%. In its present state of development, the photographic method is time consuming and expensive, although further development can be expected to improve the situation considerably. The ballistic pendulum technique will continue to be of great value; besides providing a convenient means of checking the photographic method, it can be used for screening potential load lines on the basis of impact rupture energy.

The work described here, besides resulting in significant improvements in impact-test measurement technology, has yielded data on the impact performance of high strength Kevlar structures that, until now, has not been available. In one case a Kevlar webbing showed a rupture energy increase of 75% over the Instron value when tested at approximately 5000%/sec. However, a different Kevlar structure, tested at about 7500%/sec, showed an increase of 42%, indicating that much remains to be learned about structural differences. In fact, that data recorded thus far indicates that several aspects of the impact performance of Kevlar warrant much more study. Behavior over a range of strain rates, the effect of structural differences, the significance of specimen flutter, jaw penetration, high-speed abrasion, joint efficiency under impact conditions, and the impact behavior of webbings under load are all areas in which there is a great, if not total, lack of information, although the required test technology now exists.

XII. PARACHUTE PACKS

As part of the requirements of this contract, 25 parachute pack and harness assemblies, AF Drawing 65K1533, were fabricated by ILC Steinthal, Inc., using materials designed and made for the purpose by FRL. The design of these materials is included in previous tables in this report, and need not be listed separately here.

The packs were made entirely of Kevlar, including the sewing thread, except for a few small pieces of heavy stiffening material which were nylon, though even these were covered with Kevlar. No unusual difficulties were encountered in the fabrication, and the packs were satisfactory. Because of the weight of the hardware involved, however, the weight saving was not great. In addition, the harness materials were limper than the customary nylon materials, and were somewhat thin for the hardware which was designed for the thicker, heavier nylon. Nevertheless, it was clearly demonstrated that Kevlar could be used satisfactorily in parachute packs and harnesses, if desired.

XIII. CONCLUSIONS

The work described has demonstrated the feasibility of using Kevlar fiber in parachute component materials of widely varying types. A potential weight and volume reduction of at least 50% is possible when all nylon componenets of a parachute system are replaced by Kevlar or, alternately, significantly larger parachutes can be made from Kevlar to replace a nylon parachute with no increase in weight and volume.

A study of the actual performance of Kevlar parachutes was not a part of the current work, but information from other sources indicates that Kevlar may offer other advantages over nylon, and shows promise of becoming an important fiber in parachutes. The structures described herein form the basis for the design of components for Kevlar parachute systems, and have been described in a series of tentative draft military specifications which are currently being considered by the Air Force for adoption.

APPENDIX

Laboratory Simulation of Impact Between
AQM-34R Drone Surfaces and Nylon Loadlines

Loadline failure during recent aerial recovery operations has resulted in the loss of two operational AQM-34R drones. In both instances, it was suspected that failure was precipitated by loadline impact with retrieval hook tines or any of several thin edges on the drone itself.

The objective of this program, confirmation of the specific cause of loadline failure, was sought through laboratory simulation of impact between loadlines and the suspect surfaces. Data recorded during the impact events and subsequent examination of the damaged elements provided substantial support for the theory that loadline failures were the result of cutting. Laboratory simulators of two of the four suspect surfaces were capable, under several specific conditions, of inducing premature tensile failure due to cutting.

Operational Procedure

The equipment and operational procedures employed in this work are essentially unchanged from those described in Section XI.

In brief, the measuring system consists if (1) a missile launching device, (2) a free flying missile, and (3) a mechanical and photographic means for measuring missile velocity before, during, and after impact.

A high speed rotating drum camera provides a means for visually recording a behavior of a webbing during impact. Gage marks are placed on the specimen prior to impact, making it possible to measure webbing extension-time behavior photographically by noting the changes in spacing which occur during the test. Furthermore, if the deceleration of the missile during impact can be determined, then the buildup of force in the webbing can be calculated for the same time interval. Combining the two sets of data produces an impact force-extension curve for the material under study.

It has been found previously that the method currently being used assumes that the missile mass can be selected such that its velocity will be reduced significantly during specimen rupture. With less than a fifty percent velocity reduction, for example, it is impossible to accurately measure the small incremental velocity time curve. As will be shown shortly, the constraints imposed by loadlines and impact velocities of interest in the present program caused severe problems with the measuring system as currently designed. It soon became apparent that it would be impossible to obtain force-time curves. However, the combination of an extension-time curve and energy to rupture gives a good indication of what the rupture force must be, so that despite the lack of a true force-extension curve, it is still possible to characterize the impact behavior of each material under test in a meaningful way.

102

TABLE 24

MISSILE MASSES REQUIRED TO EVALUATE
HIGH STRENGTH NYLON SUSPENSION LINES
AT VARIOUS IMPACT VELOCITIES

Nominal Webbing Strength (lb)	Missile Striking Velocity (ft/sec)							
	150		200		350		500	
	M_1 (lb)	M_2 (lb)	M_1 (lb)	M_2 (lb)	M_1 (lb)	M_2 (lb)	M_1 (lb)	M_2 (lb)
9,000	13	26	7	14	2	4	1	2
12,000	17	34	10	20	3	6	2	4
14,000	20	40	11	22	4	8	2	4

M_1 is mass required to break webbing with zero residual velocity.
M_2 is double M_1 and provides the necessary safety factor.

Table 24 lists the missile masses needed to provide double the kinetic energy input needed to break each of the test webbings under Instron test conditions. Our experience indicates that the 100 percent excess is needed for safety to insure that after rupturing the webbing the missile has sufficient velocity to reach, enter into, and be contained in the catching pendulum.

Missile Design

Given the limitations described above it became nessary to modify the standard missile shape to one which would accommodate the masses required. The heaviest mass fired previously had been an approximately 8-inch long, 2-1/2 inch diameter brass bar weighing approximately 10 pounds. Since the diameter of the cold gas gun barrel is fixed, it became necessary to lengthen the missile to approximately 18 inches in order to achieve the heavier weights required to break the test specimens. Increasing the missile length beyond twelve inches introduces a serious potential safety hazard, however. If the missile is deflected from its normal trajectory during a webbing break, it can easily strike, but not enter, the front of the catching pendulum and not be contained therein. The ricocheting missile can then damage other equipment in the area, particularly the camera and/or light source. In order to minimize the chances of such an occurrence, it is necessary to always provide sufficient excess energy so that the missile maintains a straight path. Strict adherence to this rule introduces the problem of getting sufficient missile deceleration to make the desired force-time measurements.

Two impacting metal surfaces were studied, steel and aluminum. Different surface areas and shapes were also to be studied (e.g., drone edges versus hooks), but in order to minimize the number of complete missiles to be fabricated, it was decided to utilize as many of the existing missile body masses as possible, adding only the various shapes as nosepieces which would actually be in contact with the test specimen. Two such nosepieces were constructed, one of steel and the other of aluminum. Both were eventually slotted to accept

the various blade inserts designed according to the dimensions provided, and had base weights of approximately 9 pounds for the steel and 2-1/2 pounds for the aluminum. These nosepieces, in combination with the lightest bodies of reasonable length, provided a means for firing masses of approximately 5, 12, and 15 pounds. An exploded view of a typical missile is shown in Figure 64. As can be seen it consists of the following:

(1) an approximately ten inch tapered nosepiece with a slot in front for carrying the various blades (the blades project approximately 3/8 of an inch ahead of the nosepiece),

(2) a five-inch long body section to provide stability,

(3) a light tailpiece,

(4) a one-half-inch-diameter threaded rod to connect the nose and tail pieces.

The masses selected were sufficient to provide a method of obtaining meaningful data within the limited time and funding established for the task. Now that some initial information has been obtained on the response of materials to the various impact shapes, it might be possible in future work to alter the missile mass and catching pendulum in order to get greater deceleration and thereby obtain the desired force-extension data.

Discussion of Results

Data obtained for each of the three tensile members that were studied includes low strain rate (Instron) tensile stress-strain diagrams and rupture energy determinations and high strain rate strain-time diagrams and rupture energy determinations. All high strain rate data was obtained under unique conditions, described in the previous section, that combined tensile impact and loading with several degrees of cutting action. These combinations of destructive elements simulated, in an elemental and closely-controlled way, those thought to have contributed to two recent failures to complete aerial recovery operations involving AQM-34R drones. Analysis of the recorded data lends support to the hypothesis that impact between the loadlines tested and certain surfaces simulating those of an AQM-34 drone will result in premature tensile failure of the loadlines.

Prior to the specialized impact testing that comprised the major portion of the work, a limited number of routine tensile tests was performed using an Instron tensile tester to provide bases of comparison. Force-strain diagrams typical of those obtained are shown in Figure 65, and average values of rupture force, strain and energy are shown in Tables 25, 26, and 27. For the 12,000 and 14,000 lb loadlines, the tables show two sets of slightly differing values that are designated according to the sheath color of the loadline, since, in both cases, not enough material with exactly the same tensile properties was available for high strain rate testing. Notice also, that the actual strength of these webbings is generally less than the rated value; as much as 20% less in the case of the one inch wide, 9000 lb webbing.

104
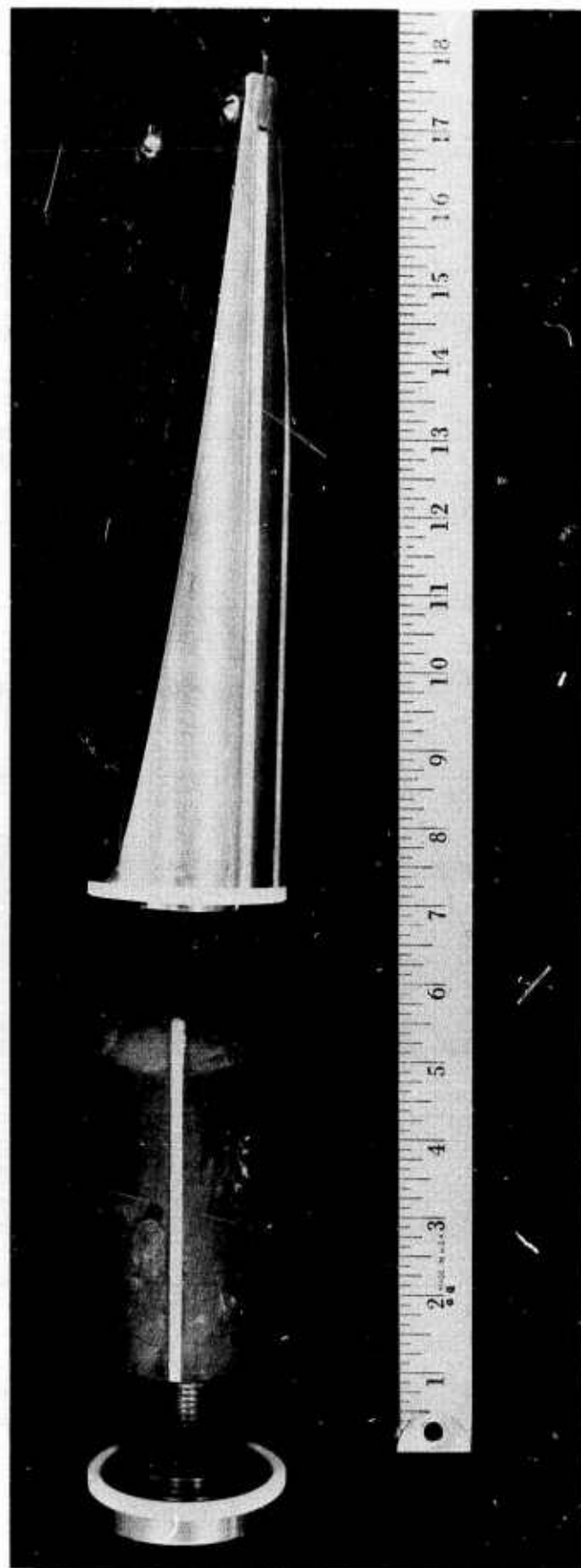
Figure 64. One of the Two Missile Configurations Employed - Leading Edge Inserts are Replaceable
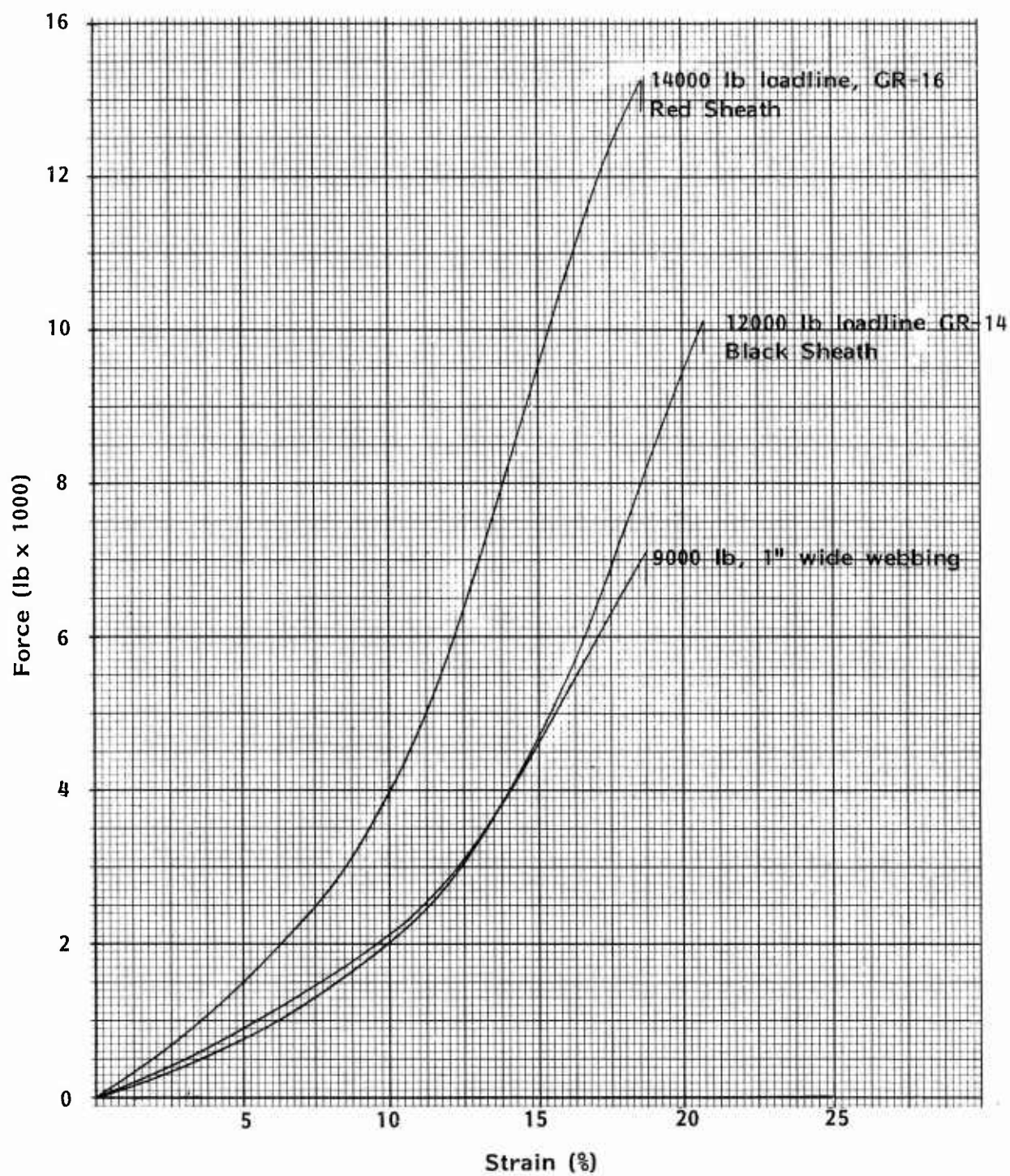
Figure 65. Typical Force-Strain Diagrams for the Three Loadlines under Study, Obtained Using a Strain Rate of Approximately 10%/Min

106

TABLE 25

TENSILE PROPERTIES OF ONE INCH WIDE, 9000 LB WEBBING
SUBJECTED TO SEVERAL MODES AND RATES OF STRAIN

	Instron – Standard Test			High Strain Rate Missile Nose as Noted		
	Rupture Load (lb)	Rupture Strain (%)	Rupture Energy (ft-lb/ft)	Rupture Strain (%)	Rupture Energy (ft-lb/ft)	Time to Rupture (msec)
Hook simulating steel nose with 0.09" R fired at 150 ft/sec	7225	18.8	487		403	
					370	
					435	
Hook simulating steel nose with 0.09" R fired at 200 ft/sec					455	
					470	
					480	
				18.0	447	2.6

TABLE 26

TENSILE PROPERTIES OF 12,000 LB GR-14 LOADLINE
SUBJECTED TO SEVERAL MODES AND RATES OF STRAIN

	Instron - Standard Test			High Strain Rate Missile Nose as Noted		
	Rupture Load (lb)	Rupture Strain (%)	Rupture Energy (ft-lb/ft)	Rupture Strain (%)	Rupture Energy (ft-lb/ft)	Time to Rupture (msec)
1/8" alminum nose white webbing 200 ft/sec	11,520	17.2	680	15.3	351 329	2.0
1/8" aluminum nose black webbing 350 ft/sec	10,230	20.8	710		460 452	
1/8" aluminum nose black webbing 500 ft/sec					362 818	
1/16" aluminum nose white webbing 200 ft/sec				17.0	609 720	3.0
1/16" aluminum nose white webbing black webbing 350 ft/sec					664 643	
1/16" aluminum nose black webbing 500 ft/sec				17.8	921 1019	1.3
1/16" stainless steel black webbing 500 ft/sec				15.4	~20	0.6
blunt nose black webbing 500 ft/sec				15.0	716	1.3
1/64" stainless steel nose white webbing 200 ft/sec					367	
1/64" stainless steel nose white webbing 500 ft/sec					1018	

TABLE 27

TENSILE PROPERTIES OF 14,000 LB GR-16 LOADLINE
SUBJECTED TO SEVERAL MODES AND RATES OF STRAIN

	Instron - Standard Test			High Strain Rate Missile Nose as Noted		
	Rupture Load (lb)	Rupture Strain (%)	Rupture Energy (ft-lb/ft)	Rupture Strain (%)	Rupture Energy (ft-lb/ft)	Time to Rupture (msec)
1/8" aluminum nose						
red webbing	13,400	18.8	920	18.4	~450	2.4
red webbing					356	
red webbing					382	
white webbing	14,310	21.4	1120		349	
200 ft/sec						
1/8" aluminum nose						
red webbing					190	
350 ft/sec					293	
					560	
1/8" aluminum nose						
red webbing					185	
500 ft/sec					261	
					473	
1/16" aluminum nose						
red webbing				16.4	791	3.1
200 ft/sec					732	
1/16" aluminum nose						
red webbing					692	
350 ft/sec						
1/16" aluminum nose						
red webbing				20.1	1205	1.7
500 ft/sec					1102	
1/64" stainless steel nose						
white webbing					451	
200 ft/sec						
1/64" stainless steel nose						
white webbing					342	
500 ft/sec						

The data generated as each of three loadline types was impacted at various velocities with missiles designated to simulate hook and drone surfaces is also presented in Tables 25, 26, and 27, to facilitate comparison with low strain rate (Instron) data. Although the Statement of Work specified two tests for each combination of loadline type, surface simulator, and impact velocity, a greater number was frequently made to confirm significant differences in energy absorption values recorded for the first two tests. In other instances, as trends in the results became obvious, fewer than two tests per condition were made in order to comply with time and budget reqirements.

The intent was that specimens of one inch wide, 9000 lb webbing be impacted and punctured with a steel hook tine at velocities of 150 and 200 fps. However, the problem of penetrating a webbing with a sharp-nosed missile was felt to be a dangerous, time-consuming endeavor that clearly would not fall within the budgetary limitations of this work. After consideration of possible alternatives, and with the consent of AFML, a steel missile nose that represented a one-dimensional replica of the smallest radius of curvature of the tine of a retrieval hook was fabricated. A photograph of a projectile nose about to impact a test specimen, seen in Figure 66, illustrates one plane of the simulated retrieval hook tine. If a photo were taken of this same projectile nose at 90° to the side view, however, it would show a 2-1/2 inch straight edge that ensured square, full contact between missile and webbing specimen and made the experimental plan workable. Rupture of 9000 lb webbing specimens impacted with this type of projectile nose at both 150 and 200 fps required only slightly less energy than that required to rupture the same material in an Instron tensile tester (see Table 25). Information taken from the film record obtained by using the high speed camera during one of these tests is shown in Figure 67 where strain is plotted as a function of time. Notice that a rupture strain of 18%, approximately equal to that measured during an Instron test, is achieved approximately 2.4 milliseconds after initial impact by the missile. Since rupture energy and rupture strain recorded during impact with the simulated hook do not differ significantly from corresponding values measured during an Instron test, one can assume that the rupture force remains at approximately the same level. These determinations, which are highly dependent upon the simplified projectile nose and specimen configuration used, are not wholly conclusive with regard to the potential for webbing damage by a hook in an actual drone recovery operation, where penetration of the webbing by the tip of the tine might occur. However, the likelihood of this happening is probably remote, and it is likely that premature tensile failure would not be expected to occur as a result of non-sliding impact with the hook. Heat generated by sliding the hook along the webbing could produce a different form of failure not studied at this time.

The 12,000 lb GR-14 and GR-16 loadlines were also impacted by each of three drone surface simulators at impact velocities of 200, 350, and 500 fps. The surface simulators represented a 1/8 inch thick aluminum spoiler, a 1/16 inch thick aluminum vertical stabilizer, and a 1/64 inch thick steel elevator. Since the precise alloy and temper of the actual drone components was unknown, FRL selected the material for the simulators based upon estimates of the general material type that would probably be employed and, to some degree, on the availability of stock. The two aluminum simulators were of a moderately high
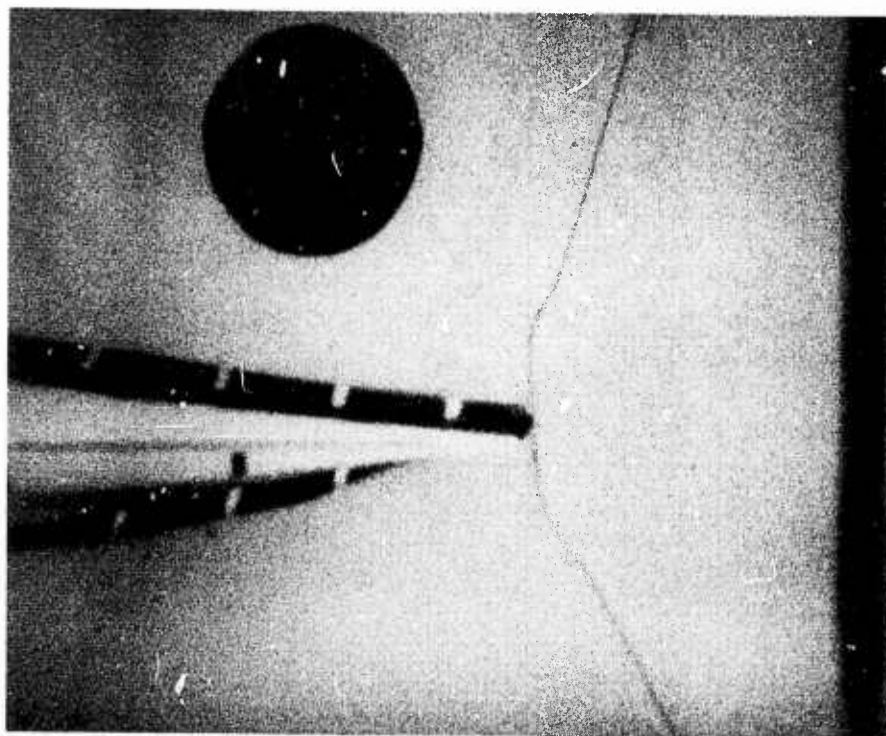
110

Figure 66. Enlargement of a Single Film Frame from Among
the Many Obtained for Each Test in which the
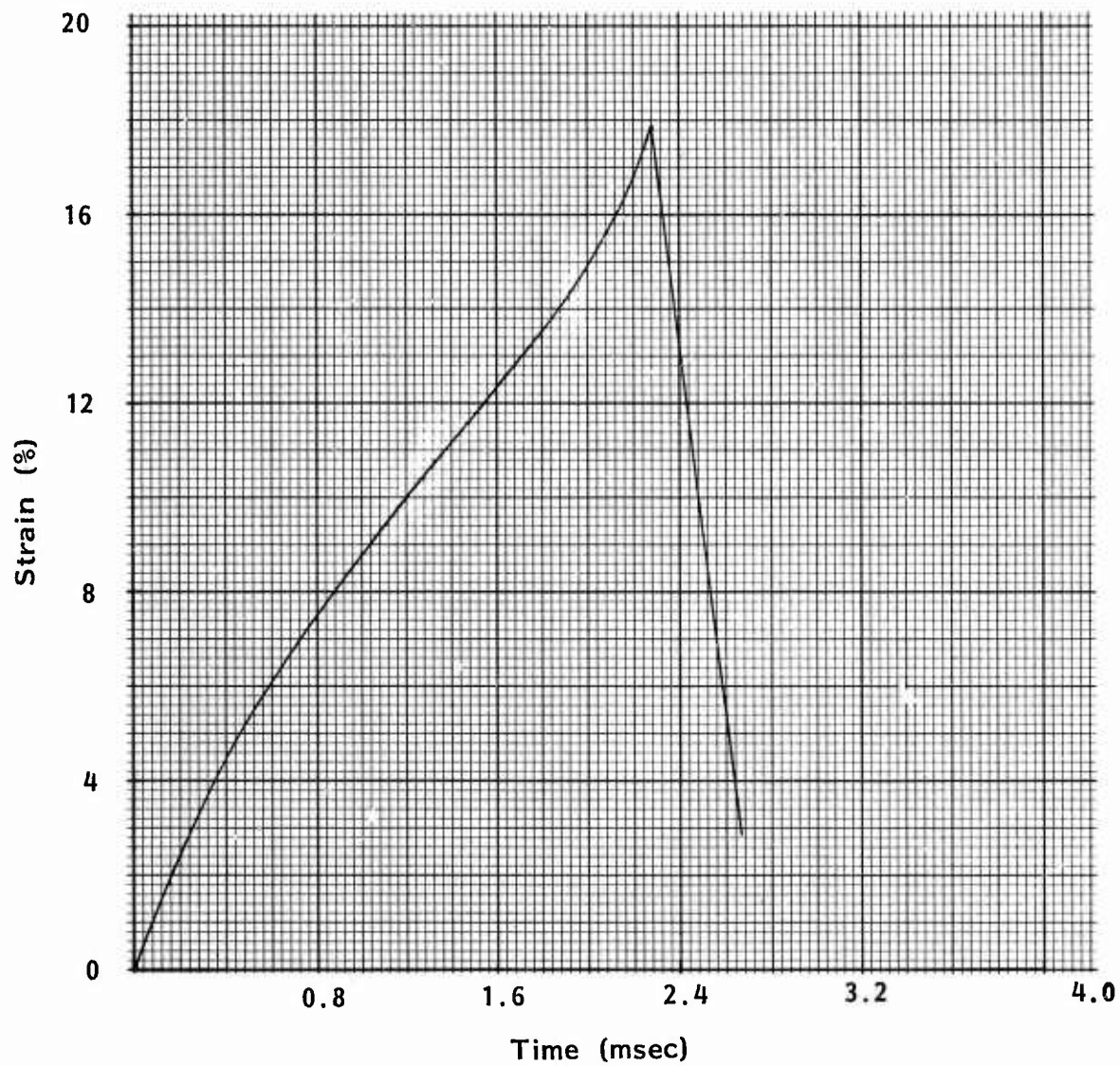High Speed Camera was Employed

Figure 67. Strain as a Function of Time During a Test of a 9,000
lb Webbing Impacted by a Steel Hook Tine Simulator at
a Velocity of 200 fps

112

strength alloy, 6061-T6, that is frequently used in aircraft applications, and the steel elevator simulator was of stainless steel, chosen because it was the stiffest (highest bending modulus) of the steels available. Tables 26 and 27 include summaries of all data obtained by impacting 12,000 lb GR-14 and 14,000 lb GR-16 loadlines with projectiles carrying noses which simulated the sharp-edged surfaces of the drone. In addition to rupture energies obtained by the ballistic pendulum method for each test, rupture strain and time-to-rupture values are shown for selected tests in which the high speed camera was employed. In Figures 68 and 69 a summary of the effect of simulator material and edge thickness upon the rupture energy of each of the loadlines impacted at three different velocities is shown graphically. This information and careful visual assessments of the surface simulating projectile nose after each test made clear the type of loadline damage suffered under each set of conditions. In every case in which a surface simulator collapsed during impact, the rupture energy of the loadline was found to be close to, or somewhat higher than, the energy required to break the loadline in a low strain rate (Instron) tensile test. However, in cases in which the surface simulator received little or no damage, low loadline rupture energies were measured. It became apparent that collapsed edge simulators allowed the blunt, 1/2-in wide projectile nose to transmit energy to the loadline and the effect became that of a routine high strain rate tensile test, while simulators that were not severely damaged during initial impact did, in fact, cut, or partially cut, the loadline. Notice in Figures 68 and 69 that tests using relatively stiff 1/8-inch aluminum impacting edges generally resulted in loadline rupture energies that were significantly lower than those recorded during Instron testing, while loadline rupture energies measured during tests involving 1/16-inch aluminum impacting edges, which completely collapsed upon impact, were similar to Instron values. Edges of 1/64-inch stainless steel, although damaged during impact, cut the loadlines with resultant low rupture energies being recorded in all except one test. In this test it is probable that the thin blade did not initially strike the center of the V-shaped specimen and folded over prior to making full contact. Other exceptions to the foregoing can be noted in two or three instances, all for tests at an impact velocity of 500 fps in which relatively high values of rupture were reported. Previous work [ASD Technical Report 60-511, II, February 1962, Coskren and Chu], however, has shown that in general nylon webbings require significantly greater energy for rupture when impacted at velocities as high as 500 fps.

To corroborate the influence of a thin edge with a high resistance to buckling on loadline cutting, two additional test firings were made. The first firing was of a projectile with a nosepiece of 1/16-inch stainless steel that represented an extreme combination of a thin and relatively stiff edge. The second firing was of a projectile with a blank insert in its nose that offered no protruding edge and thus represented the extreme condition of a case of an easily collapsible impacting edge. The loadline in both tests was 12,000 lb GR-14 and the impact velocity was 500 fps. The contrast in results obtained (see Table 26) provided convincing proof of the prime importance of the nature of the impacting edge; the rupture energy measured in the test with the 1/16-inch stainless steel edge was close to nil, indicating that cutting was the sole cause of failure, while the rupture energy measured using the blunt edge was approximately equal to the Instron value, tensile strain being the primary cause of failure. Examination of strain-time diagrams (Figure 70 and 71)
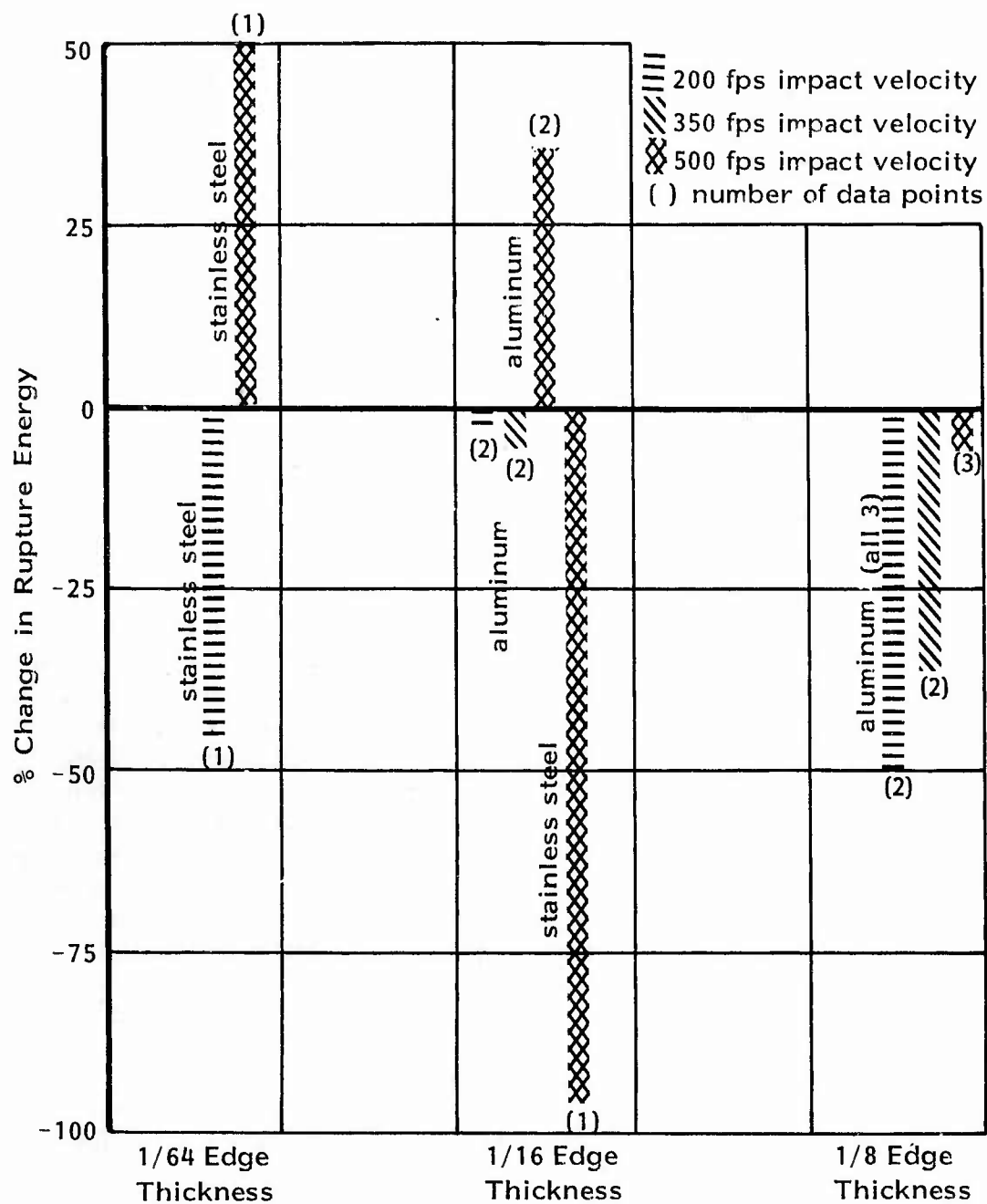
Figure 68.   Change in Rupture Energy of 12000 lb, GR-14 Loadline at High Strain Rate (compared to Instron value) as a Function of Thickness and Material of the Impacting Edge
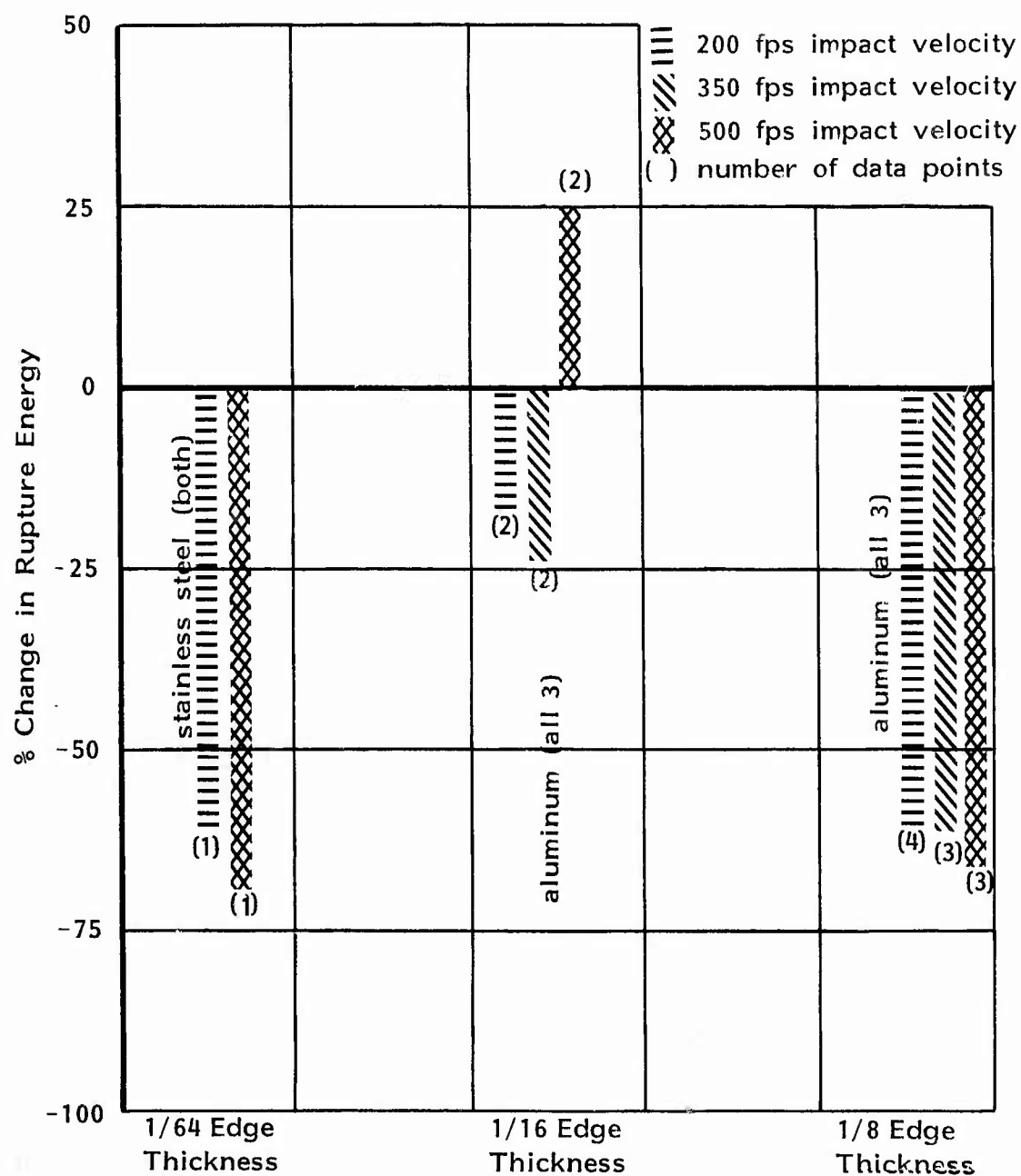
114

Figure 69. Change in Rupture Energy of 14000 lb, GR-16 Loadline at
High Strain Rate (compared to Instron value) as a Function
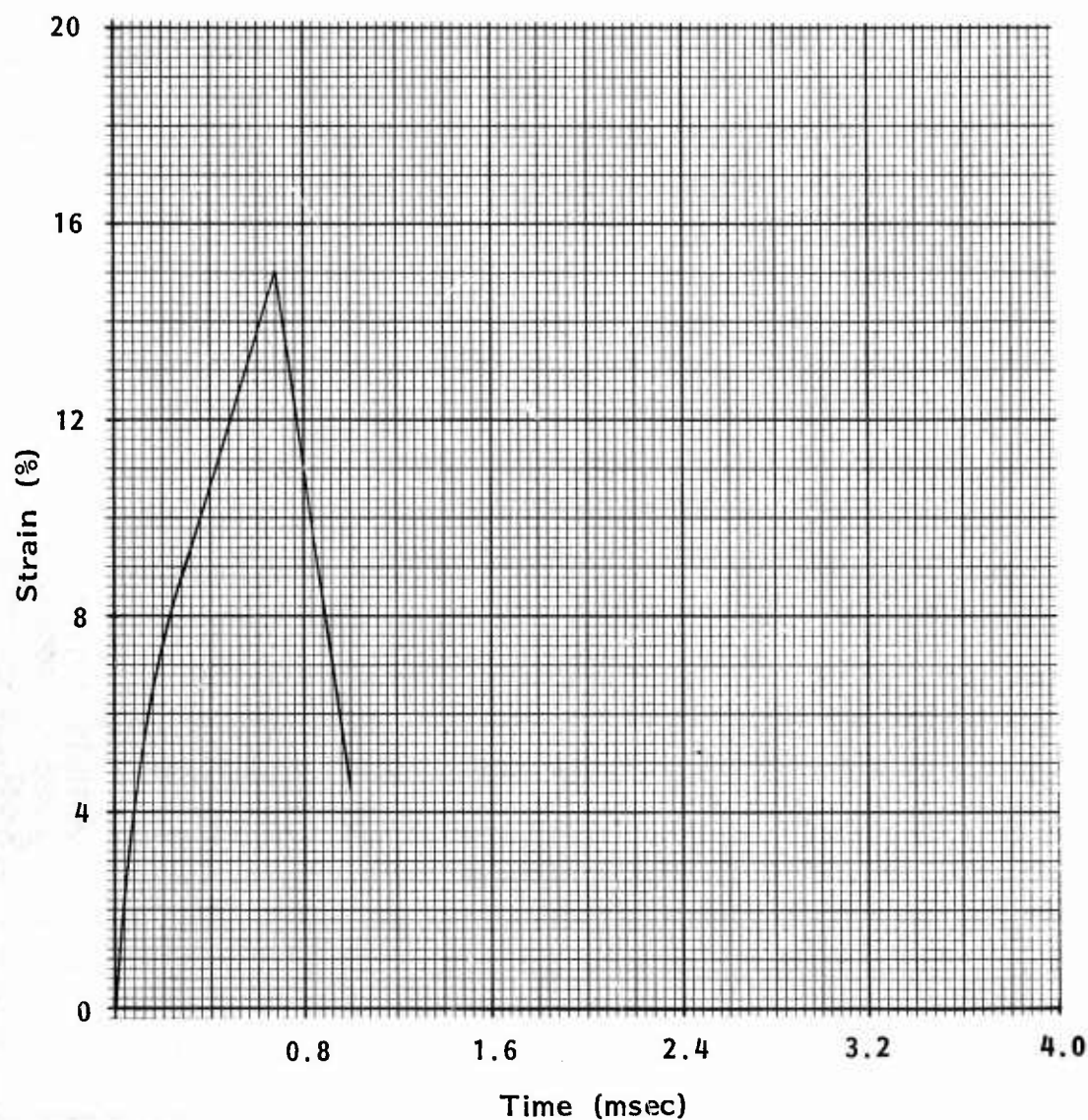of Thickness and Material of the Impacting Edge

115

Figure 70. Strain as a Function of Time During a Test of 12,000 lb, GR-14 Loadline Impacted by a 1/16-Inch Thick Stainless Steel Edge
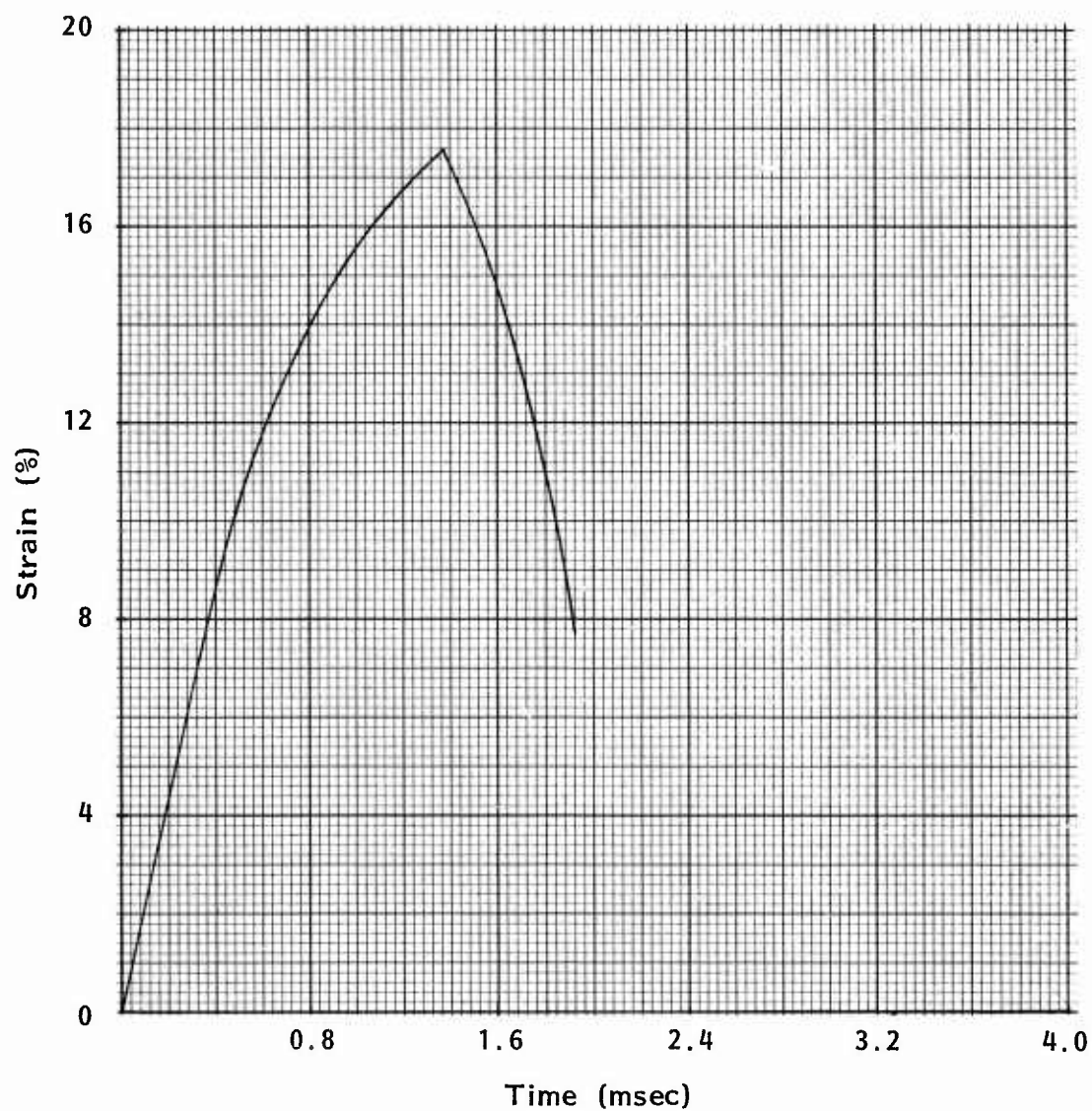
116

Figure 71. Strain as a Function of Time During a Test of 12,000
          lb, GR-16 Loadline Impacted by a 1/2-Inch Thick
          Aluminum Projectile Nose

obtained using the high speed camera during the two tests, results in additional confirmation of the cutting theory. Notice that the duration of the event involving the steel nose insert was approximately one half that of the event in which the blunt projectile nose was employed. Rupture strains recorded during these two tests (again, see Figures 70 and 71) were of the same magnitude only because the gage marks were placed very close to the point of impact. Rupture strain in the cut specimen, if measured over the full specimen length, would be significantly lower.

Careful visual examination was made of the ruptured ends of all loadline specimens as testing progressed. Upon completion of the testing program, five specimens were selected for further scrutiny under an optical microscope, and of these five, two were chosen for detailed examination with a scanning electron microscope. Although a considerable amount of time was spent observing broken fiber ends with both the optical microscope and the SEM, and several dozen SEM photographs were taken for additional study, the most pertinent observations were made with the unaided eye. it was clearly established that the cleanness of loadline breaks was directly related to the amount of cutting involved, using rupture energy and a knowledge of the nature of the impacting edge to estimate degrees of cutting action. For example, an observer, who had no knowledge of how the loadlines had been broken, was asked to rank, according to cleanness of break, five specimens of 12,000 lb GR-14 loadline, all tested at an impact velocity of 500 fps. He ranked them in this order:

Cleanness of Break (No. 1 being most clean)	Nature of Impacting Edge	Rupture Energy (ft-lb/ft)
1	1/16-inch stainless steel	~ 20
2	1/8-inch aluminum	362
3	1/8-inch aluminum	818
4	1/16-inch aluminum	1019
5	blank insert; blunt projectile nose	716

Photographs of two of the specimens from this group, those ranked Nos. 1 and 4, are shown in Figures 72 and 73 to illustrate the great contrast in appearance between the ends of a cut loadline and one that failed primarily due to tensile strain. Although a number of SEM photographs were taken of broken fiber ends from these same two specimens, characteristic features were not readily distinguishable; examples of fiber ends that were similar in appearance could be found in both specimens, as shown in Figures 74 and 75.

Conclusions and Recommendations

The failure mode of 12,000 lb GR-14 and 14,000 lb GR-16 loadlines, when impacted by AQM-34R drone surface simulators at velocities within the range of 200 to 500 fps, was shown to be dependent upon the stiffness of the impacting surface. In tests in which the impacting edge collapsed on impact, relatively
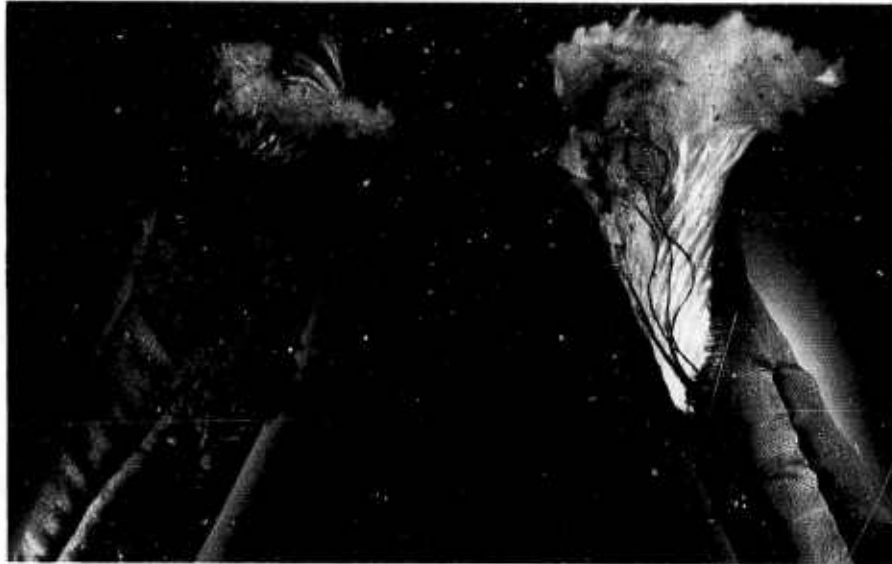
118

Figure 72. Ruptured Ends of 12000 lb, GR-14 Loadline
after Impact with a 1/16 Inch Stainless Steel
Edge at a Velocity of 500 fps (actual size)

Figure 73. Ruptured Ends of 12000 lb, GR-14 Loadline
after Impact with a 1/2 Inch Wide Blunt
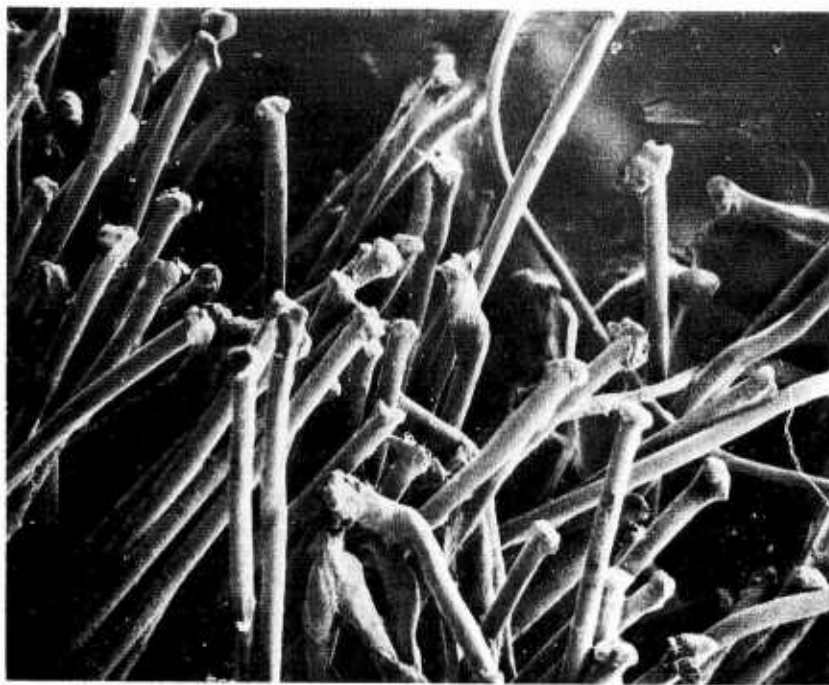Missile Nose (actual size)

119

Figure 74. SEM Photograph of Ruptured Fiber Ends from a 12000 lb,
GR-14 Loadline that was Impacted at 500 fps by a Blunt-
Nosed Projectile

Figure 75. SEM Photograph of Ruptured Fiber Ends from a 12000 lb,
GR-14 Loadline that was Impacted at 500 fps by a 1/16 inch
Stainless Steel Edge

high tensile energy measurements were recorded, but in tests in which the simulator edge suffered little or no damage, low energy values were obtained, indicative of premature failure due to cutting. Surfaces simulating spoilers (6061-T6 aluminum, 1/8-inch thick) and drone elevators (stainless steel, 1/64 inch) generally cut these loadlines, while the vertical stabilizer simulator (6061-T6 aluminum, 1/16 inch) collapsed and permitted the lines to function fully as tensile members. In applying this finding to the problem at hand, several limitations of the laboratory simulation must be recognized: 1) to achieve tensile loading, a V-shaped loadline configuration was employed; 2) impact was relatively clean without prior projectile-loadline abrasion; and 3) the unsupported depth of the impacting edge was 3/8 inch; in practice, the corresponding dimension is probably much greater.

No definite conclusions were possible in the case of a retrieval hook tine impacting a 9,000 lb loadbearing member, as safety and budget considerations severely limited the scope of this laboratory simulation. However, under the conditions employed in the tests, no evidence of webbing damage causing premature failure was found.

Visual correlation of failure mode with the appearance of ruptured loadline ends could readily be accomplished with the naked eye. Although in practice, flailing of ruptured ends subsequent to failure may tend to obscure identifying features, this sample approach should be exploited as fully as possible. Before the scanning electron microscope can become a practical tool in this application, a great deal of work will be necessary to accurately catalogue the appearance of nylon filaments subjected to many types of combinations of failure-producing strains.

Complete force-strain diagrams for loadlines subjected to impact by various surface simulators would undoubtedly be of great interest, but obtaining such diagrams is an extremely time-consuming task and could not successfully be accommodated within the scope of this program. The data obtained to date, however, provides required background information in the event that a decision is made to pursue the task of obtaining force-strain diagrams.

It would also be valuable to determine how webbings made from Kevlar, which are unusually hard to cut with a pair of scissors, would respond to impact of sharp-nosed missiles such as have been used in the current study. If they showed higher resistance to cutting than the nylon webbings presently being used, serious consideration might be given to using Kevlar suspension lines in the drone recovery parachute.

121

SUPPLEMENTARY

INFORMATION

DEPARTMENT OF THE AIR FORCE

WRIGHT LABORATORY (AFMC)
WRIGHT-PATTERSON AIR FORCE BASE, OHIO

ERRATA

25 February 1994

~~WL/DOA, Bldg 22~~

FROM: 2690 C St Ste 4
Wright-Patterson AFB OH 45433-7411

SUBJ: Notice of Changes in Technical Report(s) __AFML-TR-74-65__

TO: Defense Technical Information Center
Attn: DTIC-OCC
Cameron Station
Alexandria VA 22304-6145

Please change subject report(s) as follows:

AFML-TR-74-65, Part I - AD ~~B000360~~
Part II - ~~AD B002047~~
Part III - ~~AD B006949~~
Part IV - AD B017280

All parts have been approved for public release; distribution is
unlimited as of 23 Feb 1994.

ERRATA - AD - B017280

WM J. WHALEN
Chief, Tech. Editing & STINFO Branch
Resource Management